



Publicly Accessible Penn Dissertations


1-1-2016

Increased Expression of Frontotemporal Dementia Risk Factor Tmem106b Alters Lysosomal and Autophagosomal Pathways

Johanna Irene Busch

University of Pennsylvania, johannaibusch@gmail.com

Follow this and additional works at: <http://repository.upenn.edu/edissertations>

 Part of the [Cell Biology Commons](#), and the [Neuroscience and Neurobiology Commons](#)

Recommended Citation

Busch, Johanna Irene, "Increased Expression of Frontotemporal Dementia Risk Factor Tmem106b Alters Lysosomal and Autophagosomal Pathways" (2016). *Publicly Accessible Penn Dissertations*. 1630.
<http://repository.upenn.edu/edissertations/1630>

This paper is posted at ScholarlyCommons. <http://repository.upenn.edu/edissertations/1630>
For more information, please contact libraryrepository@pobox.upenn.edu.

Increased Expression of Frontotemporal Dementia Risk Factor Tmem106b Alters Lysosomal and Autophagosomal Pathways

Abstract

Frontotemporal lobar degeneration (FTLD) is an important cause of dementia in individuals under age 65. Common variants in the TMEM106B gene were previously discovered by genome-wide association (GWAS) to confer genetic risk for FTLD-TDP, the largest neuropathological subset of FTLD ($p=1 \times 10^{-11}$, OR=1.6). Prior to its discovery in the GWAS, TMEM106B, or Transmembrane Protein 106B, was uncharacterized. To further understand the role of TMEM106B in disease pathogenesis, we used immortalized as well as primary neurons to assess the cell biological effects of disease-relevant levels of TMEM106B overexpression and the interaction of TMEM106B with additional disease-associated proteins. We also employed immunostaining to assess its expression pattern in human brain from controls and FTLD cases.

We discovered that TMEM106B is a highly glycosylated, Type II late endosomal/lysosomal transmembrane protein. We found that it is expressed by neurons, glia, and peri-vascular cells in disease-affected and unaffected regions of human brain from normal controls in a cytoplasmic, perikaryal distribution. In brain from FTLD patients, we discovered a striking loss of subcellular localization with highly disordered TMEM106B immunostaining patterns in a subset of FTLD-TDP cases. Evidence suggests that TMEM106B variants increase risk for developing FTLD-TDP by increasing TMEM106B mRNA and protein expression levels. We therefore investigated the cell biological effects of increased TMEM106B expression. Increased TMEM106B results in a decrease in the average number of late endosomes/lysosomes per cell, loss of lysosomal acidification, and impaired lysosomal degradation. In addition, lysosomal deficits are accompanied by the appearance of enlarged organelles ($>2-3\mu\text{m}$) demonstrating ultrastructural characteristics of late autophagic vacuoles (autolysosomes/amphisomes). We observed these effects in both immortalized cell lines and in primary neurons overexpressing TMEM106B. Furthermore, we show that the effects of increased TMEM106B expression can be abrogated by (1) a single point mutation to a lysosomal sorting motif in TMEM106B newly identified here, or (2) knockdown of C9orf72 protein. In sum, our results suggest that TMEM106B exerts its effects on FTLD-TDP disease risk through alterations of lysosomal and autophagic pathways and that TMEM106B and C9orf72 may interact in disease pathophysiology.

Degree Type

Dissertation

Degree Name

Doctor of Philosophy (PhD)

Graduate Group

Cell & Molecular Biology

First Advisor

Alice Chen-Plotkin

Keywords

C9orf72, Frontotemporal dementia, FTD, FTL, Lysosome, TMEM106B

Subject Categories

Cell Biology | Neuroscience and Neurobiology

INCREASED EXPRESSION OF FRONTOTEMPORAL DEMENTIA RISK FACTOR TMEM106B
ALTERS LYSOSOMAL AND AUTOPHAGOSOMAL PATHWAYS

Johanna I. Busch

A DISSERTATION

in

Cell and Molecular Biology

Presented to the Faculties of the University of Pennsylvania

in

Partial Fulfillment of the Requirements for the

Degree of Doctor of Philosophy

2016

Supervisor of Dissertation

Alice Chen-Plotkin, M.D.
Assistant Professor of Neurology

Graduate Group Chairperson

Daniel S. Kessler, Ph.D.
Associate Professor of Cell and Developmental Biology

Dissertation Committee

Erika L. F. Holzbaur, Ph.D., Professor of Physiology (Chair)
Robert W. Doms, M.D., Ph.D., Professor of Pathology and Laboratory Medicine
Virginia M.-Y. Lee, Ph.D., John H. Ware 3rd Endowed Professor in Alzheimer's Research,
Professor of Pathology and Laboratory Medicine
Michael S. Marks, Ph.D., Professor of Pathology and Laboratory Medicine

ACKNOWLEDGMENT

I would like to thank my mentor, Dr. Alice Chen-Plotkin, for giving me the opportunity to study the exciting new world of TMEM106B and for providing me with advice, mentorship, and scientific discourse throughout the past few years. I would also like to thank the members of the lab and the members of my thesis committee for their insights and support throughout. I also thank my family and those who are like family to me for their emotional support and for the fun, both inside and outside the lab, we have had over the past years.

I thank Margie Maronski and the "Neurons R Us" core facility for providing primary murine neurons, the Electron Microscopy Resource Laboratory for processing and assistance with electron microscopy, Dr. Fenghua Hu for providing the GFP-TMEM106B construct, Robert Arauz Perez, Emily Bill, Nimansha Jain, Jordan Mak, Tyler Skrinak, and Travis Unger for their assistance, and Dr. Mickey Marks for his input and advice regarding lysosomal targeting motifs.

Finally, I would like to thank the patients and their families, whose contributions and dedication to understanding this disease make this work possible.

ABSTRACT

INCREASED EXPRESSION OF FRONTOTEMPORAL DEMENTIA RISK FACTOR TMEM106B ALTERS LYSOSOMAL AND AUTOPHAGOSOMAL PATHWAY

Johanna Busch

Dr. Alice Chen-Plotkin

Frontotemporal lobar degeneration (FTLD) is an important cause of dementia in individuals under age 65. Common variants in the *TMEM106B* gene were previously discovered by genome-wide association (GWAS) to confer genetic risk for FTLD-TDP, the largest neuropathological subset of FTLD ($p=1 \times 10^{-11}$, OR=1.6). Prior to its discovery in the GWAS, TMEM106B, or Transmembrane Protein 106B, was uncharacterized. To further understand the role of TMEM106B in disease pathogenesis, we used immortalized as well as primary neurons to assess the cell biological effects of disease-relevant levels of TMEM106B overexpression and the interaction of TMEM106B with additional disease-associated proteins. We also employed immunostaining to assess its expression pattern in human brain from controls and FTLD cases.

We discovered that TMEM106B is a highly glycosylated, Type II late endosomal/lysosomal transmembrane protein. We found that it is expressed by neurons, glia, and peri-vascular cells in disease-affected and unaffected regions of human brain from normal controls in a cytoplasmic, perikaryal distribution. In brain from FTLD patients, we discovered a striking loss of subcellular localization with highly disordered TMEM106B immunostaining patterns in a subset of FTLD-TDP cases. Evidence suggests that *TMEM106B* variants increase risk for developing FTLD-TDP by increasing *TMEM106B* mRNA and protein expression levels. We therefore investigated the cell biological effects of increased TMEM106B expression. Increased TMEM106B results in a decrease in the average number of late endosomes/lysosomes per cell, loss of lysosomal acidification, and impaired lysosomal degradation. In addition, lysosomal deficits are accompanied by the appearance of enlarged organelles (>2-3 μ m) demonstrating ultrastructural characteristics of late autophagic vacuoles

(autolysosomes/amphisomes). We observed these effects in both immortalized cell lines and in primary neurons overexpressing TMEM106B. Furthermore, we show that the effects of increased TMEM106B expression can be abrogated by (1) a single point mutation to a lysosomal sorting motif in TMEM106B newly identified here, or (2) knockdown of C9orf72 protein. In sum, our results suggest that TMEM106B exerts its effects on FTLD-TDP disease risk through alterations of lysosomal and autophagic pathways and that TMEM106B and C9orf72 may interact in disease pathophysiology.

TABLE OF CONTENTS

ACKNOWLEDGMENT	II
ABSTRACT	III
TABLE OF CONTENTS	V
LIST OF TABLES	VII
LIST OF ILLUSTRATIONS.....	VIII
CHAPTER 1: INTRODUCTION.....	1
1.1 PART I: Frontotemporal dementia and disease-associated mutations	1
1.1.1 Frontotemporal Lobar Degeneration.....	1
1.1.2 Epidemiology.....	2
1.1.3 The ALS-FTLD disease spectrum.....	2
1.1.4 Neuropathology.....	3
1.1.5 Major disease-associated mutations.....	3
1.1.5.1 <i>TARDBP</i>	6
1.1.5.2 <i>MAPT</i>	7
1.1.5.3 <i>GRN</i>	8
1.1.5.4 <i>C9orf72</i>	11
1.1.6 Summary.....	18
1.2 PART II: Introduction to the endolysosomal/autophagosomal network	19
1.2.1 Endosomes	21
1.2.2 Lysosomes.....	24
1.2.3 Autophagosomes and autophagy	25
1.2.3.1 Autophagosome-lysosome fusion	28
1.2.3.2 Resolution of autophagy.....	29
1.2.4 The endolysosomal/autophagosomal pathway in neurons and neurodegenerative diseases 30	
1.2.4.1 Autophagy in neurons	30
1.2.4.2 Endolysosomal/autophagosomal dysfunction in adult neurodegenerative disease	31
1.2.5 Summary.....	34
1.3 PART III: TMEM106B.....	36
1.3.1 The discovery and initial characterization of TMEM106B.....	36
1.3.2 Increased levels of TMEM106B are implicated in disease	37
1.3.3 TMEM106B and progranulin	39
1.3.4 TMEM106B and C9orf72	40
1.3.5 Summary.....	40
CHAPTER 2: EXPRESSION OF TMEM106B IN NORMAL AND DISEASED HUMAN BRAIN..	41
2.1 INTRODUCTION.....	42
2.2 RESULTS.....	47
2.2.1 TMEM106B expression by cell type in normal human brain tissue	47

2.2.2	TMEM106B expression by brain region in normal human brain tissue	47
2.2.3	TMEM106B expression in FTLD-TDP brain	50
2.3	DISCUSSION	54
2.4	MATERIALS AND METHODS	57
CHAPTER 3: INCREASED EXPRESSION OF THE FRONTOTEMPORAL DEMENTIA RISK FACTOR TMEM106B CAUSES C9ORF72-DEPENDENT ALTERATIONS IN LYOSOMES....		59
3.1	INTRODUCTION.....	60
3.2	RESULTS.....	62
3.2.1	Increased expression of TMEM106B in results in altered endolysosomal morphology.....	62
3.2.2	Increased expression of TMEM106B results in multiple lysosomal abnormalities	70
3.2.3	Increased TMEM106B alters autophagosomal and lysosomal populations	74
3.2.4	Increased TMEM106B levels may decrease cell survival.....	76
3.2.5	The cell biological effects of increased TMEM106B expression are dependent on localization of TMEM106B to lysosomes	78
3.2.6	Lysosomal acidification and cytotoxicity effects of increased TMEM106B expression are dependent on C9orf72.....	87
3.3	DISCUSSION.....	94
3.4	MATERIALS AND METHODS	100
CHAPTER 4: DISCUSSION		109
4.1	Changes in TMEM106B expression levels result in alterations to the endolysosomal/autophagosomal pathway	110
4.1.1	Increased levels of TMEM106B result in enlarged LAMP1 organelle size	110
4.1.2	Increased levels of TMEM106B results in lysosomal acidification and degradative defects	112
4.1.3	Increased levels of TMEM106B may impact autophagy pathways	114
4.1.4	TMEM106B overexpression may skew the endolysosomal/autophagosomal pathway towards a net increase in fusion products	115
4.1.5	Point mutations in an extended dileucine lysosomal sorting motif abrogates TMEM106B overexpression phenotypes	123
4.1.6	The endolysosomal/autophagosomal disturbances caused by increased TMEM106B are cytotoxic to cells.....	124
4.1.7	TMEM106B knockdown may alter lysosomal size and trafficking	125
4.2	TMEM106B and C9orf72	126
4.3	TMEM106B and progranulin	130
4.3.1	TMEM106B overexpression may disrupt neuroprotective progranulin pathways	131
4.4	The endolysosomal/autophagosomal pathway in disease pathogenesis	132
4.5	Future Directions	135
4.6	Conclusion.....	138
BIBLIOGRAPHY		139

LIST OF TABLES

Characteristics of cases and brain regions evaluated for TMEM106B expression.....	45
---	----

LIST OF ILLUSTRATIONS

Figure 1.1: Major disease-associated mutations.....	5
Figure 1.2: Major genes and cellular pathways implicated in FTLD.....	5
Figure 1.3: The endolysosomal / autophagosomal pathway.....	20
Figure 2.1: TMEM106B expression in neurons, glial and endothelial cells or pericytes in cortical specimens from normal controls.....	48
Figure 2.2: TMEM106B protein expression in brain tissue from normal controls.....	49
Figure 2.3: Scoring of neuronal TMEM106B protein expression.....	52
Figure 2.4: TMEM106B expression is more disorganized in neurons from <i>GRN</i> -associated FTLD-TDP cases.....	53
Figure 3.1: Increased expression of TMEM106B alters endolysosomal morphology.....	63
Figure 3.2: TMEM106B does not co-localize with EEA-1 and SV-2.....	65
Figure 3.3: Ultrastructural characterization of TMEM106B-induced vacuolar phenotype.....	67
Figure 3.4: Flow cytometry of GFP-TMEM106B-transfected HeLa cells.....	69
Figure 3.5: TMEM106B overexpression alters lysosomal acidification and function.....	72
Figure 3.6: TMEM106B co-localizes with LC3 and overexpression of TMEM106B alters autophagosome and lysosome populations.....	75
Figure 3.7: Increased levels of TMEM106B are cytotoxic to cells.....	77
Figure 3.8: ENQLVALI is a potential lysosomal sorting motif for TMEM106B.....	80
Figure 3.9: ENQLVAAA TMEM106B is not retained in the endoplasmic reticulum.....	82
Figure 3.10: Characterization of lysosomal motif mutants.....	84
Figure 3.11 The effects of increased TMEM106B expression depend on proper localization of TMEM106B to lysosomes.....	85
Figure 3.12: Knockdown of C9ORF72 rescues TMEM106B-induced vacuolar phenotype..	89

Figure 3.13: Knockdown of C9orf72 mitigates TMEM106B-induced acidification defects and cytotoxicity.....	91
Figure 3.14: Overexpression and knockdown of C9orf72.....	92
Figure 4.1: Model 1.....	117
Figure 4.2: Model 2.....	121
Figure 4.3: Endolysosomal/autophagosomal dysfunction in neurodegeneration.....	134

CHAPTER 1: INTRODUCTION

PREFACE:

This body of work aims to provide an initial characterization of Transmembrane Protein 106B, or TMEM106B – a protein associated with the neurodegenerative disease, frontotemporal lobar degeneration (FTLD) – and to demonstrate how elevated levels of TMEM106B, as seen in disease, perturb endolysosomal and autophagosomal pathways. In this Introduction, I will describe FTLD, discuss known mutations that cause the disease, detail the discovery of TMEM106B, and give an overview of endolysosomal/autophagosomal pathways and their role in neurodegeneration.

1.1 PART I: Frontotemporal dementia and disease-associated mutations

1.1.1 Frontotemporal Lobar Degeneration

Frontotemporal lobar degeneration (FTLD), otherwise known by its clinical designation “frontotemporal dementia (FTD),” refers to a clinically and genetically heterogeneous group of neurodegenerative disorders that are characterized by the selective and progressive degeneration of the frontal and temporal lobes of the brain (Ratnavalli et al., 2002; Neary et al., 2005). FTLD is the second most common cause of dementia in patients under the age of 65 after Alzheimer’s, and accounts for approximately 5-15% of all patients with dementia (Seelaar et al., 2011; Ratnavalli et al., 2002; Mercy et al., 2008). Reflecting the location of degeneration within the brain, patients initially exhibit changes in behavior, language, and personality, in contrast to the prominent memory impairments typically associated with Alzheimer’s disease (Mackenzie et al., 2011). These changes are progressive and ultimately result in global dementia with a disease duration of four to eight years from diagnosis to death (Garcin et al., 2009; Hodges et al., 2003; Neary et al., 2005). There are currently no treatments for the disease; therefore, elucidating the mechanisms underlying disease pathogenesis is important in order to identify potential therapeutic avenues.

1.1.2 Epidemiology

The mean age at onset of FTLD is ~58 years, but disease onset can range from ~40 to 75 years old (Hodges et al., 2003; Rosso et al., 2003). Some studies estimate equal incidence of disease in men and women (Johnson et al., 2005), while others have demonstrated increased incidence in men (Ratnavalli et al., 2002). In the 45- to 64-year-old population demographic, the incidence of disease has been estimated to be 15 per 100,000 people (Ratnavalli et al., 2002), although these estimates are likely to be conservative due to misdiagnosis of FTLD as psychiatric illnesses due to the striking personality changes and loss of inhibition sometimes exhibited by patients.

1.1.3 The ALS-FTLD disease spectrum

It has been increasingly recognized that FTLD and amyotrophic lateral sclerosis (ALS) exist on a disease spectrum, with pure forms of the diseases at either extreme and clinical and genetic overlap in between (Mackenzie and Feldman, 2005). ALS is classically described as a neurodegenerative disease that selectively affects both upper and lower motor neurons and is usually fatal between 3-5 years after diagnosis (Swinnen and Robberecht, 2014). Approximately half of ALS patients exhibit functional loss in tests of frontal lobe function and ~15% of patients have enough deficits to be diagnosed with FTLD (Ringholz and Greene, 2006). Conversely, ~40% of FTLD cases have some level of motor dysfunction, with ~15% meeting the criteria for ALS diagnosis (Burrell and Hodges, 2010).

In addition to this clinical overlap, genetic and pathological evidence likewise support an FTLD-ALS continuum. A major discovery came in 2006, when pathological inclusions of TAR-DNA binding protein 43 (TDP-43) were identified as the major ubiquitinated protein found in brain tissue of both sporadic ALS and FTLD (Neumann et al., 2006; Arai et al., 2006). In addition, disease-causing missense mutations in the gene encoding TDP-43 (*TARDBP*) were also found to account for ~3% of familial ALS and a small number of FTLD cases (Borroni et al., 2009; Sreedharan et al., 2008; Van Damme et al., 2008; Kabashi et al., 2008; Lagier-Tourenne and Cleveland, 2009). Finally, in 2011, expansion of an intronic hexanucleotide repeat in *C9orf72* was

identified as the most common cause of both FTLD and ALS (DeJesus-Hernandez et al., 2011; Renton et al., 2011; Beck et al., 2013). Mutations in *TARDBP*, *C9orf72*, and other disease-associated genes are described in further detail below.

1.1.4 Neuropathology

FTLD pathology includes atrophy of the frontal and temporal cortices with associated neuronal loss, gliosis, and spongiosis (Sieben et al., 2012; Seelaar et al., 2011). There are two major neuropathological subtypes of FTLD – FTLD with tau-positive inclusions (FTLD-tau) and FTLD with TDP-43-positive inclusions (FTLD-TDP) (Mackenzie et al., 2011; Sieben et al., 2012; Mackenzie et al., 2010). The genetic data to date suggest that there are likely distinct mechanisms of disease pathogenesis for FTLD-tau and FTLD-TDP, with specific mutations associated solely with each subtype. The neuropathological subtypes and their known disease-associated gene mutations are depicted in **Figure 1.1**. FTLD-tau represents approximately 45% of FTLD and is characterized by abnormal accumulations of the microtubule-associated protein tau in neurons and glia. In contrast, FTLD-TDP cases make up the largest proportion of FTLD, at approximately 45-60% of total FTLD cases (Ling et al., 2013). FTLD-TDP is the neuropathological subtype of most interest to this work, as *TMEM106B* variants were found to confer risk of disease in the FTLD-TDP subtype. FTLD-TDP cases harbor neuronal inclusions of ubiquitinated, hyperphosphorylated TAR DNA binding protein 43 (TDP-43) (Arai et al., 2006; Neumann et al., 2006). Briefly, TDP-43 is an RNA/DNA binding protein which has been reported to regulate gene expression, transcription, and multiple aspects of RNA processing and functioning; the role of TDP-43 in disease will be discussed in further detail below. Other neuropathological subtypes include FTLD-FUS (Fused in Sarcoma), which makes up ~9% of FTLD, and FTLD-UPS (ubiquitin-protease system). These subsets are beyond the scope of this work, but notably lack both TDP-43 and tau pathology (Ling et al., 2013).

1.1.5 Major disease-associated mutations

FTLD can be either sporadic or familial; approximately 40% of patients have a family history positive for dementia or psychiatric diagnoses, but the inheritance pattern of FTLD is not

always clear, with only 10-25% of patients exhibiting a clear Mendelian inheritance pattern (Hodges et al., 2003; Knibb et al., 2006; Goldman et al., 2005). Currently, Mendelian FTLD has been linked to mutations in many different genes, most notably *MAPT*, *GRN*, *C9orf72*, *OPTN*, *TARDBP*, *FUS*, *UBQLN2*, *VCP*, and *CHMP2B*. Autosomal dominant mutations with high penetrance in *MAPT*, *GRN*, *C9orf72*, together explain ~15% of familial FTLD. Disease-associated mutations in *MAPT* correlate with FTLD-tau pathology whereas mutations in *GRN* and *C9orf72* are associated with FTLD-TDP pathology. In addition, mutations in *VCP* and *CHMP2B* are important albeit rare causes of disease that hint at disturbances of endolysosomal/autophagosomal pathways in the development of disease (Sieben et al., 2012). Mutations in *MAPT*, *GRN*, *TARDBP*, *C9orf72*, *VCP*, and *CHMP2B* are discussed in more detail below, as they pertain most to this body of work. These genes implicate dysregulation of various cellular pathways in the development of disease, including membrane trafficking, autophagy and endolysosomal pathways, DNA/RNA processing, and accumulation of toxic aggregates; these pathways are summarized in **Figure 1.2**. For additional genes implicated in FTLD, the reader is directed to Bennion Callister 2014 for a comprehensive review (Bennion Callister and Pickering-Brown, 2014).

Figure 1.1:

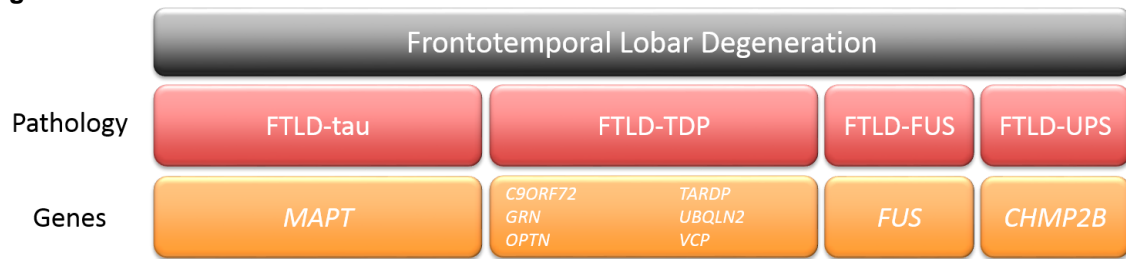


Figure 1.1: Major disease-associated mutations

The major neuropathological subtypes of frontotemporal lobar degeneration are depicted in red. The genes associated with each neuropathological subtype are depicted below in orange.

Figure 1.2:

Gene	Gene name	Location	Possible pathways
C9ORF72	Chromosome 9 open reading frame 72	9p21.2	Membrane trafficking; aggregates of toxic RNA and/or repeat dipeptides; autophagy; endolysosomal pathway
CHMP2B	Charged multivesicular body protein 2B	3p11.2	Autophagy; endolysosomal pathway
GRN	Progranulin	17q21.32	Autophagy; endolysosomal pathway; inflammation
MAPT	Microtubule-associated protein tau	17q21.1	Toxic aggregation
OPTN	Optineurin	10p13	Autophagy
TARDBP	TAR DNA binding protein	1p36.22	DNA/RNA metabolism
UBQLN2	Ubiquilin 2	Xp11.21	Autophagy
VCP	Valosin-containing protein	9p13.3	Autophagy

Figure 1.2: Major genes and cellular pathways implicated in FTLD

Genes correlating with FTLD-TDP pathology are highlighted in yellow. Disturbances of membrane trafficking and autophagosomal/endolysosomal pathways are one major theme; a second major theme is alterations in DNA/RNA processing and metabolism.

Adapted from (Guerreiro et al., 2015).

1.1.5.1 *TARDBP*

Human TDP-43 was first discovered in a screen as a transcriptional repressor of the trans-activation response (TAR) element of HIV, earning its name TAR DNA Binding Protein (*TARDBP*) (Ou et al., 1995). The protein encoded by *TARDBP* is thus named TDP-43 due to its molecular weight of 43 kDa (Neumann et al., 2006; Ou et al., 1995). Disease-associated mutations in *TARDBP* itself are a unifying cause of both FTLD and ALS; to date, 34 different missense mutations in *TARDBP* have been reported in 131 ALS and FTD families (Cruts et al., 2012). Additionally, hyperphosphorylated, ubiquitinated, and N-terminally truncated TDP-43+ inclusions were found in 2006 to be the pathological hallmark of *all* of FTLD-TDP, regardless of the underlying mutation, thus, strongly implicating TDP-43 in FTLD-TDP pathogenesis (Neumann et al., 2006). In normal states, TDP-43 is found predominantly in the nucleus, but shuttles back and forth between the nucleus and cytoplasm. However, in postmortem samples from patients with FTLD-TDP and ALS, TDP-43+ inclusions are often found mislocalized to the cytoplasm of neurons within disease-affected regions of the brain (Neumann et al., 2006).

TDP-43 is a ubiquitously expressed DNA- and RNA-binding protein and has been shown to have myriad functions, many of which are still being elucidated. TDP-43 has been shown to play a major role in RNA processing and homeostasis (Lee et al., 2011a; Da Cruz and Cleveland, 2011; Buratti et al., 2010). Data supporting such a role are as follows. TDP-43 depletion from mouse brain by anti-sense oligonucleotides resulted in changes in levels of 601 mRNAs, including *FUS* and *GRN* (Polymenidou et al., 2011). Additionally, TDP-43 depletion was then shown to result in altered splicing patterns of ~1500 RNAs in mammalian brain (Tollervey et al., 2011; Polymenidou et al., 2011). To date, more than 6000 TDP-43 RNA targets have been identified from *in vivo* studies in human brain (Tollervey et al., 2011), rat and mouse cortical neurons (Sephton et al., 2011), a murine NSC-34 line (Colombrita et al., 2012) and a human neuroblastoma cell line (Xiao et al., 2011). TDP-43 has been found to preferentially bind to introns, 3' UTRs, and non-coding RNAs (Tollervey et al., 2011); intriguingly, a number of TDP-43

regulated targets have been shown to be involved in neuronal development or neurological disease (Tollervey et al., 2011).

TDP-43 has also been implicated in ncRNA stability and miRNA biogenesis (Robberecht and Philips, 2013; Kawahara and Mieda-Sato, 2012). Specifically, TDP-43 has been found in a macromolecular complex containing Dicer (Gregory et al., 2004; Kawahara and Mieda-Sato, 2012) and Drosha (Ling et al., 2010); additionally, levels of TDP-43 have been reported to affect the stability of Drosha, with knockdown of TDP-43 causing a 66% decrease in Drosha levels in SK-N-BE cells (Di Carlo et al., 2013). TDP-43 binds directly to a subset of pri-miRNAs to promote the production of their pre-miRNAs (Kawahara and Mieda-Sato, 2012), supporting a role for TDP-43 in miRNA biogenesis. Corroborating this, Buratti et al. have reported that TDP-43 depletion results in downregulation of let-7b miRNA (Buratti et al., 2010). Thus, evidence for a RNA-regulatory role for TDP-43 comes from multiple different groups, working in cell culture, tissue, and in vivo animal contexts.

Despite these advancements in our understanding of TDP-43 within the cell, much more needs to be elucidated to begin to understand the pathogenic link between FTLD-TDP TDP-43 neuropathology and mutations in *TDP-43*, *GRN*, *C9orf72*, *VCP* and other genes.

1.1.5.2 MAPT

In 1994, initial genetic linkage evidence implicated a locus on chromosome 17q21 in familial FTLD (Wilhelmsen et al., 1994). These cases harbored neuronal and glial inclusions that contained the microtubule-associated protein tau. Intriguingly, the gene encoding tau, *MAPT*, is located on 17q21; this led to the identification of multiple mutations in *MAPT* that were found to segregate with FTLD (Clark et al., 1998; Hutton et al., 1998; Spillantini et al., 1998) in affected family members. To date, there are >40 mutations in *MAPT* associated with disease, with cases harboring these mutations all demonstrating FTLD-tau pathology. The tau protein normally functions to promote the assembly of tubulin microtubules and to regulate axonal transport, with six different isoforms expressed in adult brain (Goedert et al., 1989; Ebner et al., 1998; Sato-Harada et al., 1996). Half of these isoforms contain three repeats of a ~32 amino acid motif in the

microtubule-binding domain (3R tau), while the other half contain four repeats (4R tau); the 4R tau isoforms exhibit a stronger association with microtubules than 3R tau isoforms. FTLD-associated mutations are predominantly missense or splice-site mutations, disrupting the ratio of tau isoform expression with an overall increase in the ratio of 4R:3R tau isoforms (Gustke et al., 1994; Ingelsson et al., 2007; Spillantini et al., 2006; Hutton et al., 1998). This alteration in the ratio of tau isoforms favors tau aggregation, forming hyperphosphorylated tau filaments (Hutton et al., 1998), with toxic consequences for the cell. In neurons in particular, mutations in *MAPT* may interfere with axonal transport processes. Neurons are highly sensitive to dysregulation of axonal transport, as they depend on it to deliver cellular components to the distal axon. Overexpression of tau has been shown to alter the distribution of various organelles and to impair mostly plus-end-directed (synapse-directed) transport (Ebner et al., 1998; Trinczek et al., 1999).

1.1.5.3 GRN

Heterozygous loss-of-function mutations in the progranulin gene (*GRN*) were first reported in 2006 (Baker et al., 2006; Cruts et al., 2006) and account for ~10% of FTLD-TDP (Gass et al., 2006) and up to 20% of familial FTLD-TDP (Gijssels et al., 2008). Disease-associated mutations cause haploinsufficiency of *GRN*'s protein product, progranulin (Cruts et al., 2006). Over 90% of disease-associated mutations in *GRN* result in premature termination codons, leading to nonsense-mediated decay and decreased levels of progranulin (Gijssels et al., 2008); other missense mutations may impair secretion of progranulin, which also results in lower circulating levels of progranulin (Cruts et al., 2006; Shankaran et al., 2008; Mukherjee et al., 2008). Indeed, progranulin levels in the serum or cerebral spinal fluid (CSF) of patients harboring disease-associated *GRN* mutations are decreased by ~30-50% as compared to normal controls (Van Damme et al., 2008; Finch et al., 2009; Ghidoni et al., 2008; Sleegers et al., 2009).

The *GRN* gene encodes a 593 amino acid secreted protein, progranulin. Progranulin is a highly conserved, widely expressed growth factor with highest levels of expression in the rapidly dividing cells of skin and gastrointestinal tract and in peripheral immune tissues (Daniel et al., 2000). The protein contains seven and a half tandem repeats of a conserved cysteine-rich

granulin domain; these granulin domains are separated by linker series that contain disulfide bridges (He et al., 2002). These linker series can be cleaved by matrix metalloproteinase-14 (Butler et al., 2008), elastase (Zhu et al., 2002), proteinase 3, and neutrophil elastase (Kessenbrock et al., 2008), resulting in individual granulin peptides. The functions of individual granulins and full-length progranulin have still to be fully elucidated; intriguingly they exhibit similar functions in some settings, but opposing effects in others (De Muynck et al., 2013). For example, both progranulin and daughter peptide granulin E increase neuronal survival by 20-40% when applied to cortical neuron cultures and also both positively regulate neurite outgrowth (Van Damme et al., 2008); other investigators have also corroborated progranulin's positive effect on neuronal survival and neurite outgrowth (Laird et al., 2010; Gao et al., 2010; Gass et al., 2006). However, in inflammatory processes, progranulin and individual granulins have been shown to exhibit opposing effects (He et al., 2002; Zhu et al., 2002). For example, progranulin-deficient human and mouse microglia secrete increased levels pro-inflammatory cytokines upon activation with lipopolysaccharide (LPS) compared to controls, (Martens et al., 2012; Suh et al., 2012), suggesting that progranulin normally attenuates pro-inflammatory responses. Granulins, on the other hand, increase amounts of pro-inflammatory cytokines TNF-alpha and IL1-beta in human monocyte-derived macrophages (Okura et al., 2010; Zhu et al., 2002; Plowman et al., 1992).

Within the CNS, progranulin is mainly expressed by microglia and a subset of mature neurons, with high expression exhibited in the CA1, dentate fascia, and CA4 regions of the brain (Ahmed et al., 2007; Baker et al., 2006; Mackenzie et al., 2006; Almeida et al., 2011; Daniel et al., 2000). In addition, Hu et al. have demonstrated that progranulin is endocytosed at the surface of murine cortical neurons by a neuronal receptor, sortilin, and subsequently targeted to lysosomes (Hu et al., 2010). Sortilin is a member of the vacuolar protein sorting 10 protein (VPS10p) domain receptor family (Marcusson et al., 1994), and was first identified in a biochemical screen for orphan endocytic receptors in the human brain (Petersen et al., 1997). The same group later identified a novel interaction between progranulin and prosaposin. Prosaposin is the precursor of saposin peptides (A, B, C and D) that function as activators of lysosomal sphingolipid

metabolizing enzyme (Matsuda et al., 2007; O'Brien and Kishimoto, 1991; Qi and Grabowski, 2001). They found that prosaposin facilitates the lysosomal targeting of progranulin via mannose 6-phosphate receptor (M6PR) and low density lipo-protein receptor-related protein 1 (LRP1), as fibroblasts lacking prosaposin demonstrate loss of progranulin localization to lysosomes and increased secretion to the extracellular space. This prosaposin-mediated pathway is independent but complementary to the sortilin-mediated pathway (Zhou et al., 2015).

Initial investigations reveal that progranulin may play important roles within the CNS, including maintaining neuronal survival. First, neurons from *Grn* knockout mice exhibit decreased survival (Kleinberger et al., 2010). Secondly, exogenous administration of progranulin has been shown promote neuronal survival and to enhance neurite outgrowth in cell culture contexts (Gao et al., 2010; Van Damme et al., 2008). In addition, progranulin overexpression rescues TDP-43-induced axonopathy in zebrafish (Laird et al., 2010), although the mechanism of these neurotrophic effects remains unknown. Progranulin has been shown to be upregulated in the brain in response to infection (Johnston et al., 2001) and injury (Kanazawa et al., 2015; Tanaka et al., 2013). Its expression is also increased in activated microglia in neurodegenerative diseases such as Creutzfeldt-Jacob's and Alzheimer's (Baker et al., 2006; Pereson et al., 2009).

Recently, lentivirus-mediated progranulin overexpression was shown to decrease the plaque burden and abolish the loss of hippocampal neurons when injected in 5xFAD mice, an aggressive amyloid mouse model of familial Alzheimer's disease (Minami et al., 2014). Moreover, *Grn* ablation resulted in increased plaque load and impaired phagocytosis in microglia in APP_{low} mice, a model which expresses low levels of hAPP (Minami et al., 2014). Indeed, *reduced* progranulin may result in endolysosomal/autophagosomal disturbances. Notably, complete loss of progranulin through homozygous *GRN* deletion mutations (c.813_816del (p.Thr272Serfs*10)) found in a human sibling pair has been shown to result in adult-onset neuronal ceroid lipofuscinosis (NCL), a fatal neuronal lysosomal storage disease with progressive neuronal loss (Smith et al., 2012). These human findings complement prior findings in previous *Grn* knockout mouse models, which demonstrate lipofuscin accumulation, ubiquitin, and p62

protein aggregates, hallmarks of lysosomal dysregulation often found in lysosomal storage diseases (Ghoshal et al., 2012; Petkau et al., 2010; Wils et al., 2012; Ahmed et al., 2007). The data I present in Chapter 2 further implicates endolysosomal disturbances within the FTLD-TDP subgroup with *GRN* mutations, thus adding to the growing evidence that reduced progranulin is associated with alterations to endolysosomal pathways.

As mentioned above, disease-associated *GRN* mutations result in FTLD-TDP pathology in human brain (Neumann et al., 2006). The link between mutations in *GRN* and the accumulation of TDP-43 within the brain is one of the unresolved questions of research in FTLD. While the relationship between these two disease-related proteins is still not well understood, TDP-43 binds to the 3'UTR of *GRN* mRNA and decrease its stability with a subsequent decrease in progranulin protein levels (Polymenidou et al., 2011). In addition, knockdown of TDP-43 in mice results in an increase in *GRN* mRNA and also has been shown to lead to altered splicing of sortilin with associated increased levels of progranulin protein (Polymenidou et al., 2011; Colombrita et al., 2012).

Alterations in progranulin in turn appear to affect TDP-43. Knockdown of *GRN* has been shown to result in a caspase-dependent cleavage of TDP-43 into fragments in neuroglioma cells (Zhang et al., 2007). In addition, knockdown of *GRN* in neurons results in an increase of cytoplasmic TDP-43 as compared to nuclear TDP-43 (Guo et al., 2010). Thus, much future work will be needed to tease out the complex relationship between these two disease-related proteins.

1.1.5.4 *C9orf72*

More recently, noncoding hexanucleotide repeats with the sequence GGGGCC (G_4C_2) in the *C9orf72* gene have been found to be the *most common* genetic mutation in both ALS and FTLD, with *C9orf72*-associated FTLD brain exhibiting TDP-43 pathology (DeJesus-Hernandez et al., 2011; Renton et al., 2011; Beck et al., 2013). While healthy controls have <33 repeats, *C9orf72*-associated FTLD and ALS cases harbor expansions ranging from 800-4,400 repeats (van Blitterswijk et al., 2014; Beck et al., 2013).

Currently, several major mechanisms of pathogenesis for these *C9orf72* repeat expansions have been proposed: (1) gain of toxicity through a) formation of repeat RNA species (Fratta et al., 2012; Gendron et al., 2013; Lee et al., 2013; Mizielinska et al., 2013; Chew et al., 2015), or b) through dipeptide repeats that result from repeat-associated, non-ATG (RAN) translation (Ash et al., 2013; Mizielinska et al., 2014; Mori et al., 2013), and (2) reduced levels/loss of function of the normal *C9orf72* protein, the function of which is yet unknown (Ciura et al., 2013; O'Rourke et al., 2016; DeJesus-Hernandez et al., 2011; Gijssels et al., 2008; Renton et al., 2011; Therrien et al., 2013). It is certainly possible that all three contribute to disease pathogenesis, and current efforts are underway to determine each mechanism's contribution in this process.

(1) Gain of toxicity – RNA species and dipeptide repeats

The *C9orf72* repeat expansion has been proposed to result in toxic effects via formation of RNA species as well as via toxic dipeptide protein repeats. It has been demonstrated that the *C9orf72* GGGGCC (G_4C_2) repeat transcript, as well as the antisense CCCC GG (C_4G_2) transcript, accumulate in RNA foci; these RNA foci have been observed in the frontal cortex and spinal cord of patients as well as in patient-derived iPSCs; additionally, the number of foci has been shown to correlate with age-at-onset (DeJesus-Hernandez et al., 2011; Almeida et al., 2011; Donnelly et al., 2013; Gendron et al., 2013; Mizielinska et al., 2013; Zu et al., 2013). At the same time, the hexanucleotide repeat expansion in *C9orf72* exhibits repeat-associated non-ATG dependent translation (RAN translation). As the name implies, this RAN translation does not require an ATG codon and results in the generation of dipeptide repeat proteins (DPRs) (Ash et al., 2013; Mori et al., 2013). Interestingly, DPRs are generated from both the sense and antisense directions, producing glycine-alanine (GA), glycine-proline (GP), proline-alanine (PA), glycine-arginine (GR), and proline-arginine (PR) dipeptides, depending on reading frame. These DPRs have been found to accumulate in affected regions of the brain (Mori et al., 2013; Zu et al., 2013), as well as unaffected areas.

In a recent significant development supporting a role for gain of function in disease development, Chew et al. demonstrated that intracerebroventricular administration of an AAV vector expressing 66 GGGGCC repeats ((G₄C₂)₆₆) in postnatal day 0 mice, resulted in formation of nuclear RNA foci, ubiquitin-positive dipeptide repeat inclusions, and cortical neuron and cerebellar Purkinje cell loss (Chew et al., 2015). In addition, this was the first model to demonstrate significant TDP-43 aggregates, as these were seen in ~7-8% of cells in the cortex and hippocampus. The cells containing TDP-43 aggregates also always contained RNA foci. These pathological findings were accompanied by behavioral changes – specifically, at 6 months, compared to mice with only two G₄C₂ repeats, the (G₄C₂)₆₆ mice exhibited differences in the open field assay and also decreased latency to fall in rotarod testing, suggesting both social and motor impairment (Chew et al., 2015). Thus, this model is a significant step forward as it closely models disease, exhibiting the prominent pathological hallmark of disease, TDP-43 aggregates, as well as consistent behavioral changes. However, this model does not separate out the toxic effects of the nuclear RNA foci versus the dipeptide repeats, and, notably, ~75% of cells harboring RNA foci and TDP-43 aggregates also had dipeptide inclusions. Below I discuss additional evidence for each, RNA foci and dipeptide repeat proteins, in the pathogenesis of disease and highlight approaches that have been undertaken to try to separate out each of their pathogenic contributions.

1a) Evidence for RNA foci in disease

Several reports have identified co-localization of the *C9orf72*-associated RNA foci with RNA-binding proteins (RBPs), suggesting pathogenic sequestration of RBPs may be occurring (Fratta et al., 2012; Gendron et al., 2013; Lee et al., 2013). This sequestration of RBPs may disrupt RNA processing with downstream negative consequences for the cell. Intriguingly, one study demonstrated that RNA foci burden within the frontal cortex correlates with disease severity in patients with *C9orf72*-associated FTLD (Mizielinska et al., 2013). Another study demonstrated that degradation of these foci via antisense oligonucleotides (ASOs) results in correction of neurodegenerative characteristics in *C9orf72*-expansion ALS fibroblast lines from ALS patients

and in patient-derived induced pluripotent stem cell-differentiated neurons (iPSNs) (Donnelly et al., 2013). Specifically, these iPSNs exhibited intranuclear *C9orf72*-expansion RNA foci, sequestration of the RNA binding protein ADARB2, dysregulated gene expression, and increased susceptibility to glutamate-mediated excitotoxicity as compared to normal controls; these effects were all mitigated upon treatment with novel ASOs that targeted the *C9orf72* expansion sequence (Donnelly et al., 2013).

1b) Evidence for toxic dipeptide repeats (DPRs) in disease

The major evidence for a role of DPRs in neurodegeneration is as follows. 1) Mizielinska et al. reported that expression of DPRs, but not engineered repeat RNA incapable of translation (288 repeats of G₄C₂), resulted in degeneration of the eye in a *Drosophila* model, (Mizielinska et al., 2014), suggesting that the DPRs are the major contributors to disease. Arginine-rich dipeptides specifically (GR and PR) were sufficient to cause toxicity within the eyes and nervous systems of the flies; GA also resulted in mild toxicity at later stages, but the other DPRs did not exhibit toxic effects (Mizielinska et al., 2014). 2) The toxicity of arginine-rich dipeptides was also confirmed in non-neuronal mammalian cells by another group, as synthetic peptides were shown to bind to nucleoli and to impede multiple steps in RNA biogenesis (Kwon et al., 2014). 3) Wen et al. have recently shown that the arginine-rich dipeptide repeats, especially PR, are potently neurotoxic when expressed in rat cortical and motor neurons. In addition, they reported that induced motor neurons from *C9orf72*-associated ALS patients showed increased intranuclear PR aggregates and decreased survival as compared to controls (Wen et al., 2014). However, some have questioned the role of DPRs in disease as other investigators have found that DPRs rarely co-localize with TDP-43 pathology and neurodegeneration (Gomez-Deza et al., 2015; Gendron et al., 2013).

Overall, evidence is growing for toxic gain of function mechanisms for *C9orf72*, including mechanisms associated with DPRs, but questions remain. For example, why does there seem to be a disconnect between the brains areas that show regional vulnerability in human disease cases versus areas in which DPRs are most likely to develop in model organisms? More globally,

the relevance of cellular overexpression models to actual disease pathogenesis is a major ongoing question; these studies highlight the importance of directly comparing models with patient samples and fully characterizing the DPR-containing inclusions within patient samples.

1c) Evidence for RNA and DPRs in impaired nucleocytoplasmic transport

Finally, recent evidence has emerged associating the *C9orf72* expansion with impaired nucleocytoplasmic transport and should be discussed (Boeynaems et al., 2016; Freibaum et al., 2015; Jovicic et al., 2015; Zhang et al., 2015). Whether this is due to DPRs (Jovicic et al., 2015; Boeynaems et al., 2016), RNA (Zhang et al., 2015), or a combination of both (Freibaum et al., 2015) is currently unclear. With regards to the evidence for DPRs, Jovicic et al. performed an unbiased modifier screen in yeast that overexpressed PR, identifying genes that suppress or enhance PR's toxicity. This screen identified a striking enrichment in genes involved in nucleocytoplasmic transport, such as nuclear import proteins karyopherins, components of the nuclear pore, and regulators of the Ran GTPase cycle needed to power nuclear import (Jovicic et al., 2015). Building upon these data, Boeynaems et al. performed a targeted genetic modifier screen in a *Drosophila* model, assessing for suppression and enhancement of eye degeneration in flies expressing a 25 PR repeat construct in the eye. Notably, this *Drosophila* screen found that orthologs of the top yeast genes, including the gene encoding nuclear transport receptor transportin 1, were significant modifiers of DPR toxicity (Boeynaems et al., 2016).

Freibaum et al. also screened for modifiers of eye degeneration in a *C9orf72* expansion *Drosophila* model which exhibits both RNA foci formation as well as DPR production. Strikingly, this screen identified 18 genetic modifiers which also comprised components of the nuclear pore complex and nucleocytoplasmic transport factors (Freibaum et al., 2015). In addition, they identified a defect in RNA export in *Drosophila* cells containing the *C9orf72* expansion, and found similar RNA export deficits in aged iPSCs derived from patients with *C9orf72*-associated disease (Freibaum et al., 2015).

Finally, Zhang et al. demonstrated that a dominant gain-of-function mutant of *RanGAP*, an important regulator of nucleocytoplasmic transport, is one of the strongest suppressors of eye

degeneration in a *Drosophila* model (Xu et al., 2013), building upon their prior work that showed the *C9orf72* expansion binds to the RanGAP1 protein (the human orthologue of *Drosophila* RanGAP) (Donnelly et al., 2013). RanGAP1 was mislocalized in the presence of the *C9orf72* repeat, both in *Drosophila* as well as in *C9orf72* ALS patient brain tissue, appearing as puncta rather than the smooth perinuclear appearance seen in controls. Additionally, treating *C9orf72*-associated ALS iPSCs with antisense oligonucleotides targeted against the sense strand of *RanGAP1* reduced the RNA foci and mitigated the altered nuclear-cytoplasmic distribution of Ran GTPase, implicating sense *RanGAP1* RNA in nucleocytoplasmic transport defects.

Thus, these studies used a wide array of models and techniques, but all converged on nucleocytoplasmic transport as a pathway implicated in *C9orf72*-associated FTLD and ALS. Defects in nucleocytoplasmic transport may help explain why TDP-43, FUS, and other RNA binding proteins accumulate and are pathognomonic features in disease. While it still must be fully determined if it is the DPRs or the RNA that contribute primarily to the impairment in nucleocytoplasmic transport, it should be noted that DPR-expressing only models (Boeynaems et al., 2016; Jovicic et al., 2015) identified the same pathway (nucleocytoplasmic transport) as Freibaum's and Zhang's models, which harbor *both* RNA foci and DPRs (Freibaum et al., 2015; Zhang et al., 2015). This suggests that DPRs may be the primary players implicated in derangements in nucleocytoplasmic transport. In addition, Woerner et al. recently demonstrated that targeting aggregate species such as TDP-43 to the cytoplasm, as opposed to the nucleus, results in defects in nucleocytoplasmic transport, mislocalization of nuclear pore complex components, and inhibition in nuclear mRNA export; these data may suggest that the cytoplasmic DPR inclusions similarly are largely responsible for the impairments in nucleocytoplasmic transport (Woerner et al., 2016).

(2) Reduced levels of C9orf72 protein

Another potential mechanism by which hexanucleotide repeat expansions in *C9orf72* may contribute to disease pathogenesis – and one central to my hypothesis – is via decreased levels of the *C9orf72* protein. Indeed, decreased transcript levels of *C9orf72* are seen in the brain

tissues, lymphoblast cells, and induced pluripotent stem cell (iPSC)-derived neurons of patients with *C9orf72*-associated FTL and ALS (Ciura et al., 2013; DeJesus-Hernandez et al., 2011; Gijssels et al., 2012; Donnelly et al., 2013). Another study demonstrates decreased *C9orf72* protein expression in disease-affected frontal cortex (Waite et al., 2014).

The function of *C9orf72* is currently unknown, although it is predicted to be a DENN protein through sensitive homology searches (Levine et al., 2011; Zhang et al., 2012). Members of the DENN family (Differentially Expressed in Normal and Neoplastic cells) act as GDP-GTP exchange factors (GEFs) for Rab GTPases. Rab GTPases are a family of regulatory GTPases which act as molecular switches – cycling between a GTP-bound, membrane-bound active state, and a GDP-bound, cytosolic inactive state. As GEFs, DENN proteins thus play important roles in the regulation of membrane trafficking and autophagy (Zhang et al., 2012; Zerial and McBride, 2001). However, it has yet to be determined experimentally if *C9orf72* demonstrates GEF activity, and this protein's normal function and role in disease pathogenesis are open questions.

Current animal models have yielded conflicting data as to whether loss of *C9orf72* protein can result in disease-related phenotypes. First, knockdown of the zebrafish ortholog *zC9orf72* in zebrafish demonstrated axonal degeneration of motor neurons; this degeneration could be rescued by expression of human *C9orf72* mRNA (Ciura et al., 2013). In a similar vein, knockdown of the *C9orf72* orthologue in *C. elegans* also resulted in motility defects and degeneration of GABAergic motor neurons (Therrien et al., 2013). In contrast, a neuron-specific *C9orf72* knockout mouse model did not exhibit disease-like pathology – specifically, the mice did not have motor neuron degeneration, defects in motor function, or altered survival as compared to controls (Koppers et al., 2015). However, a recent study describes that while *C9orf72*^{-/-} mice showed no evidence of neurodegeneration through 17 months, macrophages and microglia from these mice exhibit evidence of impaired late endosomal to lysosomal trafficking, and this lysosomal perturbation was associated with pro-inflammatory states, with increased IL-6 and IL-1 β by qRT-PCR (O'Rourke et al., 2016). This raises the possibility that *C9orf72* plays a role in phagosomal maturation and immune responses in microglia, the former consistent with its putative role as a

GEF. O'Rourke et al. propose a model in which decreased *C9orf72* results in diminished ability of macrophages and microglia in clearing aggregated proteins, and suggest a dual-effect mechanism whereby the RNA foci and DPRs caused by the *C9orf72* expansion compounds with *C9orf72*-deficient dysfunctional microglia to result in neurodegeneration (O'Rourke et al., 2016).

This provides evidence that disease pathogenesis may, and likely does, involve interplay between both gain of toxicity and loss of function mechanisms. In normal brain, *C9orf72* transcription levels are found to be high in neuronal subtypes known to be affected in disease (Suzuki et al., 2013). Loss-of-function of the normal *C9orf72*, as a presumed DENN protein, could result in alterations to vesicular trafficking and endolysosomal/autophagosomal disturbances. This, coupled with the accumulation of ubiquitinated dipeptide aggregates and RNA-protein aggregates could further challenge the degradative machinery of the post-mitotic neuron, resulting in increased toxicity and neuronal cell death. Additionally, O'Rourke et al.'s data highlights the importance of considering the microenvironment – not just neuron, but the microglia and other cell types as well likely play a role in the development of disease.

1.1.6 Summary

In summary, mutations in *MAPT*, *GRN*, and *C9orf72* comprise the most common Mendelian causes of FTLN, with mutations in *C9orf72* and *GRN* resulting in FTLN-TDP pathology. However, there are other interesting, albeit rarer, causes of disease which give us further insight into potential cellular pathways and processes that are dysregulated in FTLN and lead us to postulate that *TMEM106B* could be involved in these processes. Below, I will introduce the endolysosomal and autophagosomal pathways, highlighting potential roles of genes/proteins in which rare genetic mutations can cause FTLN, and discuss the implications of dysregulation of these pathways in FTLN.

1.2 PART II: Introduction to the endolysosomal/autophagosomal network

As will be described in detail in Chapter 3, increased TMEM106B levels result in alterations to the endolysosomal/autophagosomal pathways. Additionally, mutations in *CHMP2B*, *VCP*, and *GRN* hint at disturbances within these pathways as a potential mechanism underlying FTLN pathogenesis. In the following pages, I will provide an overview of endolysosomal/autophagosomal pathways and their relevance to neurodegenerative diseases and to FTLN in particular.

The endosomal and autophagosomal pathways involve many converging steps and share common players; indeed, the lysosome lies at the convergence of these pathways, linking them together in a greater connected network (hereinafter referred to as the endolysosomal/autophagosomal network or pathway, as depicted in **Figure 1.3**). Endosomes, lysosomes, and autophagosomes are constantly docking, exchanging material, fusing and separating, working together to maintain homeostasis of the cell. Internalized cargo are targeted to endosomes, where they are directed towards their final destination. Autophagosomes sequester long-lived proteins and cellular organelles, targeting them for degradation; lysosomes help degrade these and other substrates, recycling metabolites and basic building blocks. Alterations in one subset of organelles often result in perturbations to the others, reflecting their interdependence (Settembre et al., 2013).

The importance of the endolysosomal/autophagosomal network in normal cellular function is highlighted by its dysregulation in disease. Indeed, altered endolysosomal/autophagosomal states have been shown to be associated with cancer, neurodegenerative diseases, autoimmunity, and infectious diseases (Huang and Klionsky, 2007; Levine et al., 2011; Shintani and Klionsky, 2004; Deretic et al., 2009). In neurodegeneration specifically, endolysosomal/autophagosomal dysfunction has been previously described in many adult-onset diseases, including Alzheimer's disease and Parkinson's disease (Nixon and Yang, 2011), as well as in primary lysosomal disorders. The endolysosomal/autolysosomal network and its dysregulation in neurodegeneration will be discussed in further detail below.

Figure 1.3:

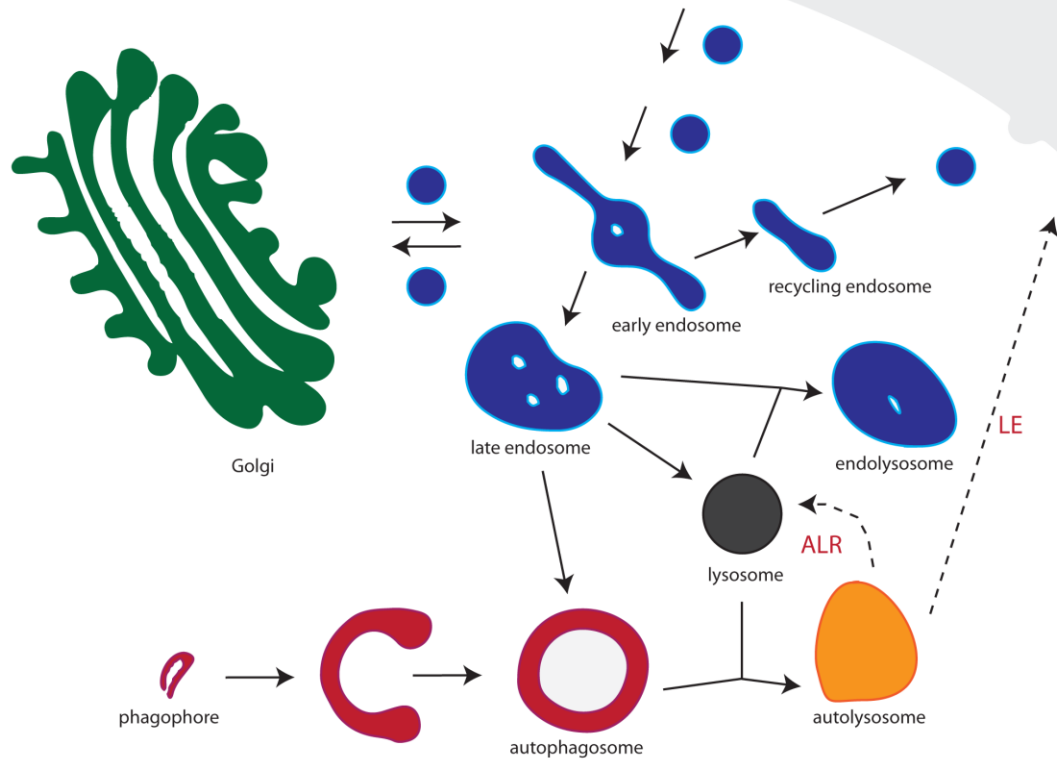


Figure 1.3: A simplified schematic of the endolysosomal / autophagosomal pathway

Lysosomes, depicted in dark gray, fuse with endosomes and autophagosomes, thus receiving incoming materials from both the endocytic and autophagic pathways. Endocytic substrates are delivered to early endosomes and then to late endosomes. Cargo destined for degradation are sorted into the intraluminal vesicles (ILVs) of late endosomes and are degraded upon lysosome fusion. The fusion of endosomes and lysosomes form endolysosomes (ELs), which are hybrid organelles that mediate much of degradation. Along the autophagic pathway, autophagosomes bind to lysosomes to form autolysosomes (ALs) or to endosomes to form amphisomes (not depicted). ALs and ELs themselves can exchange materials or fuse to form EL-AL hybrids. After degradation, lipids and other materials can be released into the extracellular environment via lysosomal exocytosis (LE). Following the completion of lysosomal degradation, autolysosomes undergo extensive tubulation, and protolysosomes are budded off these tubular autolysosomes to ultimately reform lysosomes during autophagic lysosomal reformation (ALR).

Adapted from (Tooze and Yoshimori, 2010).

1.2.1 Endosomes

The endosomal pathway involves the internalization and sorting of extracellular moieties, plasma membrane proteins, and membrane lipids. It is essential for cellular homeostasis, and is involved in myriad cellular processes including nutrient uptake, cell migration, control of signaling pathways, and establishment of cell polarity. Endocytic cargoes are internalized at the cell surface by a variety of different mechanisms, and most are ultimately delivered to early sorting endosomes. While clathrin-mediated endocytosis (Pearse and Robinson, 1990) is the best understood mechanism of endocytosis, other forms such as caveolin-mediated endocytosis, caveolin- and clathrin-independent endocytosis, macropinocytosis, and phagocytosis are becoming increasingly elucidated (Conner and Schmid, 2003). Early sorting endosomes comprise tubular and vacuolar domains and constitute the main site of cargo sorting – a highly complex and regulated process in which cargo are sorted and sent to the *trans*-Golgi network, to lysosomes for degradation, or are recycled back to the plasma membrane either directly or via distinct tubulovesicular recycling endosomes (Huotari and Helenius, 2011). For example, signaling receptors such as EGFR (Epidermal Growth Factor Receptor) can undergo endocytosis via clathrin-mediated or clathrin-independent routes; after this internalization, receptors can be recycled to the plasma membrane or, alternatively, targeted to the lysosome for degradation, thus terminating the receptor signaling pathway (Katzmann et al., 2001; Raiborg and Stenmark, 2009).

Another important endosomal function is the sorting of ubiquitinated proteins by endosomal sorting complexes required for transport (ESCRT complexes) (Katzmann et al., 2001). In this pathway, proteins are conjugated with a polyubiquitin chain or multiple mono-ubiquitins. The ESCRT complexes, of which there are four, ESCRT 0, I, II, and III, capture and sort the ubiquitinated proteins into inwardly-budded intraluminal vesicles (ILVs). These ILVs accumulate as early endosomes mature into late endosomes; the late endosomes ultimately fuse with lysosomes for subsequent degradation of their contents, including the protein and lipid contents of the ILVs (Raiborg and Stenmark, 2009).

Early endosomes mature along a continuum to become late endosomes, and, in doing so, accumulate an increased number of ILVs. Various features distinguish and indeed define early vs. late endosomes. For example, while early endosomes are weakly acidic with pH 6.8-5.9, late endosomes have a pH ranging from 6.0-4.9 (Yamashiro and Maxfield, 1987). The maturation process from early to late endosome also requires the switch from Rab5 GTPase to Rab7 GTPase at the limiting membrane (Rink et al., 2005). Rab GTPases are molecular switches that cycle between a GTP-bound, membrane-bound active state, and a GDP-bound, cytosolic inactive state. In addition, a proportion of PtdIns(3)P are converted to PtdIns(3,5)P(2) during the early endosome to late endosome maturation program (Schu et al., 1993; Behnia and Munro, 2005). Late endosomes are further characterized by a low buoyant density and a high negative surface charge. In addition, late endosomes are enriched for lysosomal transmembrane proteins such as LAMP1 as well as mannose-6-phosphate receptors (M6PRs) (Bayer et al., 1998; Falguieres et al., 2008). M6PRs bind lysosomal enzymes in the *trans*-Golgi network (TGN) and convey them to endosomes. Ultimately, fusion of endosomes with lysosomes results in the delivery of these resident lysosomal enzymes to the lysosome (Ghosh et al., 2003).

Endosomal cargo can be delivered to lysosomes by direct fusion or by “kiss and run” (Bright et al., 2005). “Kiss and run” involves a transient docking of late endosomes and lysosomes, during which small amounts of material are exchanged and then degraded within the lysosome. Alternatively, direct fusion between the endosomal and lysosomal membranes results in transient organelles termed endolysosomes (ELs) or hybrid organelles (Tjelle et al., 1996; Bright et al., 2005). The core machinery orchestrating the process of fusion between endosomes and lysosomes was elucidated using cell-free assays, which demonstrate that fusion undergoes three sequential steps: 1) tethering (the establishment of fine striations between the two organelles), 2) the formation of a trans-SNARE complex (composed of Syntaxin7, Vti1b, Syntaxin8 and VAMP7), and 3) membrane fusion. The presence of Rab7, N-ethylmaleimide-sensitive factor (NSF) as well as NSF-attachment proteins are also required (Luzio et al., 2007). Indeed, the Rab7 GTPase is a key regulator of the endolysosomal pathway, and is thought to

help mediate late endosome maturation, late endosome-lysosomal fusion, autophagosomal formation and autophagosomal-lysosomal fusion (Bucci et al., 2000; Vitelli et al., 1997).

Hybrid organelles formed from endosome-lysosomal fusion must subsequently disassociate to reform lysosomes. Preliminary research into this process of fission has demonstrated that this requires retrieval of membrane proteins and content condensation. In cell-free systems, it has been demonstrated that a proton-pumping ATPase and luminal Ca^{+2} are required for this lysosomal reformation (Luzio et al., 2007). Additionally, live-cell experiments have demonstrated that vesicular tubular structures bud off of hybrid organelles, presumably retrieving endosomal membrane proteins (Bright et al., 2005). A similar route of recovery may occur with autolysosomes (organelles formed from autophagosome-lysosome fusion), as autolysosomes have also been shown to extend tubular structures at sites concentrated with lysosomal hydrolases and lysosomal membrane proteins (Tjelle et al., 1996; Pryor et al., 2000; Yu et al., 2010; Bright et al., 2005). Further data on lysosomal reformation arising from autolysosomes, a process termed autophagic lysosomal reformation (ALR) will be discussed further below.

Along the various steps of the endolysosomal/autophagosomal pathway, Rab GTPases regulate membrane trafficking and vesicular transport within the cell, with different Rab GTPases localized to distinct organelles. This action of Rab GTPases helps to define and separate membranes and control spatial-temporal membrane trafficking events within the cell (Seabra and Wasmeier, 2004; Bock et al., 2001; Zerial and McBride, 2001). For example, Rab1 helps regulate transport from the endoplasmic reticulum to the Golgi; Rab5 regulates the vesicular trafficking of endocytosis (Zerial and McBride, 2001); Rab11 plays an important role in the regulation of endocytic recycling and exocytosis (Takahashi et al., 2012). As described above, Rab7 plays a major role at multiple steps of the pathway – late endosome-lysosome fusion, autophagosome-lysosome fusion, and autophagosome formation (Bucci et al., 2000; Meresse et al., 1995; Hyttinen et al., 2013). Control and proper regulation of Rab GTPase activity, and thus proper regulation of the endolysosomal pathway, are vital for proper neuronal function. Indeed,

mutations in *RAB7A*, which codes for Rab7, result in an autosomal dominant axonal neuropathy – Charcot-Marie-Tooth disease (Verhoeven et al., 2003). The disease-associated mutations target highly conserved residues on the surface of Rab7 and alter nucleotide exchange (BasuRay et al., 2010; Verhoeven et al., 2003). Additionally, dysregulation of DENN proteins has been shown to result in disturbed GEF activity linked to neurodegeneration (Azzedine et al., 2003; Del Villar and Miller, 2004; Hadano et al., 2010). Moreover, in Huntington's disease, an autosomal neurological disease caused by the expansion of a trinucleotide repeat in the gene encoding huntingtin (*htt*), mutant huntingtin has been shown to disrupt the association of Rab8 with the autophagy receptor optineurin at the Golgi, resulting in reduced AP-1 and clathrin-mediated trafficking to lysosomes (del Toro et al., 2009). These are a few examples that demonstrate that disruption of Rab GTPase activity can have consequences on proper regulation of the endolysosomal pathway and to the maintenance of neuronal health.

1.2.2 Lysosomes

Lysosomes are a central site of degradation for the cell, with cell and foreign material destined for degradation reaching the lysosome via endocytosis, phagocytosis, autophagy, or direct transport (Mijaljica et al., 2011; Mizushima et al., 2010). Lysosomes are acidic organelles containing hydrolases that degrade a vast variety of biological substrates; these hydrolases include proteases, glycosidases, phosphatases, lipases, nucleases, and sulfatases. Most soluble lysosomal enzymes are modified in the Golgi to generate terminal mannose-6-phosphate residues; these are recognized by mannose-6-phosphate receptors in the *trans*-Golgi network for targeting to late endosomes and ultimately to lysosomes. These enzymes are most active within the acidic environment of the lysosome, which is generated primarily by the vacuolar ATPase (vATPase). The vATPase is a large protein complex on the lysosomal membrane that pumps H⁺ ions into the lysosome (Yamashiro and Maxfield, 1987). Compared to endosomes, lysosomes are more electron-dense by electron microscopy, contain high levels of H⁺ and Ca²⁺, and are highly enriched in glycosylated transmembrane proteins such as LAMP1 and LAMP2 which help protect the lysosome from self-digestion (Luzio et al., 2007; Saftig and Klumperman, 2009).

In recent years, the lysosome has come to be appreciated beyond its role as a central site of degradation; data has demonstrated that the lysosome has myriad roles in a broad range of cellular processes, such as energy metabolism, the immune response, and cellular homeostasis (Settembre et al., 2013). For example, the mammalian target of rapamycin complex 1 (mTORC1) has been shown to recruit to the lysosomal membrane, in response to specific amino acid cues, where it encounters Rag GTPases that activate it (Sancak et al., 2010). mTORC1 is a master regulator of cell growth, positively regulating processes such as lipid biosynthesis and ATP production in response to factors such as growth factors, oxygen, and stress (Laplante and Sabatini, 2012). Inhibition of mTORC1 by starvation or drugs results in the activation of autophagy. Intriguingly, the binding of mTORC1 at the lysosomal membrane is dependent on accurate sensing of the luminal amino acid content, which is in turn dependent on the presence of the lysosome's vATPase, demonstrating the lysosome's nutrient-sensing role within the cell (Zoncu et al., 2011).

Further evidence for the interdependence of lysosomal and autophagy pathways comes from the recent finding that mTORC1 activation regulates the translocation of a master transcription factor, transcription factor EB (TFEB) (Roczniak-Ferguson et al., 2012). TFEB is a master regulator of lysosomal biogenesis and autophagy which regulates >400 genes belonging to the Coordinate Lysosomal Expression and Regulation (CLEAR) network (Settembre et al., 2011; Settembre et al., 2013; Sardiello et al., 2009). Under normal non-starvation conditions, mTORC1 inhibits the translocation of TFEB to the nucleus; however, when mTORC1 is inhibited by amino acid or glucose deprivation, TFEB translocates to the nucleus and upregulates the CLEAR network, increasing the transcription of genes involved in lysosomal biogenesis, autophagosome formation, the immune response, and lipid catabolism (Settembre et al., 2011; Palmieri et al., 2011). This results in the coordinated timing of autophagy activation and lysosomal biogenesis.

1.2.3 Autophagosomes and autophagy

Autophagy is the process by which cells sequester cytoplasmic cargo material into double-membraned organelles called autophagosomes; these cargoes are ultimately degraded upon fusion of the autophagosome with lysosomes (Mizushima et al., 2010). Autophagy is a complex process and is governed by AuTophagy-related (ATG) genes, the first of which were discovered in 1988 (Xie and Klionsky, 2007; Itakura and Mizushima, 2010; Mizushima et al., 1998). Autophagy functions within the cell to degrade material – cytoplasmic components, long-lived proteins, excess or aberrant organelles and pathogens – to allow cells to adapt to changes in the environment and external and internal stresses. Autophagy has also been shown to play role in development, immunity, and defense from pathogens (Melendez et al., 2003).

There are three major forms of autophagy – microautophagy, chaperone-mediated autophagy, and macroautophagy – all of which culminate in lysosomal degradation. In microautophagy, the lysosomal membrane invaginates, allowing small amounts of the cytoplasm into the lumen (Mijaljica et al., 2011). In chaperone-mediated autophagy, cytosolic proteins with consensus motifs are recognized by LAMP2A, a lysosomal transmembrane protein, and directly translocated across the lysosomal membrane (Cuervo and Dice, 2000). Macroautophagy, or simply “autophagy” from hereafter, is the most studied form of autophagy, and involves the formation of a double-membrane phagophore which elongates to completely surround cytoplasmic cargo material, forming the autophagosome (Mizushima et al., 2010). Selective forms of autophagy also exist, wherein specific substrates are targeted into the autophagosome by selective autophagy receptors. For example, mitophagy involves selective autophagy of dysfunctional mitochondria, whereas aggrephagy refers to the specific clearance of protein aggregates or inclusion bodies within the cell (Kopito, 2000).

The steps of autophagy are as follows: **1)** induction, **2)** substrate cargo recognition, **3)** isolation membrane (aka. phagophore) formation, **4)** double-membrane elongation, **5)** autophagosome maturation, **6)** fusion of the autophagosome with lysosomes/late endosomes to form autolysosomes/amphisomes respectively, **7)** degradation of the engulfed material, **8)** release

of the resulting macromolecules, and finally **9**) dissolution of the autolysosome/amphisome into its component parts with reformation of lysosomes (Chen and Yu, 2013; Klionsky et al., 2012).

Autophagy is initiated through phosphorylation state changes of components of the Atg1/Unc51-like kinase (ULK) complex (comprised of ULK1, ULK2, Atg13, FIP200 and Atg101) (Chan et al., 2009; Mizushima et al., 2010). Phosphorylation of ULK1 is mainly regulated by mTORC1, but can also be independently activated by the AMP-activated protein kinase (AMPK) (Mizushima et al., 2010). Stressors such as starvation, accumulation of protein aggregates, or hypoxia result in the inhibition of mTORC1 and its disassociation from the ULK complex; this results in the downstream activation of autophagy (Lamb et al., 2013).

ULK1 in turn then recruits and phosphorylates the class III phosphoinositide 3-kinase (PI3KC3) complex, resulting in its activation and relocation from the cytoskeleton to the isolation membrane in the ER, a pre-autophagosomal structure (Di Bartolomeo et al., 2010; Fimia et al., 2007; Suzuki et al., 2007). This PI3KC3 complex, consisting of, beclin-1, p150, and Atg14L, generates phosphatidylinositol 3-phosphate (Lu et al., 2013). The generation of PI3P is essential for autophagosome formation, as PI3P recruits PI3P-binding proteins called double FYVE-containing protein (DFCP1) and members of the WD-repeat protein interacting with phosphoinositides (WIPI) family, resulting in the formation of ER subdomains called omegasomes (Axe et al., 2008). WIPI proteins function as PI3P-binding effectors, mediating the downstream effects of PI3Ps, and bridging PI3P generation to the recruitment of microtubule-associated protein 1A/1B-light chain 3 (LC3) (Lamb et al., 2013).

The subsequent elongation step requires two ubiquitination-like conjugation systems, the LC3 and the Atg12-Atg5-Atg16L systems (He and Klionsky, 2009). The conjugation of phosphatidylethanolamine (PE) to LC3 is mediated by an E1-like enzyme, Atg7, and an E2-like enzyme, Atg3 (Shibutani and Yoshimori, 2014). Atg12 is covalently conjugated to Atg5 by Atg7 and the E2-like enzyme Atg10. Atg12-Atg5 then binds Atg16L (Fujita et al., 2009; Shibutani and Yoshimori, 2014). This Atg12-Atg5-Atg16L complex is recruited to the initiation site, possibly by a WIPI protein, and functions as an E3-like ligase on the LC3-PE conjugate to mediate the

lipidation of LC3 (Hanada et al., 2007; Dooley et al., 2014). LC3 itself is thought to be important for the closure of the autophagosome (Lamb et al., 2013). The full mechanism behind elongation and complete closure of the autophagosome is still under investigation, but is thought to involve several SNARE proteins, membrane components, and complexes containing ubiquitin-like proteins (Lamb et al., 2013).

1.2.3.1 Autophagosome-lysosome fusion

Autophagosomes can fuse with lysosomes, creating autolysosomes, or they can also fuse with endosomes, creating amphisomes which can also fuse with lysosomes downstream. Within the cell, lysosomes are predominantly located in the perinuclear region (Lee et al., 2011b; Roberts and Gorenstein, 1987). In neurons in particular, autophagosomes travel in a retrograde fashion towards the cell body, fusing first with the late endosomes predominant in the neuritic processes to create amphisomes (Hollenbeck, 1993; Larsen and Sulzer, 2002; Lee et al., 2011b). These amphisomes then fuse with the perinuclear lysosomes.

The mechanism underlying autophagosome-lysosome fusion has yet to be fully explicated, but multiple players have been shown to play a role in this process: Rab7, soluble *N*-ethylmaleimide-sensitive factor attachment protein receptors (SNAREs), the HOPS complex, the ESCRT-III complex, presenilin 1, UVRAG, p97VCP, LRRK2 and HSP70 to name a few (Lu et al., 2013; Gutierrez et al., 2004). Syntaxin-17 (STX17) was recently identified as the autophagosomal SNARE required for autophagosome-lysosome fusion (Itakura et al., 2012), as siRNA-mediated knockdown of syntaxin-17 resulted in a block in autophagic flux and a loss of co-localization between autophagosomal marker LC3 and late endosomal/lysosomal markers. Intriguingly, amphisomal and autolysosomal formation require many of the same players involved in the formation of late endosomes – the HOPS complex, and ESCRT components are involved in amphisomal formation (Lee and Gao, 2009; Rusten and Stenmark, 2009).

Following fusion of the autophagosome with lysosomes, the limiting membrane of the resulting autolysosome contains lysosomal membrane proteins and the vacuolar proton pump

vATPase. The cellular cargo and the inner membrane of the autophagosome are subsequently degraded by lysosomal hydrolases (Settembre et al., 2013).

1.2.3.2 Resolution of autophagy

The successful resolution of autophagy requires the lysosomal digestion of cargo and release of metabolites for reuse. It also requires the dissolution of autolysosomes/amphisomes and the reconstitution of the lysosomal pool. Recent evidence supports autophagic lysosomal reformation (ALR) as one potential process by which the lysosomal pool is renewed. In ALR, mTORC1, which is inhibited during autophagic induction, is reactivated after a delayed interval, and this reactivation is associated with the formation of tubules and protolysosomes which bud off of autolysosomes. These protolysosomes ultimately acidify and mature to become lysosomes (Yu et al., 2010; Chen and Yu, 2013). Since one autophagosome can fuse with multiple lysosomes, ALR is proposed to help maintain a pool of active lysosomes, as without a lysosomal “recycling” mechanism, the cell would soon be depleted of lysosomes. Another potential mechanism terminating the autolysosome is autolysosome exocytosis, whereby autolysosomal contents are exocytosed by fusion of the autolysosome to the plasma membrane. Recent evidence has demonstrated that if autophagosome-lysosome fusion or lysosomal acidification is impaired, autophagosomal exocytosis increases (Spampanato et al., 2013). In addition, this process may depend on TFEB, as increased expression of TFEB has been shown to result in increased exocytosis of vesicles labeled with lysosomal and autophagosomal markers (Ejlertskov et al., 2013; Martina et al., 2014; Medina et al., 2011; Spampanato et al., 2013).

Intriguingly, recent data indicates that ALR is dependent on the ability of the lysosome to degrade, as inhibition of lysosomal protease activity with leupeptin impaired mTORC1 reactivation and abolished ALR, resulting in the persistence of giant autolysosomes in rat kidney cells (Yu et al., 2010). Thus, it could be that the impairment in autolysosomal clearance seen in some neurodegenerative processes can result in the loss of mTORC1 reactivation, thereby impairing ALR and decreasing the number of available lysosomes. This could result in “stalled”

autolysosomes, as well as persistence of autophagosomes, as they have few lysosomes with which to fuse.

1.2.4 The endolysosomal/autophagosomal pathway in neurons and neurodegenerative diseases

1.2.4.1 Autophagy in neurons

Autophagic homeostasis is important for many cell types, but may be of the utmost importance for neurons. These post-mitotic cells rely heavily on the clearance mechanisms of autophagy and the degradative ability of the lysosome to help clear misfolded proteins, aggregates, and dysfunctional organelles, as they cannot clear these through cell division. In genetic murine models, knockout of essential autophagy *Atg* genes has been shown to result in severe neurodegeneration (Komatsu et al., 2005; Hara et al., 2006; Komatsu et al., 2006). Specifically, a knockout mouse model of *Atg7* within the central nervous system (*Atg7^{flox/flox}; nestin-Cre*) has been shown to result in dramatic neuronal loss in the cerebral and cerebellar cortices by postnatal day 56 (P56) with earlier onset (P14) motor and behavioral defects such as tremor and abnormal limb-clasping reflexes (Komatsu et al., 2005; Komatsu et al., 2006). Similarly, suppression of basal autophagy by knockout of *Atg5* in basal neural cells resulted in profound neurodegeneration and cytoplasmic inclusion bodies in mice (Hara et al., 2006).

The importance of autophagy to neurons is also demonstrated by human lysosomal storage diseases (LSDs). LSDs are rare inherited metabolic disorders wherein a defect in any one of functionally distinct lysosomal enzymes produces a severe neurodegenerative and multisystem phenotype with lysosomal/autophagosomal disruption evident by pathology (Pryor et al., 2000). These disorders are characterized by accumulation of undegraded material such as sphingolipids, glycoproteins, glycogen, and mucopolysaccharides within lysosomal structures, reflecting the primary enzymatic defect. How accumulation of these substrates ultimately results in cellular dysfunction and disease progression has yet to be fully understood. One possibility is that the lysosomal defect initially results in the accumulation of the undegraded substrate within the lysosome (primary storage); over time, this results in impaired overall lysosomal trafficking,

resulting in accumulation of additional lysosomal substrates (secondary storage), including dysfunctional mitochondria and polyubiquitinated proteins (Settembre et al., 2013; Settembre et al., 2008). These effects on lysosomal function feed forward to autophagy, as evidence demonstrates that many LSDs also exhibit autophagic impairment as well (Lieberman et al., 2012; Ballabio and Gieselmann, 2009). Examples of LSDs include neuronal ceroid lipofuscinoses (NCL), Gaucher's disease, and mucopolysaccharidosis IIA. In NCL, mutations in cathepsin D (*CTSD*), a typically ubiquitously expressed lysosomal protein, result in severe mental retardation or juvenile dementia (Siintola et al., 2006). In Gaucher's disease, mutations in glucocerebrosidase (*GBA*) result in impaired lysosomal hydrolysis and accumulation of sphingolipids (Sardi et al., 2011); patients with the neuronopathic type of Gaucher's typically present with progressive dementia at a young age. In mucopolysaccharidosis IIA, lysosomal sulfamidase mutations (*SGGH*) result in impaired autophagosome-lysosome fusion and patients often exhibit mental retardation (Settembre et al., 2008). Thus, these lysosomal storage diseases highlight the importance of proper lysosomal and autophagosomal function in neuronal populations.

1.2.4.2 Endolysosomal/autophagosomal dysfunction in adult neurodegenerative disease

These primary lysosomal disorders may be compared to adult onset neurodegenerative diseases, as endolysosomal and autophagosomal dysfunction has been demonstrated in multiple neurodegenerative diseases (Tresse et al., 2010; Urwin et al., 2010; Ginsberg et al., 2010; Harris and Rubinsztein, 2011), including Alzheimer's, Parkinson's, Huntington's, and FTLD.

In Parkinson's disease, mutations in genes encoding important endolysosomal/autophagosomal proteins have been shown to result in disease, and mutations in PD-associated genes with unclear functions have also been shown to result in endolysosomal/autophagosomal aberrations. For example, mutations in ATPase type 13A2 (*ATP13A2*), a component of the lysosomal acidification machinery, have been found in patients with hereditary parkinsonism (Williams et al., 2005). Fibroblasts derived from these patients exhibit defective clearance of autophagosomes and accumulation of α -synuclein (Usenovic et al.,

2012; Ramirez et al., 2006); additionally, these mutations result in decreased activity of lysosomal enzymes and reduced degradation of substrates (Dehay et al., 2012). Mutations in PINK (PTEN-induced putative kinase) and PARK2 (which encodes a component of the ubiquitin ligase complex) are also known Mendelian causes of Parkinson's disease and are associated with defective mitophagy (Geisler et al., 2010; Narendra et al., 2008; Valente et al., 2004). Additionally, mutations in VPS35, which encodes an endosomal protein involved in retrograde transport between endosomes and the *trans*-Golgi, have been shown to result in Parkinson's disease and result in decreased autophagosome biogenesis (Chartier-Harlin et al., 2011; Zimprich et al., 2011). Finally, missense mutations in leucine-rich repeat kinase 2 (*LRRK2*), which codes for a large protein called dardarin of uncertain function with functional GTPase and kinase domains, are the most common known genetic cause of Parkinson's disease (Hedrich et al., 2006). Disease-associated mutations have been shown to affect vesicular trafficking, autophagy, cytoskeletal function, and protein synthesis in both cell and animal models of Parkinson's (Martin et al., 2016; MacLeod et al., 2013).

In Alzheimer's disease (AD), most data suggesting a link to endolysosomal/autophagosomal dysfunction is more correlative. For example, affected brains from Alzheimer's patients as well as from animal models exhibit dystrophic neurites which contain accumulations of autophagosomes and autolysosomes (Lee et al., 2010; Nixon and Yang, 2011). Beclin-1, the mammalian ortholog of yeast Atg6 (Liang et al., 1998), has been shown to be decreased in AD patients and may be one of the initial signs of autophagic dysfunction in AD (Pickford et al., 2008). Abnormal upregulation of Rab GTPases, including Rab5 and Rab7, has been shown in cholinergic basal forebrain neurons microdissected from postmortem brains (Ginsberg et al., 2010) and, additionally, a genome-wide analysis shows transcriptional upregulation of autophagy-related genes in affected Alzheimer's brain (Lipinski et al., 2010), possibly indicating a compensatory mechanism in response to autophagic dysfunction. However, perhaps the strongest link between AD and lysosomal dysfunction comes from work with presenilin-1 (PS1). Mutations in *PSEN1* (presenilin 1) are one of the most common causes of

familial AD. It has been reported that loss of PS1 or AD-associated mutations in *PSEN1* result in impaired lysosomal acidification and degradative ability (Lee et al., 2010; Avrahami et al., 2013; Dobrowolski et al., 2012). In presenilin-1 knockout mouse blastocysts, Lee et al. reported defective clearance of autophagic vacuoles as well as defective lysosome acidification as measured by LysoTracker fluorescence (a pH sensitive dye whose intensity correlates with acidity). Lee et al. further provide evidence that loss of PS1 results in a failure of the V0a1 subunit of the vATPase to be properly N-glycosylated in the ER, resulting in impaired delivery of PS1 to autolysosomes and lysosomes (Lee et al., 2010).

In FTLD specifically, dysregulation of the endolysosomal/autophagosomal network has also been linked to disease. For example, mutations in the charged multivesicular body protein 2B (*CHMP2B*) gene are a known cause of disease. *CHMP2B* is a subunit of the ESCRT-III complex and plays a role in sorting ubiquitinated proteins into the intraluminal vesicles of late endosomes for ultimate degradation upon lysosomal fusion (Urwin et al., 2010; Filimonenko et al., 2007; Rusten and Stenmark, 2009; Katzmann et al., 2002). Disease-associated mutations in *CHMP2B* result in the deletion of the C-terminus of the protein (Urwin et al., 2010) and expression of these C-terminal deletion mutant *CHMP2Bs* in human neuroblastoma cells results in the formation of enlarged late endosomes (van der Zee et al., 2008). Furthermore, patient fibroblasts as well as cortical neurons also exhibit enlarged endosomes (Urwin et al., 2010). This defect was attributed to impairments of endosome-lysosome fusion, as late endosomes in *CHMP2B* mutant cells were defective in their ability to recruit the Rab7 GTPase, a key player in the fusion of endosomes-lysosomes and lysosomes-autophagosomes (Bucci et al., 2000; Hyttinen et al., 2013; Jager et al., 2004). Mutant *CHMP2B* thus disturbs endosomal and autophagic trafficking (Urwin et al., 2010; Filimonenko et al., 2007; Lee et al., 2007), intimating at a general role for endolysosomal/autophagosomal disturbances in the development of FTLD.

In addition, mutations in *VCP*, which encodes valosin-containing protein (*VCP*), also cause a familial form of FTLD. Specifically, these *VCP* mutations cause a dominantly inherited, multisystem degenerative disease that affects muscle, bone, and brain. *VCP* has been shown to

have a multitude of activities within the cell including cell-cycle regulation, DNA repair, organelle biogenesis, protein quality control, endolysosomal sorting, and autophagosome biogenesis and maturation (Ritz et al., 2011; Tresse et al., 2010; Ju et al., 2009; Braun et al., 2002). VCP is thought to be able to execute this variety of functions due to its N-terminal domain, which can interact with many different adaptor proteins. The conformation of this N-terminal domain is determined by the presence of ATP or ADP in the nucleotide binding pocket (Abramzon et al., 2012; Tang et al., 2010). FTLN-associated mutations alter the shape of the binding pocket, and this is thought to increase the interactions of VCP with some adaptors and decrease its interactions with others (Fernandez-Saiz and Buchberger, 2010).

Among its many functions, VCP has been shown to be essential for maturation of autophagosomes, as knockdown of VCP (or expression of dominant-negative VCP) results in the accumulation of immature autophagic vesicles (Tresse et al., 2010). FTLN-associated mutations in *VCP* have similarly been shown to interfere with and alter autophagosomal pathways, blocking transport of ubiquitinated cargo to lysosomes and also impairing the maturation of autophagosomes (Ju et al., 2009; Ritz et al., 2011). In addition, large LAMP1+/LAMP2+ vacuoles with accumulated LC3 and TDP-43 are seen in myoblasts of patients with VCP mutations (Ju et al., 2009; Tresse et al., 2010).

Mutations in *CHMP2B* and *VCP* thus intimate that dysregulation of endolysosomal/autophagosomal pathways may contribute to disease pathogenesis in FTLN.

1.2.5 Summary

Multiple lines of evidence are converging on dysregulation of the endolysosomal/autophagosomal network as a central common theme in neurodegenerative processes. Many neurodegenerative diseases exhibit impaired neuronal autophagy and accumulation of toxic proteins, with detrimental effects for cells. Proper lysosomal and autophagosomal function is vital to clear aggregates and maintain cellular homeostasis. This is of even more importance in the post-mitotic neuron, which cannot reduce the effects of damaged organelles or protein aggregates through cell division and must maintain cellular clearance and

recycling of proteins over long distances between the cell body and distal processes (Lee et al., 2011b).

1.3 PART III: TMEM106B

1.3.1 The discovery and initial characterization of TMEM106B

While the disease-associated mutations in *GRN*, *MAPT*, and *C9orf72* as described above account for most of the known Mendelian cases of FTLD, non-Mendelian patterns of inheritance often occur within families, suggesting that more common genetic variants conferring risk for FTLD exist (Sieben et al., 2012). In order to identify other risk factors for the most common neuropathological subtype of disease, FTLD-TDP, a genome-wide associate study (GWAS) was performed on 515 FTLD-TDP patients and 2,509 controls in 2010. Multiple SNPs within the minimally characterized gene *TMEM106B*, which codes for Transmembrane Protein 106B, at 7p21 were found to significantly associate with FTLD-TDP with and without *GRN* mutations (odds ratio 1.6, $p=1.08 \times 10^{-11}$ for top SNP rs1990622) (Van Deerlin et al., 2010). These SNPs are located within a 36-kb haplotype block that contains no other genes (Gallagher et al., 2014). The identification of the uncharacterized gene *TMEM106B* as a risk factor for FTLD-TDP has been replicated several times, including in a clinically diagnosed cohort of patients (Finch et al., 2011; van der Zee et al., 2011a). Interestingly, *TMEM106B* genotypes that increase risk for FTLD also increase the risk of dementia in ALS patients (Vass et al., 2011).

Prior to the discovery of its link to FTLD-TDP, little was known about *TMEM106B* or the 274 amino acid TMEM106B protein that it encodes (predicted molecular weight of 32 kDa). TMEM106B is conserved throughout vertebrates and has no yeast ortholog. It has 43% sequence identity with family member TMEM106A and 47% sequence identity TMEM106C, the functions of which are also both poorly understood. Since then, our laboratory and others have worked to characterize this protein. TMEM106B has been shown to be a highly glycosylated, Type II transmembrane protein which may exist as a homo- or hetero-dimer with TMEM106C (Chen-Plotkin et al., 2012; Lang et al., 2012; Stagi et al., 2014; Brady et al., 2013). Initial work from our laboratory was among the first to show that TMEM106B co-localizes with late endosomal/lysosomal marker LAMP1 as well as the pH-sensitive dyes LysoTracker and LysoSensor (Chen-Plotkin et al., 2012). Multiple investigators have independently confirmed the

late endosomal/lysosomal localization in multiple cell types with Brady et al. demonstrating that TMEM106B co-localized with the late endosomal/lysosomal protein Rab7, and did not co-localize with the early endosomal Rab GTPase, Rab5, or with recycling endosome marker Rab11 in N2a (mouse neuroblastoma) cells (Brady et al., 2013). The late endosomal/lysosomal localization of TMEM106B was subsequently also confirmed in mouse and rat primary cortical and hippocampal neurons by antibody immunofluorescence and expression of fluorescently tagged TMEM106B (Lang et al., 2012; Schwenk et al., 2014; Stagi et al., 2014). Furthermore, our laboratory and others have shown that TMEM106B does not co-localize with Golgi marker GM130, TDP-43, or synaptic vesicle markers (Schwenk et al., 2014; Brady et al., 2013; Chen-Plotkin et al., 2012). Additionally, initial work in the laboratory demonstrated that increased expression of TMEM106B by transient transfection in HEK293 and HeLa cells resulted in the striking appearance of enlarged, >2 μ m LAMP1+ organelles (Chen-Plotkin et al., 2012), an effect that was also later confirmed (Brady et al., 2013; Lang et al., 2012).

Building upon these initial discoveries by others within the laboratory, I undertook as my thesis project to provide an initial characterization of TMEM106B within cell biological and disease-associated contexts. In the following chapter, I provide the first report on the distribution of TMEM106B in normal as well as FTLD-TDP human brain. In Chapter 3, I address the cell biological sequelae of disease-relevant increased TMEM106B expression and the relationship of TMEM106B to C9orf72. Specifically, I will describe the perturbations to endolysosomal/autophagosomal pathways that occur with increased TMEM106B expression and discuss their implications for our understanding of disease development. Below I summarize some of our laboratory's initial data regarding TMEM106B, which formed the basis and rationale for my own subsequent investigations of this protein detailed in the following chapters. In particular, I will summarize data suggesting that increased TMEM106B expression may be linked to FTLD, and data suggesting specific mechanistic connections between TMEM106B and the FTLD-TDP-associated proteins progranulin and C9orf72.

1.3.2 Increased levels of TMEM106B are implicated in disease

Variants in *TMEM106B* likely increase disease risk by increasing levels of *TMEM106B* expression, suggesting that an underlying *cis*-acting genetic regulatory mechanism may explain the GWAS results (Van Deerlin et al., 2010). Data to support this claim are as follows.

First, risk genotypes at the GWAS-implicated SNPs are associated with higher expression levels in both lymphoblastoid cell lines and in human frontal cortex (Van Deerlin et al., 2010; Chen-Plotkin et al., 2012; Dixon et al., 2007). Second, *TMEM106B* mRNA levels were also found to be elevated >2.5x in FTLD-TDP cases versus controls, even after controlling for genotype (Van Deerlin et al., 2010; Chen-Plotkin et al., 2012). In brain, the highest levels of *TMEM106B* were displayed by FTLD-TDP cases harboring *GRN* mutations, the next highest in FTLD-TDP without *GRN* mutations, and the lowest levels were found in normal brain. This trend was found to be true in multiple areas of the brain, with the most striking differences seen in the frontal cortex (Chen-Plotkin et al., 2012). Third, we previously identified microRNA-132 (miR-132) in a global miRNA expression screen as the microRNA exhibiting the greatest difference between FTLD-TDP and controls ($p=0.0001$), with a 50% decrease seen in diseased brains. Intriguingly, we have shown that miR-132 targets the 3'UTR of *TMEM106B*, thus negatively regulating mRNA expression (Chen-Plotkin et al., 2012). Since miR-132 negatively regulates *TMEM106B*, the decreased levels of this miRNA seen in disease would be expected to result in overexpression of *TMEM106B*, again linking increased *TMEM106B* expression to disease states. Fourth, evidence also exists at the protein level for elevation of *TMEM106B* expression in disease, as we have shown that *TMEM106B* is elevated ~1.5x in *GRN*-associated FTLD-TDP frontal cortex by immunoblot (Chen-Plotkin et al., 2012). In addition, *TMEM106B* exhibits more intense immunohistochemical staining and is more widely distributed in the cytoplasm of neurons from FTLD-TDP brain, particularly in individuals with *GRN*-associated FTLD-TDP, than in normal or disease controls, suggesting higher levels (Chen-Plotkin et al., 2012; Busch et al., 2013; Gotzl et al., 2014). One report aimed at explaining these elevated levels of *TMEM106B* suggests that the coding variant rs3173615 (p.T185S), which is in linkage disequilibrium with the top GWAS SNP, exhibits differential degradation rates between the protective (S185) and risk (T185) isoforms

(Nicholson et al., 2013). The risk (T185) isoform is associated with higher steady state levels due to a slower protein degradation rate than the protective isoform. While this is at best a partial explanation (since differential protein degradation rates cannot explain the robust correlation observed between *TMEM106B* mRNA levels and *TMEM106B* genotypes in multiple expression quantitative trait loci datasets), it does indicate a growing convergence in the field on increased *TMEM106B* expression as a mechanism for increasing FTL-D-TDP risk.

Given these data, which together suggest that elevated *TMEM106B* levels may play a role in disease, I sought to characterize the effects of increased *TMEM106B* within the cell. The results of this investigation will be reported in Chapter 3.

1.3.3 *TMEM106B* and progranulin

Multiple lines of evidence suggest a relationship between *TMEM106B* and progranulin. First, the GWAS linking *TMEM106B* to FTL-D-TDP demonstrated that the top disease-associated SNP at the *TMEM106B* locus was more strongly associated with disease in the subset of *GRN*-associated FTL-D-TDP cases than in cases without *GRN* mutations (Van Deerlin et al., 2010); this association was subsequently replicated in an additional cohort of *GRN* mutation carriers (Finch et al., 2011). Additionally, *GRN*-mutation bearing patients who were also homozygotes for the risk allele of *TMEM106B* have a median age of onset thirteen years earlier than heterozygotes and homozygotes for the protective allele ($p=9.9 \times 10^{-7}$) (Cruchaga et al., 2011), suggesting a genetic modifier effect of *TMEM106B* on *GRN*. Finally, *TMEM106B* genotypes have also been found to correlate with plasma progranulin levels. Specifically, the major (risk) allele of the top SNP rs1990662 was associated with lower plasma progranulin levels in both normal controls and in *GRN*-associated FTL-D-TDP patients (Cruchaga et al., 2011; Finch et al., 2011).

Following up on this data, we and others have shown that *TMEM106B* and progranulin proteins co-localize within lysosomes within neurons and, furthermore, that overexpression of *TMEM106B* appears to increase intracellular levels of progranulin (Brady et al., 2013; Chen-Plotkin et al., 2012; Nicholson et al., 2013). In addition, in Chapter 2, I demonstrate that cortical neurons from *GRN* mutation-associated FTL-D-TDP human brain exhibit an altered distribution of

TMEM106B as compared to other subsets of FTLD pathology. Further investigation into a potential link between TMEM106B and progranulin is an ongoing area of active research, and I describe potential models on how these proteins may interact in the development of disease in the Discussion.

1.3.4 TMEM106B and C9orf72

In addition to TMEM106B's connection to progranulin, recent genetic evidence links *TMEM106B* to *C9orf72* as well (van Blitterswijk et al., 2014; Gallagher et al., 2014). Specifically, we have demonstrated that *TMEM106B* also acts as a genetic modifier in *C9orf72*-associated FTLD-TDP (Gallagher et al., 2014). Strikingly, the major allele of the SNP rs1990622, which associated with increased risk of FTLD-TDP by genome-wide association (Van Deerlin et al., 2010; van der Zee et al., 2011a; Finch et al., 2011) and with earlier age at disease onset in *GRN*-associated FTLD-TDP, also modulates the age at onset and age at death in *C9orf72*-associated FTLD cases from an international consortium. Building upon these genetic data, in Chapter 3, I present the first cell biological evidence that *C9orf72* and *TMEM106B* proteins may mechanistically interact within the cell, as the lysosomal effects induced by increased *TMEM106B* expression appear to be dependent on the presence of *C9orf72* protein, functionally implicating both players within the same pathway for the first time.

1.3.5 Summary

Finally, in the Discussion, I will frame my work in the context of the current understanding of FTLD and propose how risk genotypes in *TMEM106B* may contribute to disease pathogenesis. I will also propose potential models of how levels of *TMEM106B* could influence progranulin pathways; furthermore, I discuss the implications of our *C9orf72* data and what this suggests for *C9orf72*'s normal function within the cell as well as within disease.

CHAPTER 2: EXPRESSION OF TMEM106B IN NORMAL AND DISEASED HUMAN BRAIN

*This chapter has been adapted from the following manuscript: "Expression of TMEM106B, the frontotemporal lobar degeneration-associated protein, in normal and diseased human brain" by **Busch, J.I.**, Martinez-Lage, M.M., Ashbridge, E., Grossman, M., Van Deerlin, V.M., Hu, F., Lee, V.M.-Y., Trojanowski, J.Q., and Chen-Plotkin, A.S. in *Acta Neuropathologica Communications*.*

SUMMARY:

A recent genome-wide association study (GWAS) identified multiple SNPs within the *TMEM106B* gene that significantly associated with FTLD-TDP, suggesting that *TMEM106B* genotype confers risk for FTLD-TDP (Van Deerlin et al., 2010). *TMEM106B* expression levels, which correlate with *TMEM106B* genotype, may play a role in the pathogenesis of disease.

Given that little is known about *TMEM106B* and its expression in human brain, we performed immunohistochemical studies of *TMEM106B* in postmortem human brain samples from normal individuals, FTLD-TDP individuals with and without *GRN* mutations, and individuals with other neurodegenerative diseases. We find that *TMEM106B* protein is cytoplasmically expressed in both histopathologically affected and unaffected areas of the brain by neurons, glia, and perivascular cells (endothelial cells or pericytes). Furthermore, we demonstrate that *TMEM106B* expression may differ among neuronal subtypes. Finally, we show that *TMEM106B* neuronal expression is significantly more disorganized in FTLD-TDP cases with *GRN* mutations (*GRN*-associated FTLD-TDP) compared to normal and disease controls, including FTLD-TDP cases without *GRN* mutations (*GRN*-negative FTLD-TDP). Our data thus provide an initial neuropathological characterization of this newly discovered FTLD-TDP-associated protein and add to evidence that *TMEM106B* and progranulin are pathophysiologically linked in FTLD-TDP.

2.1 INTRODUCTION

Frontotemporal lobar degeneration (FTLD) is a fatal neurodegenerative disease characterized by selective degeneration of the frontal and temporal lobes (Neary et al., 2005; Ratnavalli et al., 2002). FTLD is neuropathologically classified into two major subtypes: FTLD-tau and FTLD-TDP (Chen-Plotkin et al., 2010; Mackenzie et al., 2009). FTLD-tau cases are characterized by abnormal accumulations of the microtubule-associated protein tau in neurons and glia (Mackenzie et al., 2009). In contrast, FTLD-TDP, the largest neuropathological subset of FTLD (45-60% of FTLD), is characterized by inclusions of hyperphosphorylated, ubiquitinated TAR DNA-binding protein 43 (TDP-43) (Neumann et al., 2006; Arai et al., 2006; Ling et al., 2013). Mutations in the gene *GRN*, which codes for a growth factor progranulin with neuroprotective effects (Van Damme et al., 2008; Gao et al., 2010) account for ~10% of FTLD-TDP (Gass et al., 2006; Baker et al., 2006; Cruts et al., 2006). The majority of these autosomal dominant mutations result in premature termination codons and thus progranulin haploinsufficiency (Cruts et al., 2006; Shankaran et al., 2008). In addition, expansions in the *C9orf72* gene have recently been shown to be an important Mendelian cause of FTLD-TDP (DeJesus-Hernandez et al., 2011; Renton et al., 2011). However, the majority of FTLD-TDP cases do not show clear Mendelian patterns of inheritance.

In order to identify additional genetic risk factors, we previously performed a genome-wide association study (GWAS) and identified multiple SNPs within the uncharacterized gene *TMEM106B* that significantly associated with FTLD-TDP (odds ratio 1.6, $p=1.08 \times 10^{-11}$ for top SNP rs1990622) (Van Deerlin et al., 2010). This association has been replicated in a clinically diagnosed cohort of patients (van der Zee et al., 2011b) and in a cohort of FTLD-TDP patients carrying *GRN* mutations (Nicholson et al., 2013). We and others have investigated the physiological (Lang et al., 2012; Brady et al., 2013; Chen-Plotkin et al., 2012) and pathophysiological (Finch et al., 2011; Cruchaga et al., 2011; Rutherford et al., 2012; Vass et al., 2011) function of *TMEM106B*. *TMEM106B* genetic variants may confer increased disease risk by increasing levels of *TMEM106B* expression, since mRNA expression levels of *TMEM106B* are

>2.5-fold higher in FTLD-TDP cases vs. controls (Van Deerlin et al., 2010), and are particularly increased in FTLD-TDP cases with *GRN* mutations (Chen-Plotkin et al., 2012). Moreover, *TMEM106B* risk genotypes have been associated with higher levels of *TMEM106B* expression in lymphoblastoid cell lines (Dixon et al., 2007) and in human brain tissue (Chen-Plotkin et al., 2012; Van Deerlin et al., 2010), suggesting that the variants found by GWAS tag a *cis*-acting mechanism for regulating *TMEM106B* expression. One possible mechanism was recently identified by Nicholson et al. (Nicholson et al., 2013), who demonstrated that differential isoforms at the coding SNP rs3173615 (p.T185S), which is in linkage disequilibrium with the GWAS SNP rs1990622, result in different rates of protein degradation. The risk (T185) isoform of *TMEM106B* is degraded less quickly than the protective (S185) form of *TMEM106B*. Together, these data suggest that *TMEM106B* variants resulting in higher levels of *TMEM106B* protein may increase disease risk.

Evidence further suggests that *TMEM106B* risk genotypes/increased *TMEM106B* expression may modulate disease risk by affecting progranulin pathways. For example, *TMEM106B* risk genotypes have been associated with decreased plasma progranulin levels (Finch et al., 2011), and significantly earlier onset of disease in *GRN* mutation carriers (Cruchaga et al., 2011). Moreover, *TMEM106B* has recently been described as localizing to late endosomes / lysosomes in multiple cell lines and in mouse primary cortical and hippocampal neurons where it co-localizes with progranulin (Chen-Plotkin et al., 2012; Nicholson et al., 2013; Brady et al., 2013; Lang et al., 2012). Intriguingly, expression of *TMEM106B* as compared to control results in increased intracellular progranulin (Chen-Plotkin et al., 2012; Brady et al., 2013; Nicholson et al., 2013), and changes progranulin's apparent subcellular compartmentalization as visualized by immunofluorescence microscopy (Chen-Plotkin et al., 2012).

While studies to date have established *TMEM106B* as an important risk factor for FTLD-TDP and implicated *TMEM106B* in progranulin pathways, many basic features of this protein -- including its expression patterns in human brain -- are largely unknown. To further characterize this novel disease-related protein, we investigate here the distribution and appearance of

TMEM106B in postmortem human brain samples from normal and disease controls, FTLD-TDP individuals with *GRN* mutations (hereinafter *GRN*-associated FTLD-TDP), and FTLD-TDP individuals without *GRN* mutations (*GRN*-negative FTLD-TDP). **Table 1** further details the cases and brain regions evaluated.

Table 1:

<u>Case</u>	<u>Brain Evaluated</u>	<u>Regions</u>	<u>Diagnosis</u>	<u>GRN mutation</u>	<u>Other mutation</u>	<u>Age</u>	<u>Gender</u>
1	frontal, hippocampal		AD			65	f
2	frontal		AD			87	m
3	frontal		AD			87	m
4	frontal		AD			70	f
5	frontal		AD			63	f
6	frontal		FTLD-tau			66	m
7	frontal		FTLD-tau			66	m
8	frontal		FTLD-tau			82	f
9	frontal		FTLD-tau			78	m
10	frontal		FTLD-tau			87	m
11	frontal		FTLD-tau			76	m
12	frontal, cerebellar, hippocampal, lentiform	occipital,	FTLD-TDP GRN (-)			49	f
13	frontal		FTLD-TDP GRN (-)			48	m
14	frontal		FTLD-TDP GRN (-)			53	m
15	frontal		FTLD-TDP GRN (-)			77	f
16	frontal		FTLD-TDP GRN (-)		<i>C9ORF72</i>	73	f
17	frontal, cerebellar, hippocampal, lentiform	occipital,	FTLD-TDP GRN (+)	c.1252C>T		62	f
18	frontal		FTLD-TDP GRN (+)	c.1477C>T		65	m
19	frontal		FTLD-TDP GRN (+)	c.348A>C		78	m
20	frontal		FTLD-TDP GRN (+)	c.1179+2T>C		61	m
21	frontal		FTLD-TDP GRN (+)	c.911G>A		78	f

22	frontal	FTLD-TDP GRN (+)	c.1252C>T	68	f
23	frontal	Normal		56	f
24	frontal	Normal		83	m
25	frontal	Normal		82	f
26	frontal	Normal		>90	f
27	frontal	Normal		55	f
28	frontal, cerebellar, hippocampal, lentiform	occipital, Normal		68	f
29	frontal, cerebellar, hippocampal, lentiform	occipital, Normal		85	f

Table 1: Characteristics of cases and brain regions evaluated for TMEM106B expression
GRN mutations were present in cases 17-22, as designated “FTLD-TDP GRN (+)” here. Nomenclature follows cDNA sequence NM_002087.2; all mutations are believed to be pathogenic (<http://www.molgen.ua.ac.be/admutations/>). Case 16 carries a *C9orf72* expansion -- this case was rated a “2” by both scorers for TMEM106B staining pattern. No cases had *MAPT* mutations. All FTLD-TDP cases were FTLD-TDP Type A cases.

2.2 RESULTS

2.2.1 TMEM106B expression by cell type in normal human brain tissue

We began by characterizing TMEM106B expression in normal human brain tissue. As shown in Figure 2.10, we found that TMEM106B is expressed in neurons, glia, and in cells surrounding blood vessels in frontal and occipital cortical samples from normal controls. Specifically, TMEM106B appears to be a cytoplasmic protein that assumes a polarized, perikaryal distribution in neurons (**Figure 2.1a**). Glial cells also demonstrate TMEM106B in an asymmetric, polarized pattern within the cytoplasm (**Figure 2.1b**). Finally, occasional robust TMEM106B immunoreactivity was observed perivascularly in endothelial cells or pericytes (**Figure 2.1c**). TMEM106B immunoreactivity in neurons and glia was observed throughout all layers of neocortex, with prominent expression in the pyramidal neurons of layers 3-5 (**Figure 2.2a**).

2.2.2 TMEM106B expression by brain region in normal human brain tissue

We next evaluated whether TMEM106B expression and appearance varies by brain region. In occipital cortex, a region of the brain relatively spared from TDP-43 pathology, neurons and glia had a similar perikaryal, cytoplasmic pattern of TMEM106B expression when compared to neurons and glia of frontal cortex, a brain region which typically displays a heavy burden of TDP-43 pathology (**Figure 2.2b and 2.2c**) (Geser et al., 2009).

In the hippocampus, however, whereas TMEM106B expression was clearly seen in the pyramidal neurons of Ammon's horn (**Figure 2.2d**), no significant staining of the dentate gyrus was observed (**Figure 2.2e**), suggesting neuronal subtype specificity of TMEM106B expression. Lentiform nucleus sections from normal controls showed minimal TMEM106B expression (**Figure 2.2f**); additionally, neurons of the nucleus basalis of Meynert had little to no staining (not pictured). In cerebellar sections, Purkinje cells demonstrated little TMEM106B expression (**Figure 2.2g**), and neurons of the granular layer did not stain for TMEM106B. In contrast, neurons of the deep cerebellar nuclei showed diffuse TMEM106B immunoreactivity with varying degrees of granularity (**Figure 2.2h**).

In summary, we observed variability in TMEM106B expression by neuronal subtype. However, TMEM106B expression did not demonstrate obvious differences in neocortical regions vulnerable to neurodegeneration, compared to those relatively resilient to neurodegeneration, in FTLD-TDP.

Figure 2.1:

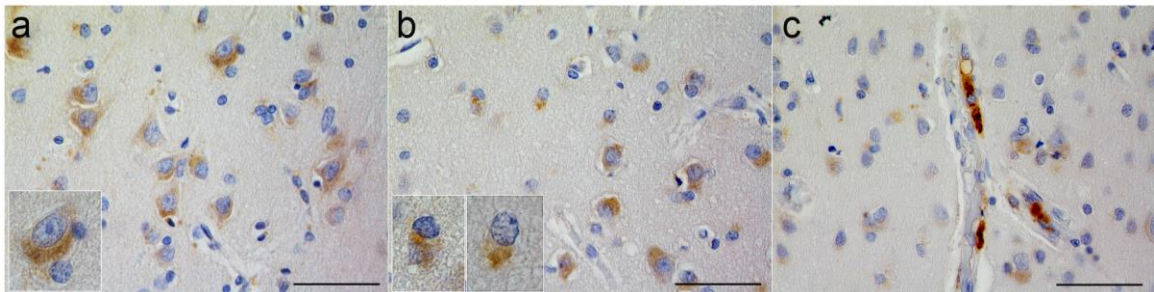


Figure 2.1: TMEM106B expression in neurons, glial and endothelial cells or pericytes in cortical specimens from normal controls

(a) Neuronal staining in cortices from normal human controls demonstrated a perikaryal, polarized cytoplasmic distribution mainly in the cell body and variably extending into processes.
(b) Glial distribution of TMEM106B similarly demonstrated an asymmetric cytoplasmic distribution.
(c) A subset of endothelial cells or pericytes demonstrated intense cytoplasmic expression of TMEM106B. Sections were stained with the anti-TMEM106B polyclonal antibody N2077.

Scale bar = 50 μ m.

Figure 2.2:

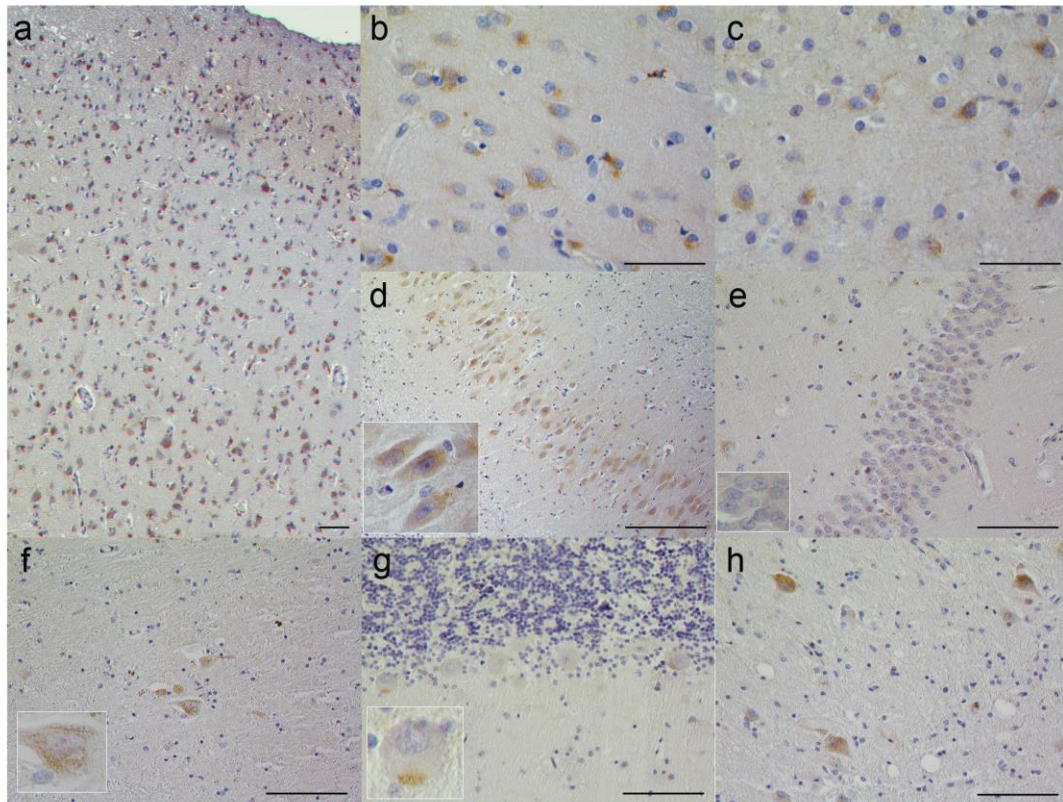


Figure 2.2: TMEM106B protein expression in brain tissue from normal controls

(a) TMEM106B protein expression in frontal cortex. TMEM106B protein expression is found throughout all layers of neocortex.

(b,c) TMEM106B neuronal and glial staining pattern is similar in both histopathologically affected areas of the brain (b, frontal cortex) and in areas of the brain that are relatively spared of TDP-43 pathology (c, occipital cortex).

(d, e) In the hippocampus, the pyramidal neurons of Ammon's horn show positive TMEM106B immunoreactivity (d), whereas those of the dentate gyrus do not (e).

(f) Lentiform nucleus sections demonstrated very rare neuronal staining.

(g) There was minimal staining of the Purkinje cells of the cerebellum; rarely, cells demonstrated a cytoplasmic, granular staining, as highlighted in the inset.

(h) Neurons of the deep cerebellar nuclei demonstrated diffuse cytoplasmic TMEM106B. Sections were stained with the anti-TMEM106B polyclonal antibody N2077.

Scale bar = 50 μ m.

2.2.3 TMEM106B expression in FTLD-TDP brain

Given the putative role of TMEM106B in FTLD-TDP, we stained frontal cortex, occipital cortex, cerebellar, hippocampal, and lentiform nucleus sections from individuals with *GRN*-associated FTLD-TDP, *GRN*-negative FTLD-TDP, and normal controls. In addition, we included FTLD-tau, and Alzheimer's disease (AD) brain samples as non-FTLD-TDP disease controls.

While FTLD-TDP is characterized by neuronal cytoplasmic inclusions (NCI) and (depending on histological subtype) neuronal intranuclear inclusions (NII) of TDP-43, these TDP-43-containing pathological inclusions did not contain TMEM106B. Furthermore, TMEM106B did not appear to form pathological inclusions of any type in the eleven FTLD-TDP cases investigated here. Comparing normal and disease-affected specimens, however, we noted greater variability in the appearance of TMEM106B cytoplasmic staining among the disease cases. Specifically, in neurons, cytoplasmic TMEM106B ranged from an organized perikaryal distribution to a disordered phenotype in which TMEM106B was expressed diffusely throughout the cell body and even extended into neuronal processes.

To further characterize these differences, we semi-quantitatively rated specimens based on their degree of apparent TMEM106B disorganization and loss of subcellular localization using an ordinal scale ranging from 0 (most polarized/organized) to 3 (most diffuse/disorganized). Specifically, two individuals blinded to disease status rated 29 frontal cortex samples for patterns of TMEM106B staining, as described in **Figure 2.3a** (normal controls n=7; AD n=5; FTLD-tau n=6, *GRN*-associated FTLD-TDP n=6, *GRN*-negative FTLD-TDP n=5).

Inter-rater reliability was moderately high (weighted kappa = 0.44). Moreover, as shown in **Figure 2.3b**, *GRN*-associated FTLD-TDP cases showed the most disorganized patterns of TMEM106B staining, with an average score (2.125) that was significantly greater when compared to all other cases (Mann-Whitney test, p=0.005). Moreover, while TMEM106B expression rarely extended into neuronal processes for normal controls, FTLD-tau, AD, or *GRN*-negative FTLD-TDP cases, in every *GRN*-associated FTLD-TDP case, we observed TMEM106B expression

extending into neuronal processes even in otherwise healthy-appearing neurons. Staining sections with a second TMEM106B antibody demonstrated similar results (**Figure 2.4**). Furthermore, TDP-43 pathology did not differ significantly between *GRN*-associated FTLD-TDP and *GRN*-negative FTLD-TDP cases (**Figure 2.4**). Of note, *GRN*-negative FTLD-TDP cases used in this study were matched by histopathological subtype to *GRN*-associated FTLD-TDP cases; all were FTLD-TDP Type A cases (Mackenzie et al., 2011).

Thus, TMEM106B expression differs significantly in frontal cortex neurons of *GRN*-associated FTLD-TDP brain. Specifically, in this genetic subtype, TMEM106B is diffusely expressed throughout the neuronal cytoplasm, with frequent extension into neuronal processes.

Figure 2.3:

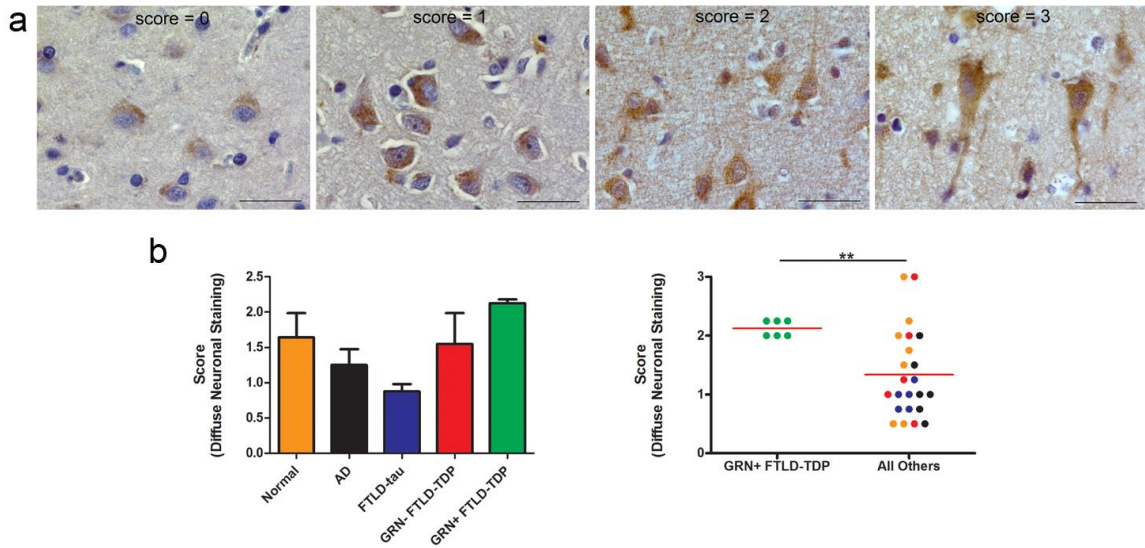


Figure 2.3: Scoring of neuronal TMEM106B protein expression

(a) Scoring schema used to grade severity of disorganization of neuronal TMEM106B expression. **Scores of 0** were assigned to sections in which almost all neurons displayed cytoplasmic TMEM106B expression with a vesicular pattern exhibiting a polarized quality. Nuclear boundaries were clear. **Scores of 1** were assigned to sections in which a sizeable number of neurons displayed more diffuse TMEM106B staining dispersed more widely in the cytoplasm, but still delimited to the soma. Polarity was still usually maintained. **Scores of 2** were assigned to sections in which most neurons recapitulated the characteristics of a score of 1. However, these sections also contained *rare*, non-degenerating neurons which displayed highly disorganized and diffuse TMEM106B staining throughout the cytoplasm with extension into processes. **Scores of 3** were assigned to sections in which *numerous* neurons displayed highly disorganized and diffuse TMEM106B staining, with extension into processes.

(b) Shown is the average scoring of the degree of diffuse neuronal TMEM106B expression by two independent, blinded scorers for N2077-stained human frontal cortical samples. Normal cases n=7; Alzheimer's disease n=5; FTLD-tau n=6, *GRN*-negative FTLD-TDP n=5, *GRN*-associated FTLD-TDP n=6. The colors in the dot plot correspond to the groups delineated in the bar graph. Weighted kappa = 0.44. *GRN*-associated FTLD-TDP cases demonstrated more disorganized patterns of TMEM106B expression ($p=0.005$ for Mann-Whitney test).

Scale bar = 30 μ m.

Figure 2.4:

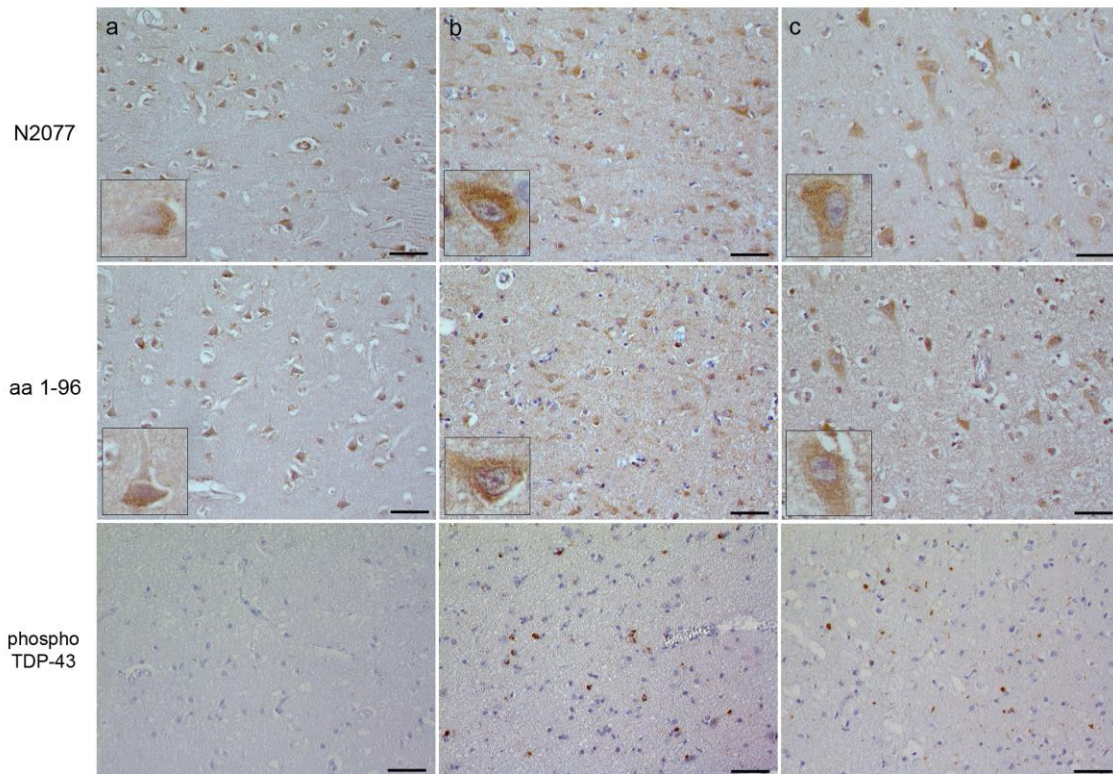


Figure 2.4: TMEM106B expression is more disorganized in neurons from *GRN*-associated FTLD-TDP cases, despite comparable levels of TDP-43 pathology

Representative frontal cortical sections from a normal control (a), *GRN*-negative FTLD-TDP (b), and *GRN*-associated FTLD-TDP (c). Both the N2077 antibody (top row) and a different polyclonal antibody (middle row) raised against the N-terminus (amino acids 1-96) of TMEM106B show similar patterns of immunoreactivity on serial sections from the same cases. *GRN*-associated FTLD-TDP cases showed more disorganized TMEM106B expression than *GRN*-negative FTLD-TDP cases, despite similar degrees of TDP-43 pathology, as indicated by staining against pathological, phosphorylated forms of TDP-43 (bottom row).

Scale bar = 50 μ m.

2.3 DISCUSSION

We have provided an initial characterization of TMEM106B protein expression in normal, *GRN*-negative FTLD-TDP, and *GRN*-associated FTLD-TDP human brain, as well as other neurodegenerative disease controls. We find that TMEM106B is normally expressed in the cytoplasm of neurons, glia, and perivascular endothelial cells or pericytes, although there may be differences based on neuronal subtype. Unlike many neurodegenerative disease-related proteins, TMEM106B does not form pathological inclusions in diseased brain. Instead, we show that neurons in *GRN*-associated FTLD-TDP cases exhibit more disorganized cytoplasmic TMEM106B expression than normal or disease controls. Specifically, TMEM106B expression in these cases demonstrates loss of polarity as well as subcellular compartmentalization.

We have recently shown that TMEM106B is localized to endosomes or lysosomes in immortalized cell lines and primary cortical neurons, with other investigators corroborating this finding (Brady et al., 2013; Chen-Plotkin et al., 2012; Lang et al., 2012; Nicholson et al., 2013). We note that the pattern of TMEM106B staining in normal human brain tissue is compatible with this subcellular localization as well, although further studies using double-label immunofluorescence would be needed to definitively demonstrate this.

The present finding that *GRN*-associated FTLD-TDP cases exhibit significantly different patterns of TMEM106B expression is intriguing. It is unlikely that this finding is due to neurodegeneration alone, since disease controls (FTLD-tau, AD) showed the least disorganization. Moreover, *GRN*-negative FTLD-TDP cases with similar patterns of TDP-43 pathology did not demonstrate TMEM106B expression extending into neuronal processes, suggesting that this effect is specific to the *GRN*-associated FTLD-TDP genetic subtype. We have previously shown that *GRN*-associated FTLD-TDP has a distinct global mRNA expression profile (Chen-Plotkin et al., 2008), suggesting that distinct pathophysiological mechanisms may exist in this molecularly defined subgroup. Moreover, recent evidence implicates TMEM106B in *GRN*-associated FTLD-TDP pathways. First, we have previously shown that TMEM106B may be expressed at higher levels in *GRN*-associated FTLD-TDP brain (Chen-Plotkin et al., 2012), which

is consistent with the histopathological pattern described here of TMEM106B expression throughout the neuronal cytoplasm in these genetic cases. Secondly, *TMEM106B* may act as a genetic modifier among *GRN* mutation carriers, influencing age at disease onset and levels of circulating progranulin (Cruchaga et al., 2011; Finch et al., 2011). Finally, we and others have recently demonstrated that overexpression of TMEM106B affects endolysosomal appearance and function as well as the distribution of progranulin in intracellular and extracellular compartments (Brady et al., 2013; Chen-Plotkin et al., 2012; Nicholson et al., 2013).

In this context, the current study provides further evidence of a relationship between TMEM106B and progranulin, although the directionality of this relationship is unclear. The observation that *GRN* mutation carriers exhibit disordered TMEM106B expression suggests that abnormalities in progranulin can influence TMEM106B expression patterns, whereas the TMEM106B overexpression studies suggest that TMEM106B levels affect progranulin. One possibility to reconcile these findings is that a feedback loop exists between TMEM106B and progranulin in the pathogenesis of FTLT-DTP. Additional studies to investigate this possibility would be a valuable addition to the data presented here.

Our current study has several limitations. First, our sample size of 29 cases may not adequately represent the full range of TMEM106B expression that might exist in a larger sample size. However, even with this small sample size, we were able to detect a significant difference in TMEM106B expression in *GRN*-associated FTLT-DTP. Second, the use of postmortem brain samples limits our ability to interpret the current finding, since non-specific effects due to postmortem interval, disease duration, cell loss and gliosis could confound our results. Finally, samples used here were not strictly age- and gender-matched among groups. However, the *GRN*-associated FTLT-DTP group did not differ significantly from the other groups in these respects (t-test $p=0.612$ for age comparison, chi-square $p=0.775$ for sex comparison), decreasing the possibility that these demographic variables may account for the observed effect.

In conclusion, we have provided the first histological characterization of TMEM106B expression in multiple regions of pathological and normal human brain. Our data add to the

growing body of evidence that TMEM106B and progranulin may be linked mechanistically in the pathogenesis of FTLD-TDP. Further characterization of this new FTLD-TDP risk factor, as well as its interactions with progranulin, may open up new avenues for the development of disease-modifying therapies.

2.4 MATERIALS AND METHODS

Brain samples:

Human postmortem brain samples were obtained from the University of Pennsylvania Center for Neurodegenerative Disease Brain Bank under IRB approval. These comprised samples from normal individuals (n=7), as well as individuals with FTLD-TDP (n=11), FTLD-tau (n=6), and Alzheimer's disease (AD, n=5). Regions sampled included midfrontal cortex, occipital cortex, cerebellum, lentiform nucleus, and hippocampus. See **Table 1** for full list of cases. Histopathological subtyping for FTLD-TDP was performed according to established criteria (Mackenzie et al., 2011). Genetic testing for *C9orf72* expansions, *GRN* mutations, and *MAPT* mutations was performed as previously described (Brettschneider et al., 2012; Van Deerlin et al., 2003). One FTLD-TDP case was found to harbor a *C9orf72* expansion – TMEM106B expression in this case did not appear atypical for the *GRN*-associated FTLD-TDP group. In addition, 6 FTLD-TDP cases had *GRN* mutations, and no cases had *MAPT* mutations.

Immunohistochemistry:

Formalin-fixed, paraffin-embedded 6 μm sections from various brain regions were cleared in a descending ethanol series then blocked with 3% H₂O₂/MeOH for 30 minutes. After washing, sections were immersed in Antigen Unmasking Solution (Vectashield) and microwaved 1x10 minutes at 50% power, then 2x6 minutes at 50% power. Slides were allowed to cool to room temperature, then washed with 0.1 M Tris buffer, pH 7.6 (Tris) for five minutes. Sections were blocked in Tris+ 2% FBS, pH 7.6 (Tris/FBS) for five minutes, before overnight incubation at 4°C with primary antibody. Specimens were immersed in Tris buffer x 5 minutes, followed by Tris/FBS x 5 minutes. Biotinylated goat anti-rabbit secondary antibody (Vectashield) was applied, and samples were incubated at room temperature in a humidified chamber for one hour. Samples were washed briefly in Tris. VECTASTAIN AB solution (Vector Labs) made up in Tris/FBS was applied to the samples and incubated for one hour at room temperature. Slides were then incubated with ImmPACT DAB solution (Vector Labs) for 2-8 minutes until desired stain intensity

was achieved. Specimens were rinsed briefly with Tris, followed by dH₂O and then counterstained with Harris' hematoxylin (Thermo-Shandon) for 10-30 seconds. Slides were washed in running tap water for 5 minutes. Coverslips were sealed with Cytoseal (Thermo Scientific) and slides were allowed to dry for at least one hour.

TMEM106B antibodies used in this manuscript included N2077, a previously validated (Chen-Plotkin et al., 2012) polyclonal rabbit antibody directed at amino acids 4–19 of TMEM106B (a peptide sequence specific to TMEM106B), used at 1ug/ml. A second polyclonal rabbit antibody raised against amino acids 1–96 of TMEM106B was also used at 1:750 to verify results; this second antibody has been previously validated as well (Brady et al., 2013). In addition, p409/410 anti-TDP-43 (phosphorylated at 409/410) was used at 1:500.

Semi-quantitative scoring of TMEM106B expression pattern in frontal cortical neurons:

Two independent, blinded observers (MML and ACP) scored stained specimens from normal controls (n=7), as well as from patients with Alzheimer's disease (n=5), FTLD-tau (n=6), *GRN*-associated FTLD-TDP (n=6), and *GRN*-negative FTLD-TDP (n=5), assessing for the nature and degree of neuronal staining. Specimens were assigned scores of 0-3 based on an ordinal scale representing increasing disorganization of staining pattern.

CHAPTER 3: INCREASED EXPRESSION OF THE FRONTOTEMPORAL DEMENTIA RISK FACTOR TMEM106B CAUSES C9ORF72-DEPENDENT ALTERATIONS IN LYSOSOMES

Portions of this chapter have been adapted from the following manuscript (submitted): "Increased expression of the frontotemporal dementia risk factor TMEM106B causes C9orf72-dependent alterations in lysosomes" by Busch, J.I., Unger, T.L., Jain, N., Skrinak, R.T., Charan, R.A., and Chen-Plotkin, A.S.

SUMMARY:

Frontotemporal lobar degeneration with TDP-43 inclusions (FTLD-TDP) is an important cause of dementia in individuals under age 65. Common variants in the *TMEM106B* gene were previously discovered by genome-wide association to confer genetic risk for FTLD-TDP ($p=1 \times 10^{-11}$, OR=1.6). Furthermore, *TMEM106B* may act as a genetic modifier affecting age at onset and age at death in the Mendelian subgroup of FTLD-TDP due to expansions of the *C9orf72* gene. Evidence suggests that *TMEM106B* variants increase risk for developing FTLD-TDP by increasing expression of Transmembrane Protein 106B (TMEM106B), a lysosomal protein. To further understand the functional role of TMEM106B in disease pathogenesis, we investigated the cell biological effects of increased TMEM106B expression. Here, we report that increased TMEM106B expression results in the appearance of a vacuolar phenotype in multiple cell types, including neurons. Concomitant with the development of this vacuolar phenotype, cells over-expressing TMEM106B exhibit impaired lysosomal acidification and degradative function, as well as increased cytotoxicity. We further identify a potential lysosomal sorting motif for TMEM106B and demonstrate that abrogation of sorting to lysosomes rescues TMEM106B-induced defects. Finally, we show that TMEM106B-induced defects are dependent on the presence of *C9orf72*, as knockdown of *C9orf72* also rescues these defects. In sum, our results suggest that TMEM106B exerts its effects on FTLD-TDP disease risk through alterations in lysosomal pathways. Furthermore, TMEM106B and *C9orf72* may interact in FTLD-TDP pathophysiology.

3.1 INTRODUCTION

Frontotemporal lobar degeneration (FTLD) is a leading cause of presenile dementia (Neary et al., 2005; Ratnavalli et al., 2002). The most common neuropathological subtype of disease, FTLD-TDP, is characterized by inclusions of TAR DNA-binding protein of 43 kDa (TDP-43) (Baborie et al., 2011). Two of the major Mendelian causes of FTLD-TDP have been identified as 1) non-coding hexanucleotide repeat expansions in *C9orf72* (DeJesus-Hernandez et al., 2011; Renton et al., 2011) and 2) haploinsufficiency mutations in *GRN*, which encodes the growth factor progranulin (Baker et al., 2006; Gass et al., 2006; Cruts et al., 2006). In addition, a recent genome-wide association study (GWAS) (Van Deerlin et al., 2010) revealed multiple common variants in the largely uncharacterized gene *TMEM106B* that significantly associated with FTLD-TDP ($p=1 \times 10^{-11}$, OR=1.6).

In addition to acting as a genetic risk factor for FTLD-TDP, *TMEM106B* has also been shown to act as a genetic modifier in both *GRN* mutation-associated FTLD-TDP (Cruchaga et al., 2011) and *C9orf72* expansion-associated FTLD-TDP (van Blitterswijk et al., 2014; Gallagher et al., 2014), affecting age at onset of disease and age at death. Moreover, while genotypes at *TMEM106B* do not appear to confer risk for development of amyotrophic lateral sclerosis (ALS), another disease defined by TDP-43 proteinopathy (Chen-Plotkin et al., 2010), *TMEM106B* variants associated with increased FTLD-TDP risk correlate with development of dementia in ALS (Vass et al., 2011). Most recently, *TMEM106B* variants associated with increased FTLD-TDP risk have been reported to correlate with increased burden of TDP-43 proteinopathy in aged individuals without overt clinical FTLD (Yu et al., 2015).

Since its initial discovery as an FTLD-TDP risk factor, *TMEM106B* has been characterized as a Type II transmembrane protein localized to late endosomes/lysosomes (Stagi et al., 2014; Schwenk et al., 2007; Lang et al., 2012), with widespread expression in human brain (Busch et al., 2013). Recent data suggests that *TMEM106B* regulates lysosomal transport in neurons, with knockdown of *TMEM106B* resulting in increased retrograde lysosomal transport in

one report (Schwenk et al., 2007) and increased bidirectional transport in another report (Stagi et al., 2014). TMEM106B has also been demonstrated to affect lysosomal size, acidification, and degradative capacity in immortalized cell lines (Stagi et al., 2014; Brady et al., 2013; Chen-Plotkin et al., 2012), and lysosomal size and number in neurons (Stagi et al., 2014).

While functional characterization of FTLD-TDP-associated genetic variants at *TMEM106B* remains incomplete, we and others have demonstrated that *TMEM106B* genotypes associated with disease also correlate with increased TMEM106B expression (Chen-Plotkin et al., 2012; Van Deerlin et al., 2010; Nicholson et al., 2013; Yu et al., 2015). To further understand the contribution of TMEM106B to FTLD-TDP disease pathogenesis, we investigated the cell biological effects of disease-associated increases in TMEM106B expression.

3.2 RESULTS

3.2.1 Increased expression of TMEM106B in results in altered endolysosomal morphology

We (Chen-Plotkin et al., 2012) and others (Brady et al., 2013) have previously shown that increased expression of TMEM106B results in enlargement of organelles positive for the lysosomal marker LAMP1 in immortalized cells. By live cell imaging, we confirmed this effect of increased TMEM106B expression, using a GFP-tagged TMEM106B construct (Brady et al., 2013). These enlarged organelles were readily visible by brightfield imaging and did not occur with increased expression of another lysosomal protein, LAMP1 (**Figure 3.1a**).

We next extended our investigations of TMEM106B overexpression to neurons. As shown in **Figure 3.1b**, primary mouse hippocampal neurons overexpressing TMEM106B also exhibited multiple, enlarged vacuolar structures $>2\text{-}3\mu\text{m}$ in size in the cell body and extending into processes. In contrast, overexpression of LAMP1 in neurons did not result in the appearance of these enlarged vacuolar structures (**Figure 3.1c**). These enlarged vacuoles appeared within a day post-nucleofection and were observed in both hippocampal and cortical neurons (data not shown). Mirroring our prior results in immortalized cell lines (Chen-Plotkin et al., 2012), these vacuoles were positive for both TMEM106B itself and for LAMP1, which co-localized with TMEM106B at the limiting membrane of these vacuoles. Indeed, the average size of LAMP1+ organelles in neurons overexpressing TMEM106B was $\sim 50\%$ larger than a control non-overexpressing condition (**Figure 3.1d**). Moreover, vacuoles were also negative for EEA-1, a marker of early endosomes, and SV2, a marker of synaptic vesicles; neither of these markers demonstrated strong co-localization with TMEM106B (**Figure 3.2a, b**).

Figure 3.1:

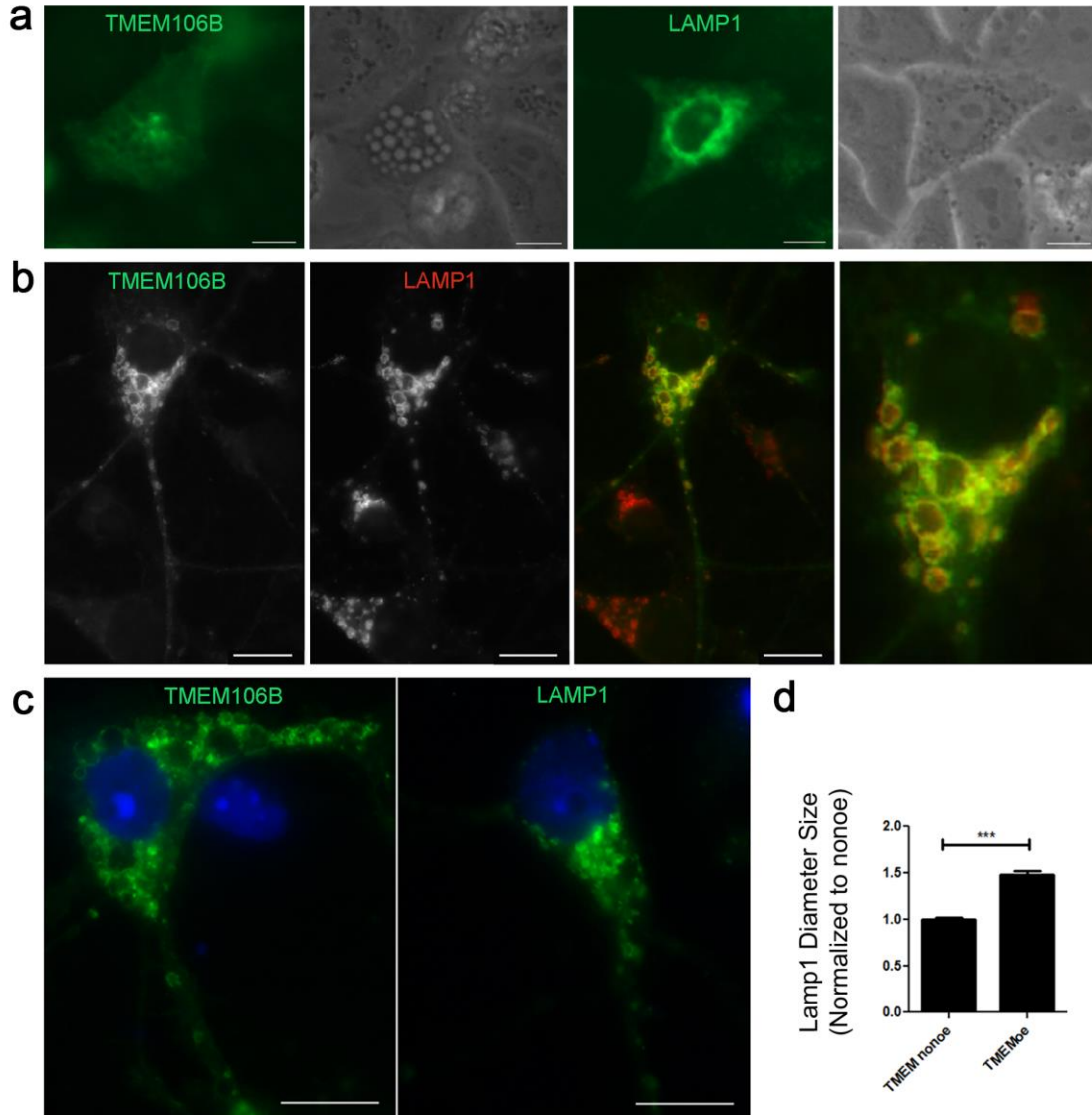


Figure 3.1: Increased expression of TMEM106B alters endolysosomal morphology

(a) Live image of HeLa cells transfected with GFP-TMEM106B or GFP-LAMP1. Expression of TMEM106B resulted in the appearance of enlarged vacuolar structures (left) visible by fluorescence or brightfield microscopy. This phenotype was not observed upon expression of GFP-LAMP1, another transmembrane lysosomal protein (right).

(b) In primary mouse hippocampal neurons nucleofected with GFP-TMEM106B, the enlarged vacuolar structures demonstrate co-localization of TMEM106B (green) and the lysosomal marker LAMP1 (red). The two right panels show the merged images, which are shown in monochrome in the first and second panels. Scale bar for images excluding magnified right panel = 10 μ m.

(c) Primary mouse hippocampal neurons nucleofected with GFP-TMEM106B exhibited enlarged >2 - 3 μ m vacuolar structures (left), whereas GFP-LAMP1-expressing neurons did not (right).

(d) The diameter of LAMP1+ organelles in TMEM106B overexpressing neurons is significantly larger than that of neighboring neurons not overexpressing TMEM106B. $p < 0.001$ for four replicate experiments.

Scale bar = 10 μm .

*** $p < 0.001$.

Figure 3.2:

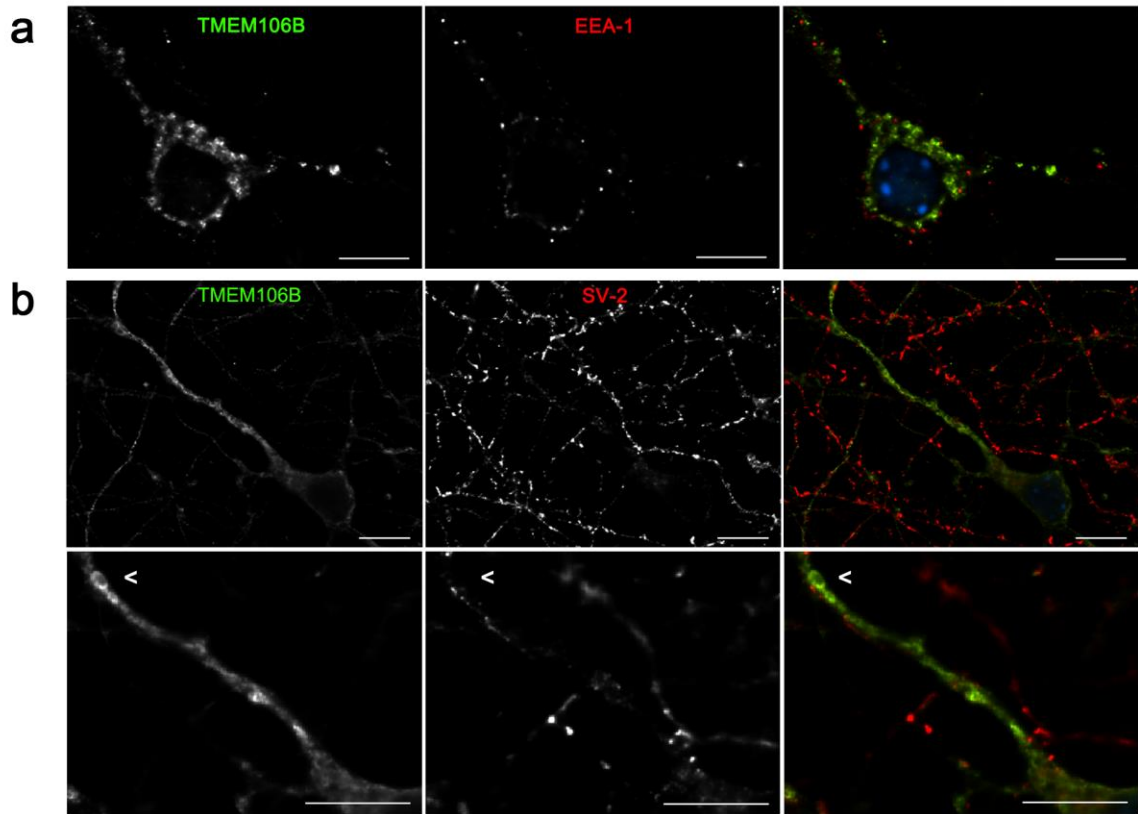


Figure 3.2: TMEM106B does not co-localize with EEA-1 and SV-2

(a) Primary mouse hippocampal neurons nucleofected with FLAG-TMEM106B and immunofluorescently labeled with N2077 (green) and early endosomal marker EEA-1 (red); individual channels are shown in monochrome in left and middle panels with the merged channels shown on the right. Little co-localization was seen between TMEM106B and EEA-1.

(b) Primary mouse hippocampal neurons nucleofected with GFP-TMEM106B (green) and labeled with synaptic vesicle marker SV-2 (red). Minimal co-localization was noted between TMEM106B+ organelles and SV-2 in GFP-TMEM106B+ neurons. In the top and bottom panels, GFP-TMEM106B (green) is shown in monochrome in the left panel, while SV-2 (red) is shown in the middle panel; merged channels are shown on the right. The bottom panel provides a higher magnification view of TMEM106B+ organelles along the axon.

Scale bar = 10 μ m.

To better characterize these enlarged LAMP1+ TMEM106B+ organelles, we performed ultrastructural analyses by electron microscopy. Exogenous expression of empty vector, GFP, or LAMP1 resulted in no notable changes in ultrastructure (data not shown). However, in HeLa cells (**Figure 3.3a, b**), COS-7 cells (**Figure 3.3c**), HEK293 cells (**Figure 3.3d**), and DIV7 mouse hippocampal neurons (**Figure 3.3e, f**), expression of TMEM106B resulted in the appearance of a striking vacuolar phenotype. Specifically, TMEM106B overexpressing cells contained multiple enlarged, electron-lucent, single-membrane-delimited cytoplasmic organelles >2 μ m in diameter. These enlarged organelles often appeared largely empty, although at times they contained multilamellar structures and cytoplasmic material or organelles in varying states of degradation. In addition, smaller organelles resembling intraluminal vesicles (ILVs) were also observed within a subset of the enlarged vacuoles (**arrows**), as seen in late autophagic vacuoles (amphisomes and autolysosomes) and late endosomes. Because of the “empty” appearance of some of these vacuoles, we investigated the possibility that they could be lipid droplets. However, immunofluorescence microscopy in HeLa cells demonstrated that these enlarged vacuoles were negative for BODIPY 493/503, which labels neutral lipids (**Figure 3.3g**).

We next quantified this ultrastructural phenotype in both HeLas and primary neurons. Because TMEM106B was overexpressed in cells by transient transfection or nucleofection, not all cells overexpressed TMEM106B. Thus, we enriched for TMEM106B-expressing cells by expressing GFP-TMEM106B and sorting into GFP-positive and GFP-negative populations using flow cytometry (**Figure 3.4**). In GFP-positive TMEM106B-transfected HeLa cells, 26% (26/100) exhibited enlarged vacuoles >1 μ m in diameter. In the corresponding GFP-negative population (cells which presumably express little or no TMEM106B), only 4% (4/100) displayed this phenotype ($p < 0.001$, Fisher exact test). As GFP sorting of nucleofected neurons was complicated by cell death, we could not similarly confine our quantitative analyses to neurons with confirmed GFP-TMEM106B expression. However, 22% (11/50) of the total primary hippocampal neurons nucleofected with TMEM106B exhibited the enlarged organelles, whereas only 2% (1/50) of GFP-LAMP1-nucleofected neurons did ($p = 0.004$, Fisher exact test).

Figure 3.3:

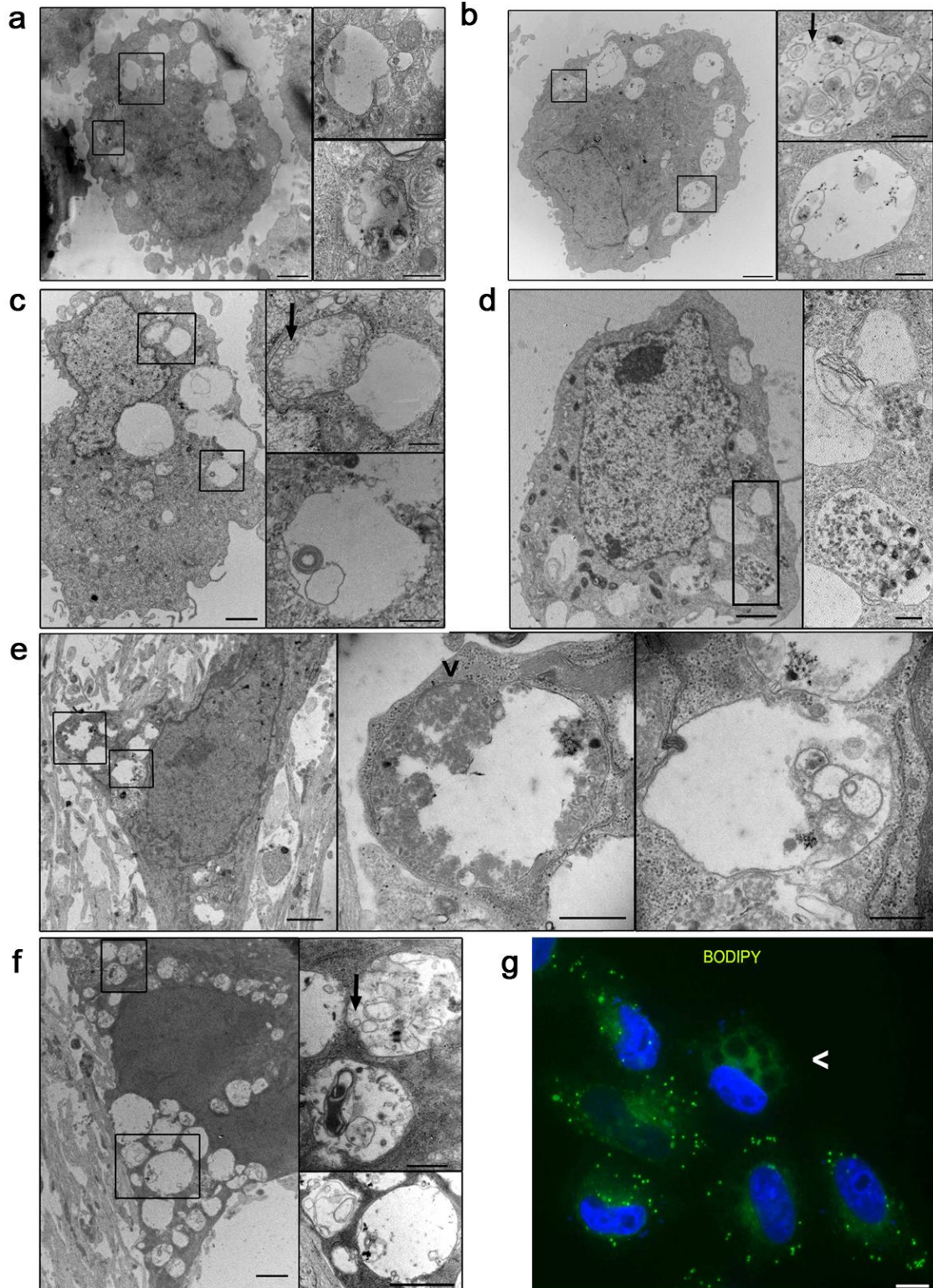


Figure 3.3: Ultrastructural characterization of TMEM106B-induced vacuolar phenotype

(a, b) HeLa cells transfected with TMEM106B exhibit multiple large electron-lucent, single-membraned organelles. These organelles often contain cytosolic components in varying states of degradation and multilamellar structures (see insets), an ultrastructural phenotype consistent with late autophagic vacuoles (autolysosomes or amphisomes).

(c) COS-7 cells transfected with TMEM106B also display a similar phenotype, with intraluminal vesicles (ILVs, arrow) and multilamellar structures within the enlarged vacuoles (see insets).

(d) HEK293 cells transfected with TMEM106B also display the enlarged vacuoles, some containing components in varying states of degradation (see inset).

(e, f) Primary mouse hippocampal neurons nucleofected with TMEM106B display the same ultrastructural phenotype. The organelle depicted in the middle panel of (e) demonstrates a small area of still visible double membrane (arrowhead), consistent with identification as a late autophagic vacuole (double membrane-autophagosome fusing with a lysosome, resulting in degradation of the inner membrane). Occasional internal ILVs are similarly noted as well (arrow in top inset for (f)).

(g) HeLa cells transfected with TMEM106B demonstrate the same vacuolar appearance (arrowhead) seen by electron microscopy when visualized by fluorescence microscopy. Vacuoles do not stain with BODIPY 493/503, as would be expected with lipid droplets.

Scale bar = 2 μ m for the lower-power view, and 0.5 μ m for the insets in electron microscopy. Scale bar = 10 μ m for BODIPY panel.

e, f imaged by R. Tyler Skrinak.

Figure 3.4: Flow cytometry of GFP-TMEM106B-transfected HeLa cells

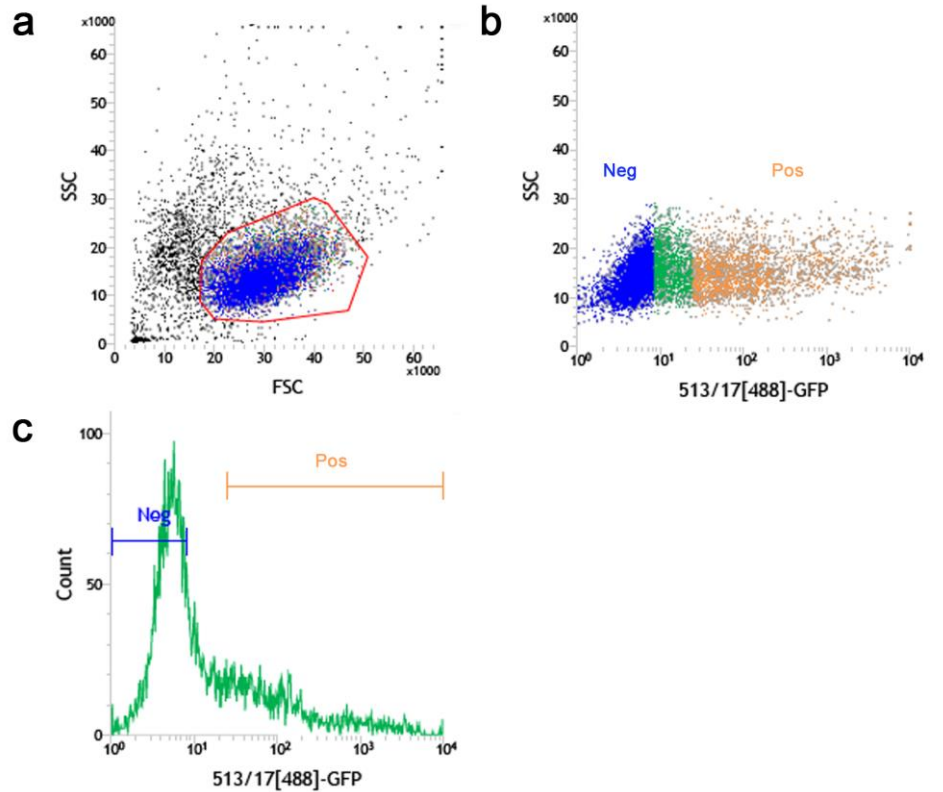


Figure 3.4: Flow cytometry of GFP-TMEM106B-transfected HeLa cells

(a) Flow cytometry of HeLa cells transfected with GFP-TMEM106B. Forward scatter is shown on the x-axis, and side-scatter is shown on the y-axis, with the cell population gated as delimited in red.

(b) A spectrum of GFP expression levels was present in the cell population. GFP fluorescence is shown at a log scale on the x-axis and side scatter is shown on the y-axis. The GFP-low population (Neg) was defined as indicated in blue, whereas the GFP-high population (Pos) was defined as indicated in orange.

(c) Histogram of the GFP-low (Neg) and GFP-high (Pos) populations.

Experiments conducted with R. Tyler Skrinak.

3.2.2 Increased expression of TMEM106B results in multiple lysosomal abnormalities

Having observed that TMEM106B overexpression results in a striking vacuolar phenotype, we next asked what the functional consequences of this phenotype might be. Previous data in immortalized cell lines has also demonstrated that TMEM106B overexpression results in impaired acidification of the lysosomal compartment as well as compromised lysosomal degradative capability (Brady et al., 2013; Chen-Plotkin et al., 2012). To expand this to more disease-relevant cell types, we overexpressed TMEM106B in primary mouse hippocampal neurons and assessed lysosomal acidification with the pH-sensitive dye, LysoTracker. As shown in **Figure 3.5a**, TMEM106B overexpressing neurons showed visibly decreased mean fluorescence intensity (MFI) of LysoTracker compared with non-overexpressing neurons, suggesting that elevated levels of TMEM106B impaired acidification. Indeed, quantification of the LysoTracker MFI for TMEM106B overexpressing neurons revealed a significant decrease compared to neighboring non-overexpressing neurons ($14.23 \pm 2.75\%$ decrease, $p=0.002$). In contrast, LAMP1 overexpression did not result in significant changes in LysoTracker MFI comparing LAMP1 overexpressing cells to neighboring non-overexpressers (**Figure 3.5b**).

The loss of lysosomal acidification observed here in neurons and previously described in other cell types has consequences for lysosomal degradative function. Corroborating the reports of others (Brady et al., 2013), we found that overexpression of TMEM106B results in impaired lysosomal degradation of the epidermal growth factor receptor (EGFR) (**Figure 3.5c**). Under normal conditions, EGFR rapidly targets to the lysosome for degradation upon internalization via endocytosis of its ligand epidermal growth factor, (EGF) (Eden et al., 2009; Katzmann et al., 2002). Quantification of EGFR degradation demonstrated a significant delay in EGFR degradation in the context of increased TMEM106B expression vs. vector-expressing control (two-way ANOVA $p=0.011$, **Figure 3.5d**).

The delay in EGFR degradation upon conditions of increased TMEM106B expression could be solely due to inefficient lysosomal degradation. Alternatively, trafficking defects induced by increasing TMEM106B expression could also be playing a role. To assess these possibilities,

we evaluated the trafficking of fluorescently-labeled EGF from introduction into the cell culture medium to internalization in a LAMP1+ vesicle. As shown in **Figure 3.5e and 3.5f**, TMEM106B overexpression resulted in delayed delivery of EGF to LAMP1+ vesicles at both higher and lower concentrations of EGF (two-way ANOVA $p=0.001$ for 50 ng/ml EGF, $p<0.001$ for 400 ng/ml EGF). Quantification of EGF-488's co-localization with LAMP1 over time demonstrates that EGF reaches its peak level of co-localization with LAMP1 (i.e. time to reach the lysosome) at 90 minutes in control cells (**Figure 3.5e**). In contrast, in cells transfected with TMEM106B, EGF-488 was significantly delayed in reaching the lysosome (two-way ANOVA $p=0.001$). EGF delivery to LAMP1+ vesicles was also delayed when using a higher concentration of EGF, 400ng/ml (**Figure 3.5f**). This concentration may utilize other internalization mechanisms in addition to receptor-mediated endocytosis (Sorkin and Duex, 2010; Mineo et al., 1999). Thus, both trafficking of EGF to the lysosome as well as lysosomal degradation of EGFR may be impaired upon increased expression of TMEM106B.

Figure 3.5:

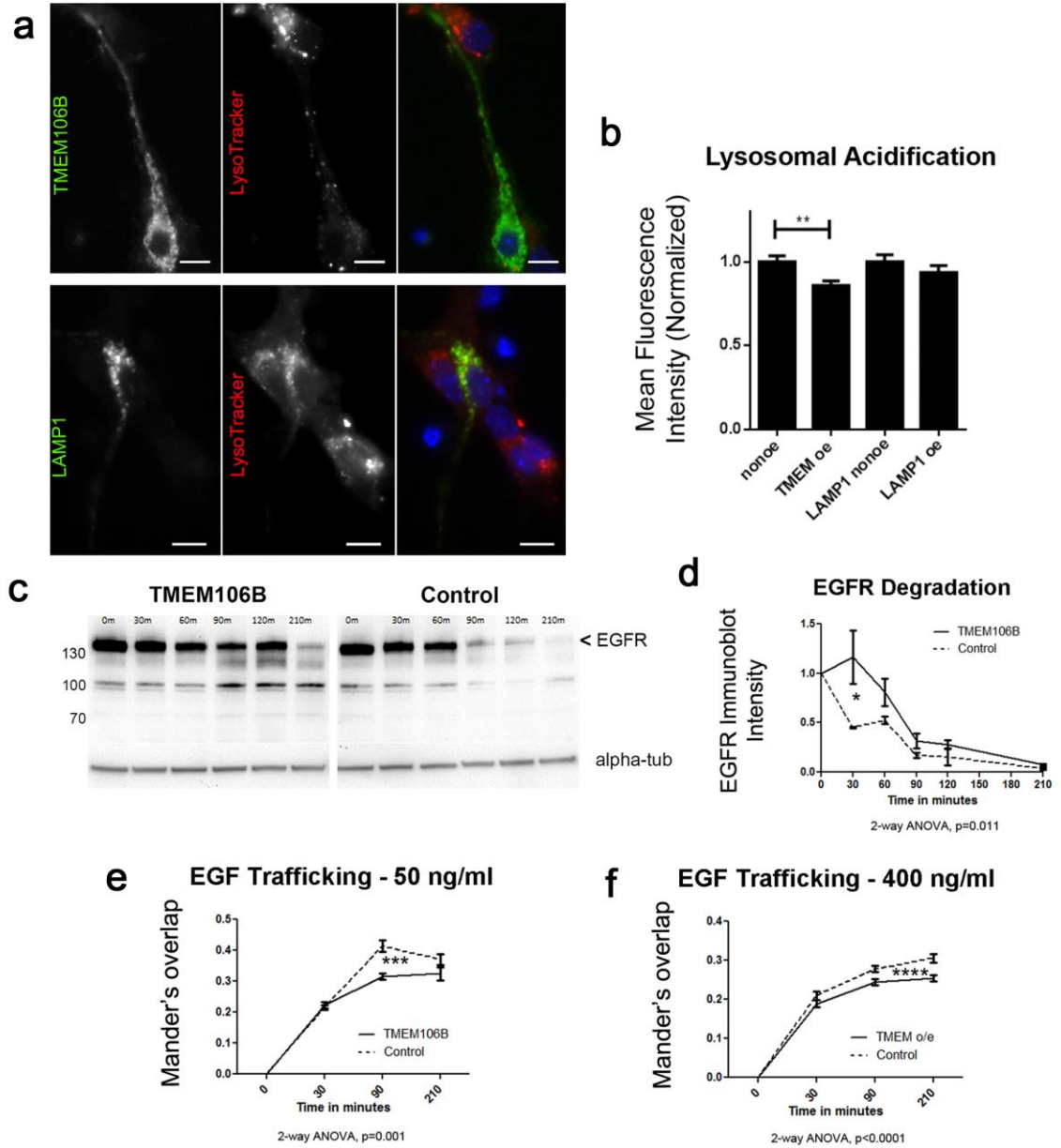


Figure 3.5: TMEM106B overexpression alters lysosomal acidification and function

(a) Expression of GFP-TMEM106B (top three panels) in DIV4 primary mouse hippocampal neurons results in an apparent decrease in intensity of LysoTracker, a pH-sensitive dye that fluoresces intensely at low pH and weakly at higher pH. Expression of GFP-LAMP1 (bottom three panels) does not affect LysoTracker intensity. In each set of three panels, the right-most panel shows the merged images, with LysoTracker in red, and TMEM106B or LAMP1 in green. Cells

overexpressing TMEM106B or LAMP1 fluoresce brightly in green compared to non-overexpressing neighbors.

(b) Quantification of lysosomal acidification combined from four independent experiments. TMEM106B-overexpressing neurons demonstrate a significant decrease in mean fluorescence intensity (MFI) of LysoTracker, compared to neighboring non-overexpressers. Overexpression of LAMP1 does not affect LysoTracker MFI.

(c) A representative immunoblot is depicted of the EGFR degradation assay. Addition of EGF in the presence of cycloheximide results in rapid EGFR lysosomal degradation in vector-transfected cells (right immunoblot). EGFR degradation in TMEM106B-transfected cells, however, was impaired, as EGFR was still present in high quantities at 120 minutes (left immunoblot). EGFR is as indicated; other bands are non-specific.

(d), Quantification of four replicates of the EGFR degradation assays demonstrated a significant delay in EGFR degradation in TMEM106B-transfected versus vector-transfected control cells (mean \pm SEM; $p=0.011$).

(e,f) The endolysosomal trafficking of EGF to lysosomes (LAMP1+ organelles) is significantly delayed in TMEM106B overexpressing cells, as demonstrated by decreased co-localization between EGF and LAMP1, as compared to control cells (mean \pm SEM; $p=0.001$). Two different concentrations of EGF were tested, as the lower concentration is internalized via EGFR-mediated endocytosis, and the higher concentration may also utilize other internalization mechanisms. In both cases, TMEM106B overexpression delayed the delivery of EGF to lysosomes. Co-localization was quantified by Mander's overlap; quantification with Pearson's coefficient demonstrated similar results (data not shown).

Scale bars = 10 μ m. FLAG-TMEM106B is detected by FLAG antibody in the bottom row.

* $p<0.05$, ** $p<0.01$, *** $p<0.001$, **** $p<0.0001$.

3.2.3 Increased TMEM106B alters autophagosomal and lysosomal populations

Our ultrastructural analyses suggested that a proportion of the enlarged organelles seen on TMEM106B overexpression could be late autophagic vacuoles. Thus, we evaluated cells overexpressing TMEM106B for subcellular localization of TMEM106B, LAMP1, and the autophagosome/autolysosome marker LC3, using triple-label immunofluorescence microscopy. While LC3 staining was minimal and did not co-localize well with TMEM106B under endogenous conditions, upon TMEM106B overexpression, many enlarged LAMP1+ organelles also expressed LC3, with TMEM106B, LAMP1, and LC3 demonstrating co-localization (**Figure 3.6a**). In addition, cells overexpressing TMEM106B displayed a marked increase in the number of LC3+ organelles (**Figure 3.6b**), compared to neighboring non-overexpressers. Quantification of the number of LC3+ organelles demonstrated that TMEM106B-expressing cells had a significant increase in the average number of LC3+ organelles per cell compared with controls expressing GFP or vector (**Figure 3.6c**). This suggested that increased TMEM106B expression increases the number of autophagosomes (APs), potentially through increased autophagosomal formation or via blocking downstream autophagic flux, possibly through the previously described impairment of lysosomal acidification.

However, in contrast to the increase seen in LC3+ organelles, we observed a *decrease* in the number of LAMP1+ organelles (late endosomes/lysosomes) with TMEM106B overexpression (**Figure 3.6d**). Specifically, we found a significant decrease in the average number of LAMP1+ organelles in cells with increased expression of TMEM106B compared to controls (71.56 ± 4.29 LAMP1+ organelles for TMEM106B-overexpressing cells vs. 97.2 ± 5.56 for GFP-overexpressing cells vs. 92.3 ± 8.41 for non-overexpressing cells).

Figure 3.6:

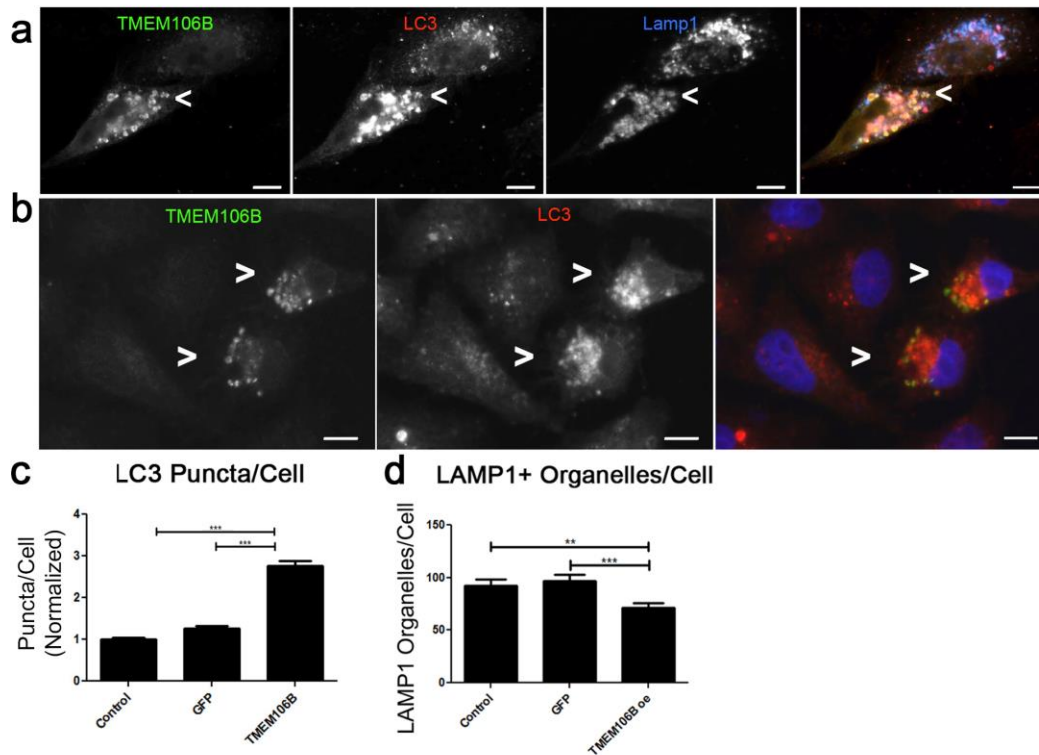


Figure 3.6: TMEM106B co-localizes with LC3 and overexpression of TMEM106B alters autophagosome and lysosome populations

(a) Immunofluorescence microscopy demonstrates co-localization of the autophagosomal marker LC3 (red) with TMEM106B+ (green) and LAMP1+ (blue) organelles in HeLa cells overexpressing TMEM106B. Right-most panel merges channels, which are shown individually in monochrome in left three panels. Two cells are shown, with the bottom one demonstrating increased TMEM106B expression.

(b) Expression of TMEM106B results in a visible increase in the number of LC3+ organelles/cell (arrows), compared to neighboring cells in which TMEM106B expression is not increased. Right-most panel shows merged TMEM106B (green) and LC3 (red) channels, which are shown individually in monochrome in the left panels. Four HeLa cells are shown in the field, with the two on the right demonstrating increased TMEM106B expression.

(c) Quantification of the average number of LC3+ puncta per cell shows a significant increase in LC3+ puncta in TMEM106B-transfected HeLa cells, compared to GFP- or vector-transfected controls.

(d) The number of LAMP1+ organelles decreased significantly in TMEM106B-overexpressing HeLa cells, compared to GFP-overexpressing HeLa cells or non-overexpressing (control) HeLa cells (mean \pm SEM; $p=0.000642$ for TMEM106B vs. GFP, $p=0.00271$ for TMEM106B vs. non-overexpressing cells; quantifications performed for three experiments).

Scale bars = 10 μ m. ** $p<0.01$, *** $p<0.001$. TMEM106B is detected by N2077 in (a) and by the FLAG tag in panel (b).

b, c imaged and quantified by Robert Arauz Perez

3.2.4 Increased TMEM106B levels may decrease cell survival

Notably, the endolysosomal disturbances associated with TMEM106B overexpression appear to be associated with decreased cell survival, since we observed that HeLa cells expressing TMEM106B “disappeared” from culture approximately forty-eight hours post-transfection, whereas LAMP1-expressing cells remained readily apparent (**Figure 3.7a**). To further quantify these observations, we assessed cytotoxicity in several ways. First, we measured LDH release from cultured cells, which occurs when cell membranes are compromised. After transient transfection with TMEM106B or control constructs, we assessed cytotoxicity at multiple timepoints. Compared with both vector control and LAMP1-overexpressing cells, cells overexpressing TMEM106B exhibited significantly higher cytotoxicity at 48 hours post-transfection (two-way ANOVA $p=0.026$ compared to vector control, $p=0.010$ compared to LAMP1, **Figure 3.7b**), suggesting that TMEM106B overexpression is toxic to cells. Second, because we were concerned that LDH result could also result from our transfection methods, we also quantified the proportion of Trypan Blue (+) cells in HeLa cells expressing TMEM106B or controls GFP or LAMP1 to quantitated non-viable cells in each condition. These studies corroborated the cytotoxic effect of increased TMEM106B expression (**Figure 3.7c**). Finally, in order to investigate the contribution of apoptotic cell death mechanisms to the cytotoxicity observed with TMEM106B expression, we performed TUNEL staining. Corroborating the results of others (Brady et al., 2013), we did not see a difference in numbers of cells undergoing apoptosis in conditions with vs. without TMEM106B overexpression, with very few TUNEL+ cells in both conditions (**Figure 3.7d**).

Taken together, our findings suggest that increased expression of TMEM106B in multiple cell types, including neurons, results in prominent morphological alterations in LAMP1+ organelles such as late endosomes, lysosomes, or autolysosomes. Moreover, these alterations affect trafficking to lysosomes, lysosomal acidification and degradative function, ultimately resulting in cytotoxicity.

Figure 3.7:

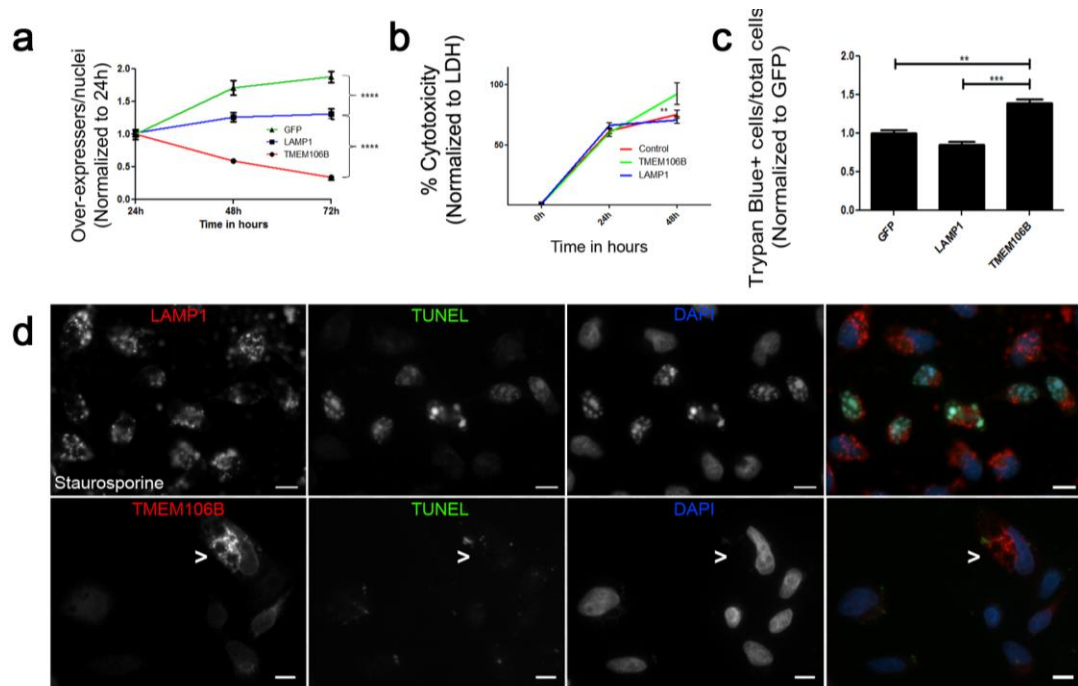


Figure 3.7: Increased levels of TMEM106B are cytotoxic to cells

(a) Growth and survival of HeLa cells transfected with FLAG-TMEM106B, LAMP1, and GFP. The proportion of TMEM106B-overexpressing cells to total number of cells decreases over time compared with overexpression controls (mean \pm SEM; **** p <0.0001 for two independent experiments). Overexpressing cells were identified by immunofluorescent labeling with N2077, LAMP1, and GFP antibodies; the total number of cells was enumerated by counting the number of DAPI+ nuclei. Results are normalized to the 24 hour timepoint.

(b) Increased expression of TMEM106B results in cytotoxicity. Cytotoxicity was quantified in HeLa cells overexpressing TMEM106B or controls (LAMP1, vector) using measurements of LDH release (which accompanies loss of cell membrane integrity); data is combined for eighteen replicates performed on three days. Over a 48h time-course, TMEM106B overexpression (green) resulted in significantly greater cytotoxicity than overexpression of LAMP1 (blue, two way ANOVA p <0.001) or vector control (red, two-way ANOVA p =0.026).

(c) Trypan Blue labeling demonstrates that TMEM106B overexpression decreases cell viability. HeLa cells were transfected with controls (GFP and LAMP1) or myc-TMEM106B and analyzed for uptake of Trypan Blue. The proportion of blue cells normalized to the GFP-expressing condition is shown (mean \pm SEM; ** p <0.01, *** p <0.001 for nine replicates performed on three separate days).

(d) HeLa cells treated with 1 μ M of the positive control staurosporine exhibit TUNEL staining (top row), while TMEM106B overexpressing HeLa cells (arrowhead, bottom row) do not. For the top row, the right panel shows the merged channels of LAMP1 (red), TUNEL (green), and DAPI (blue). Individual channels are shown in monochrome in the left three columns. For the bottom row, the right panel demonstrates the merged channels of TMEM106B (red), TUNEL (green), and DAPI (blue).

Scale bars = 10 μ m. FLAG-TMEM106B is detected by FLAG antibody in the bottom row.

** p <0.01, *** p <0.001 *b, c* conducted with Travis L. Unger

3.2.5 The cell biological effects of increased TMEM106B expression are dependent on localization of TMEM106B to lysosomes

The preceding experiments demonstrate that increased expression of TMEM106B results in changes in lysosomes, autophagosomes, and autolysosomes, with concomitant cytotoxic effects. Furthermore, these effects are relatively specific to TMEM106B, since they are not seen upon overexpression of another lysosomal protein, LAMP1, or a control protein, GFP. We next asked whether the localization of TMEM106B to lysosomes is necessary for these changes to occur.

To answer this question, we first had to determine, and then abrogate, potential lysosomal sorting motifs for TMEM106B. Inspection of the cytosolic, N-terminal domain of TMEM106B revealed three potential canonical lysosomal sorting motifs (**Figure 3.8a**) – two tyrosine-based (YDGV, YVEF) and one extended dileucine-based motif (ENQLVALI), fitting the tyrosine consensus sequence YXXØ and dileucine motif [DE]XXXL[LI], respectively (Bonifacino and Traub, 2003). We therefore used site-directed mutagenesis to individually mutate each potential motif. The potential lysosomal sorting motifs are identified in **Figure 3.8b** along with the mutations introduced: YDGV → ADGV, YVEF → AVEF, and ENQLVALI → ENQLVAAA. We assessed the subcellular localization of each of these motif mutants by immunofluorescence microscopy.

While the constructs containing mutated tyrosine-based motifs (YDGV → ADGV, YVEF → AVEF) continued to localize to lysosomes, mutation of the leucine and isoleucine residues within the extended dileucine-based motif abrogated lysosomal localization of TMEM106B, as demonstrated by decreased co-localization with LAMP1 (**Figure 3.8c**). Instead, in the ENQLVAAA TMEM106B mutant, TMEM106B expression appeared more diffusely cytoplasmic. In addition, we verified that the ENQLVAAA TMEM106B mutant was not retained in the endoplasmic reticulum (ER) by confirming cell surface expression under non-permeabilized immunofluorescence microscopy conditions (**Figure 3.9a**) and by Endoglycosidase H (EndoH) and Peptide-N-Glycosidase F (PNGaseF) deglycosylation experiments (**Figure 3.9b**).

Specifically, both wild-type TMEM106B and ENQLVAAA TMEM106B showed similar EndoH-resistant bands ~35kDa by immunoblot, demonstrating that ENQLVAAA TMEM106B achieves complex glycosylation in the Golgi and is not retained in the ER. This 35kDa band fully collapsed down to TMEM106B's predicted 31 kDa size when deglycosylated with PNGaseF for both ENQLVAAA TMEM106B and wild-type TMEM106B.

Accompanying the abrogation of lysosomal localization, ENQLVAAA TMEM106B also demonstrated a striking loss of the vacuolar phenotype (**Figure 3.8c, 3.10a**). In fact, on brightfield microscopy, cells expressing ENQLVAAA TMEM106B showed virtually no vacuoles (**Figure 3.10a**). We considered the possibility that the loss of phenotype might be due to lower expression levels of this construct. We found, however, that, whereas our wild-type TMEM106B construct demonstrated overexpression levels 2-10X over baseline, the ENQLVAAA TMEM106B mutant construct showed much higher expression (**Figure 3.10b, c**).

Given the loss of the vacuolar phenotype in cells overexpressing ENQLVAAA TMEM106B, we asked if the other cell biological effects of TMEM106B overexpression were also abrogated upon mutation of this motif. Indeed, ENQLVAAA TMEM106B expressing cells did not exhibit decreased lysosomal acidification as seen with wild-type TMEM106B (**Figure 3.11a, b**). In addition, ENQLVAAA TMEM106B-expressing cells showed only a modest increase in the number of LC3 puncta, compared to the >1.5X-increase in LC3 puncta observed with increased wild-type TMEM106B expression (**Figure 3.11c, d**). Finally, the cytotoxicity effects exerted by wild-type TMEM106B were also rescued in this point mutant, since expression of ENQLVAAA TMEM106B caused no more toxicity than controls (**Figure 3.11e, f**).

Figure 3.8:

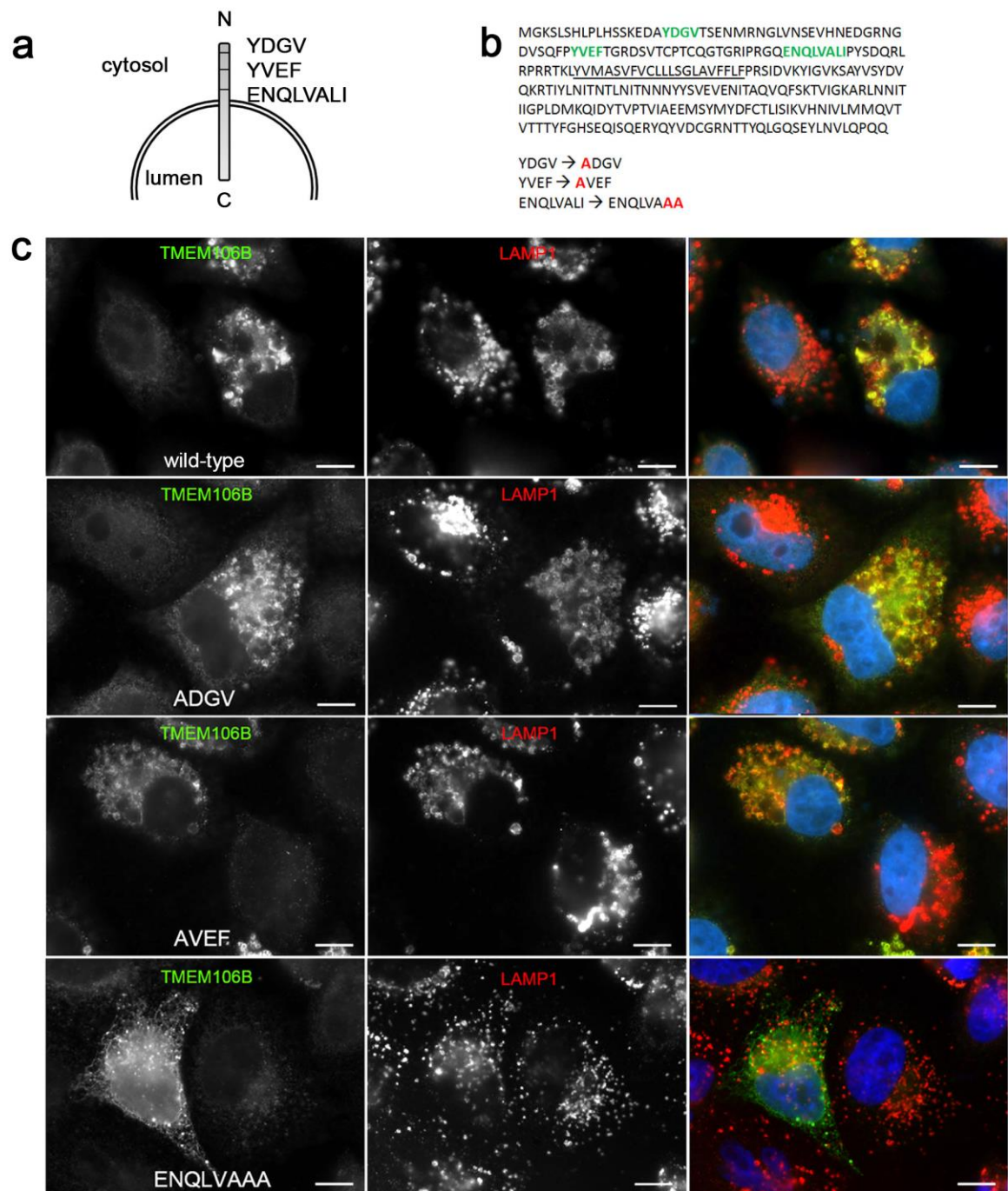


Figure 3.8: ENQLVALI is a potential lysosomal sorting motif for TMEM106B

(a) Three potential classical lysosomal targeting motifs – two tyrosine motifs and one isoleucine/dileucine motif – were identified in the N-terminal domain of TMEM106B.

(b) The primary amino acid sequence of TMEM106B is shown, with lysosomal targeting motifs depicted in green. These motifs were individually mutated to alanine residues, with mutated residues indicated in red.

(c) SDS-PAGE and immunoblotting of the lysosomal motif mutants demonstrates that expression levels in HeLa cells are comparable to wild-type TMEM106B; overexpression levels of all TMEM106B constructs are only moderately increased over endogenous levels. Endo=endogenous TMEM106B, WT=wild-type TMEM106B, ENQ=ENQLVAAA TMEM106B, AVEF=AVEF-TMEM106B, and ADGV=ADGV-TMEM106B. Two bands (arrows) for TMEM106B at 70kDa (dimer) and 40kDa (monomer) are detected by the N2077 antibody.

Scale bars = 10 μ m. FLAG-TMEM106B is detected by FLAG antibody.

Figure 3.9:

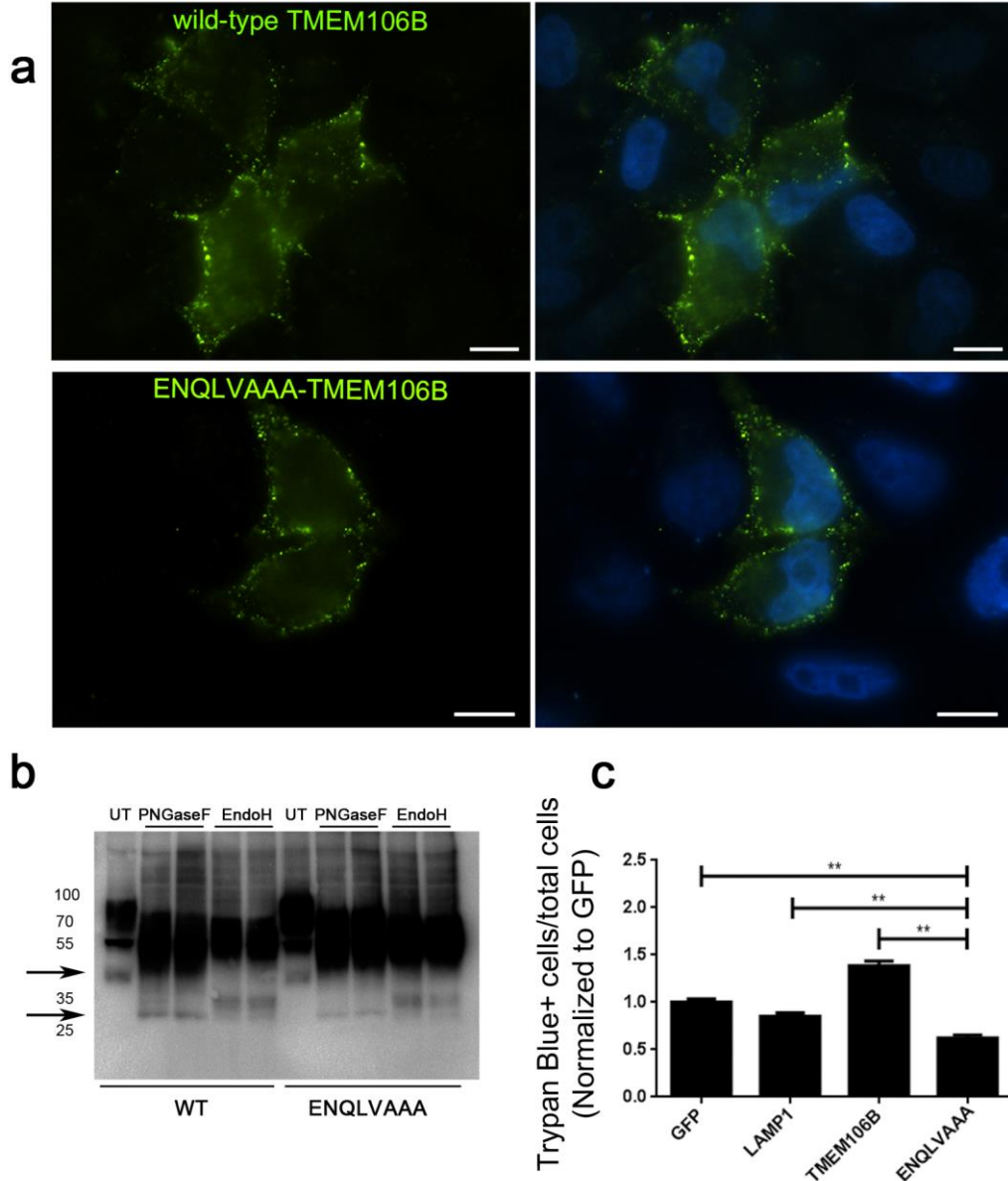


Figure 3.9: ENQLVAAA TMEM106B is not retained in the endoplasmic reticulum

(a) Mutation of a dileucine-based motif in TMEM106B abrogates lysosomal localization but does not prevent the mutated protein from leaving the endoplasmic reticulum (ER). HeLa cells were transfected with either wild-type TMEM106B (top panel) or the ENQLVAAA TMEM106B mutant (bottom panel), and expression was visualized on the cell surface by staining under non-permeabilized conditions. Antibodies directed at a FLAG-tag on the TMEM106B construct were used to ensure that staining was specific for the expressed construct. Both wild-type and ENQLVAAA TMEM106B demonstrated surface expression of TMEM106B. Scale bar = 10 μ m.

(b) Immunoblot patterns for wild-type TMEM106B (five lanes on left) and ENQLVAAA TMEM106B (five lanes on right) expressed in HeLa cells are similar under conditions of Endo H digestion and

PNGase F digestion. The presence of Endo H-resistant bands by immunoblot demonstrates that the ENQLVAAA TMEM106B mutant achieves complex glycosylation in the Golgi and is not retained within the ER. The top arrow indicates the 40 kDa band of monomeric TMEM106B which collapses down to TMEM106B's predicted molecular weight of 31 kDa upon complete deglycosylation with PNGase F (bottom arrow). Digestion with Endo H reveals Endo H-resistant complex glycosylation, with a resulting intermediate molecular weight of ~35 kDa. The blot is developed with a long exposure so as to show the 40 kDa species of TMEM106B.

(c) Trypan Blue staining confirms LDH assay results suggesting that HeLa cells transfected with ENQLVAAA-TMEM106B (ENQLVAAA) do not have increased cell death over controls (LAMP1 and GFP over-expressing conditions), whereas wild-type TMEM106B-transfected cells do show increased toxicity (mean \pm SEM; ** $p < 0.01$ for nine replicates performed on three independent days). GFP, LAMP1, and TMEM106B data are the same as shown in Supplementary Fig. 4b, with ENQLVAAA-TMEM106B results added for comparison.

Scale bar = 10 μ m.

c conducted with Travis L. Unger.

Figure 3.10:

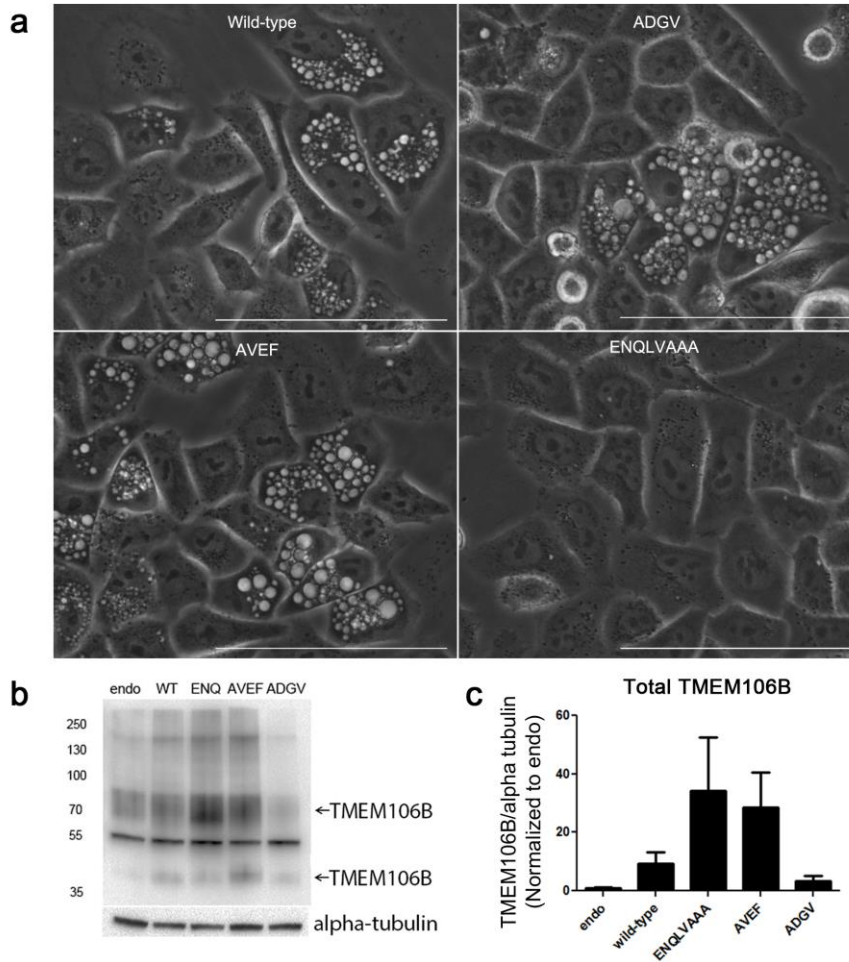


Figure 3.10: Characterization of lysosomal motif mutants

(a) Live imaging of HeLas overexpressing either wild-type TMEM106B or lysosomal motif mutants by bright-field microscopy demonstrates loss of the vacuolar phenotype in cells expressing the ENQLVAAA TMEM106B mutant. In contrast, cytoplasmic vacuoles ranging in size were readily seen in cells expressing wild-type, ADGV-, or AVEF-TMEM106B.

(b, c) Lysosomal motif mutants all exhibit expression levels that are comparable to, or higher than, wild-type TMEM106B, with the ENQLVAAA TMEM106B construct expressing at the highest levels in HeLa cells. Endo=endogenous TMEM106B, WT=wild-type TMEM106B, ENQ=ENQLVAAA TMEM106B, AVEF=AVEF-TMEM106B, and ADGV=ADGV-TMEM106B. In the example immunoblot (b), two bands (arrows) for TMEM106B at 70kDa (dimer) and 40kDa (monomer) are detected (N2077 antibody). Quantification for four replicate experiments is shown in (c), normalized to the endogenous condition (mean \pm SEM).

Scale bar = 100 μ m.

b conducted by R. Tyler Skrinak.

Figure 3.11:

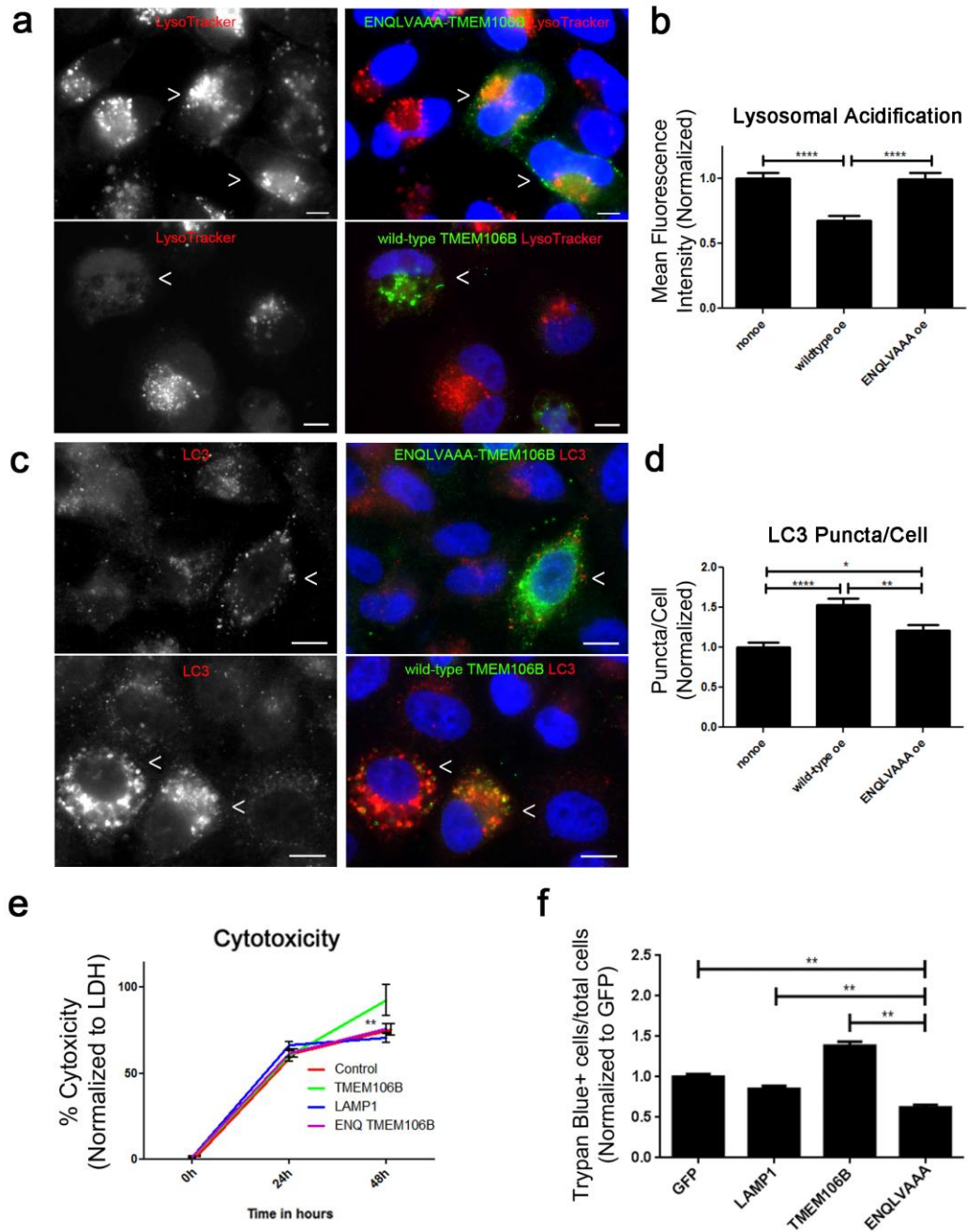


Figure 3.11: The effects of increased TMEM106B expression depend on proper localization of TMEM106B to lysosomes

(a,b) While expression of wild-type TMEM106B impairs lysosomal acidification (as demonstrated by decreased LysoTracker mean fluorescence intensity), expression of ENQLVAAA TMEM106B does not significantly alter organelle acidification. Representative images are shown in (a), and quantification is shown in (b) (mean \pm SEM; $p=8.44 \times 10^{-5}$ for wild-type TMEM106B overexpressing cells (oe) vs. neighboring non-overexpressing (nonoe) cells; no significant difference in ENQLVAAA TMEM106B overexpressing cells vs. neighboring non-overexpressing cells).

(c,d) ENQLVAAA TMEM106B-expressing HeLa cells demonstrate a modest increase in the number of LC3+ puncta, whereas wild-type TMEM106B-expressing cells exhibit a $>1.5x$ increase compared to neighboring non-over-expressers. Representative images are depicted in (c), whereas quantification from two independent experiments is depicted in (d) (mean \pm SEM; $p=4.85 \times 10^{-2}$ for wild-type vs. non-expressers, $p=0.0288$ for ENQLVAAA TMEM106B vs. non-expressers).

(e) Cytotoxicity is quantitated by measurement of LDH in the cell culture medium, as LDH release accompanies compromise of the plasma membrane. While wild-type TMEM106B expression in HeLa cells induces cytotoxicity by 48 hours (TMEM106B, green line), the loss of lysosomal localization (ENQ TMEM106B, pink) rescues this cytotoxicity to levels seen with transfection of vector only (Control, red line, almost entirely overlapped by pink line). Cytotoxicity seen with expression of LAMP1 (blue line) is also shown for comparison purposes. Beyond the 48 hour time point, wild-type TMEM106B-expressing cells are largely lost from the culture medium due to cell death. % cytotoxicity is calculated in comparison to the maximal LDH release induced by treatment with Triton X as described in Materials and Methods.

(f) Trypan Blue staining confirms LDH assay results suggesting that HeLa cells transfected with ENQLVAAA TMEM106B (ENQ) do not have increased cell death over controls (LAMP1 and GFP overexpressing conditions) (mean \pm SEM; $**p<0.01$ for nine replicates performed on three independent days).

Scale bars = 10 μ m.

* $p<0.05$, ** $p<0.01$, **** $p<0.0001$. Wild-type TMEM106B and ENQLVAAA TMEM106B are detected by their FLAG tags in panels a and c.

d, e, f conducted with R. Tyler Skrinak and Travis L. Unger.

3.2.6 Lysosomal acidification and cytotoxicity effects of increased TMEM106B expression are dependent on C9orf72

We have previously demonstrated that *TMEM106B* is a genetic modifier affecting age at death in *C9orf72*-associated FTLD-TDP (Gallagher et al., 2014), suggesting that *TMEM106B* and *C9orf72* may interact in the pathophysiology of FTLD-TDP (Cooper-Knock et al., 2014; Deming and Cruchaga, 2014; van Blitterswijk et al., 2014). The protein product of the *C9orf72* gene, in which hexanucleotide repeat expansions are the most common Mendelian cause of both FTLD-TDP and ALS (Renton et al., 2011; DeJesus-Hernandez et al., 2011), is predicted to be a DENN protein by structural analysis (Levine et al., 2013a). As DENN proteins are guanine exchange factors (GEFs) regulating Rab GTPases, which in turn regulate cell biological events such as vesicular trafficking and fusion (Zhang et al., 2012), we asked whether *TMEM106B*'s cell biological effects might be dependent on *C9ORF72*.

Strikingly, siRNA-mediated knockdown of *C9ORF72* expression abrogated the vacuolar phenotype seen upon overexpression of *TMEM106B*. This effect was found in multiple cell types, and did not occur with control siRNA knockdown (**Figure 3.12a, b**). Moreover, quantification of LAMP1+ organelle size demonstrated that siRNA knockdown of *C9orf72*, but not control siRNA knockdown, rescued the LAMP1+ organelle diameter size in *TMEM106B* over-expressing cells to levels near that of cells with endogenous levels of *C9orf72* and *TMEM106B* (**Figure 3.12c, d**). Intriguingly, in HEK293 cells but not in HeLa cells, concomitant overexpression of both *C9orf72* and *TMEM106B* resulted in the most dramatic increases in vacuolar size (**Figure 3.12d**). Moreover, in both cell types, knockdown of *C9orf72* without overexpression of *TMEM106B* resulted in a small, but significant, decrease in the LAMP1+ organelle diameter size, compared to cells without knockdown of *C9orf72* (**Figure 3.12c, d, right graph**).

We then asked if other cell biological phenotypes observed with *TMEM106B* overexpression are similarly dependent on the presence of *C9orf72* protein. Specifically, we evaluated cytotoxicity as well as the lysosomal acidification defect induced by *TMEM106B* overexpression. As shown in **Figure 3.13a and b**, the difference in LysoTracker MFI typically

seen in TMEM106B overexpressing HeLa cells as compared to non-overexpressing cells is abrogated in the context of C9orf72 knockdown, but maintained in the context of control siRNA knockdown. In addition, knockdown of C9orf72 abrogated the cytotoxic effects of TMEM106B overexpression (**Figure 3.13c**).

To ensure that the reversal of TMEM106B overexpression effects by C9orf72 knockdown were not due to off-target effects of the siRNA used, we repeated our experiments with an shRNA targeting C9orf72. As shown in **Figure 3.14a**, knockdown of C9orf72 by this second method in TMEM106B overexpressing cells again rescued LAMP1+ organelle diameter sizes to baseline. Additionally, knockdown of C9orf72 by shRNA also rescued the cytotoxicity of TMEM106B overexpression (**Figure 3.14b**).

Of note, immunoblots were run in parallel to confirm C9orf72 knockdown for all experiments and demonstrated nearly complete disappearance of the endogenous C9orf72 band; validation of the specificity for the C9orf72 antibody used was demonstrated with C9orf72 knockdown and overexpression in immortalized cells (**Figure 3.14c**). Additionally, quantitative PCR experiments demonstrated efficient knockdown and overexpression of C9orf72 in our siRNA experiments (**Figure 3.14d**). Finally, we considered the possibility that C9orf72 knockdown and overexpression might secondarily affect TMEM106B expression levels, thus rescuing TMEM106B overexpression phenotypes. However, manipulation of C9orf72 levels minimally affected TMEM106B expression (**Figure 3.14e, f**).

Figure 3.12:

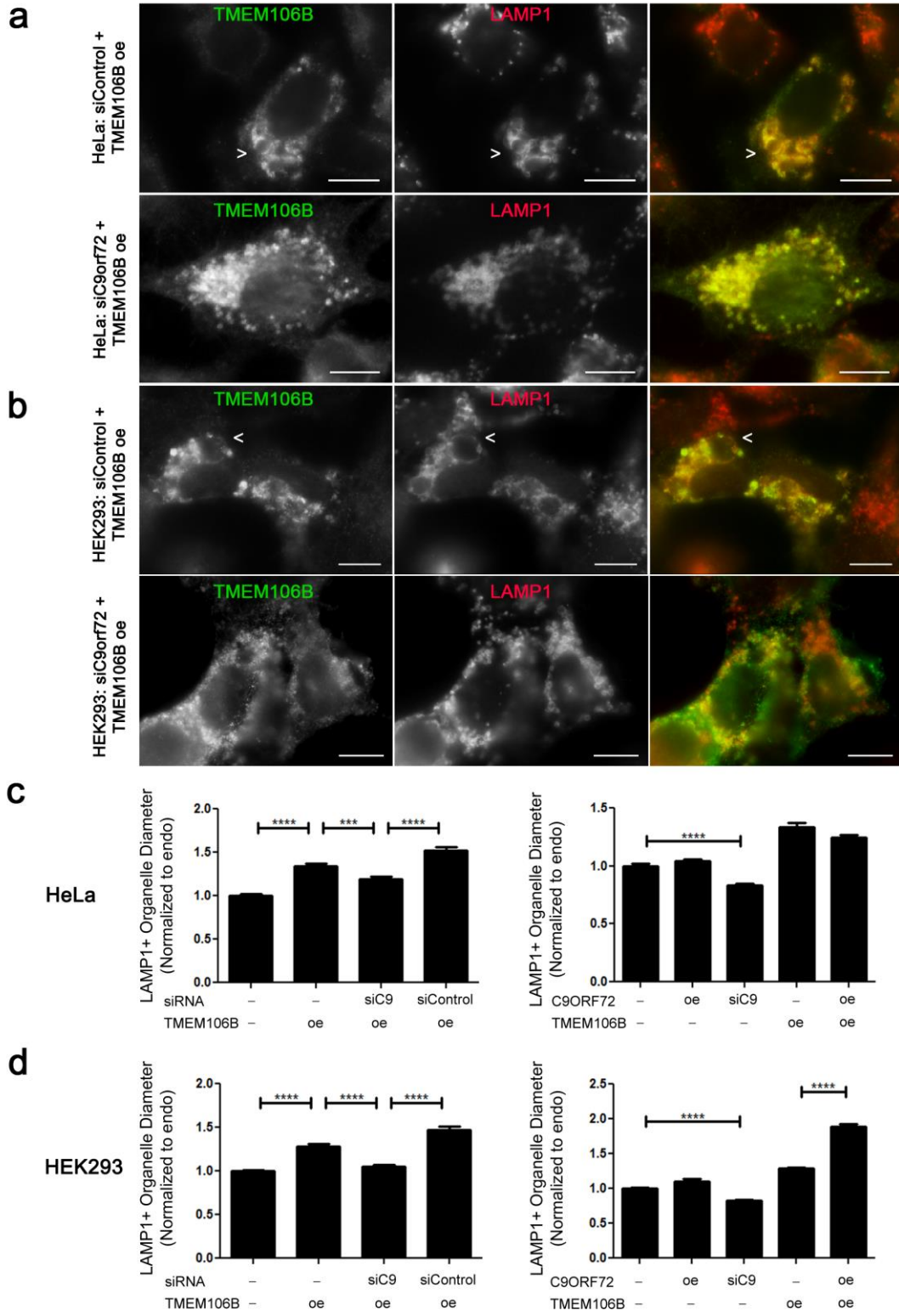


Figure 3.12: Knockdown of C9ORF72 rescues TMEM106B-induced vacuolar phenotype

(a,b) In HeLa cells (a) and in HEK293 cells (b), treatment with control siRNA does not affect the LAMP1+ vacuolar phenotype seen in TMEM106B over-expressing cells (arrows, top row), but siRNA knockdown of C9orf72 mitigates the phenotype (bottom row). For all panels, the right panel shows the merged channels for TMEM106B (green) and LAMP1 (red); individual channels are shown in monochrome in the left and middle panels. Scale bars = 10 μ m. TMEM106B detected by N2077 antibody.

(c,d) The diameter of LAMP1+ organelles was quantified in HeLa (c) and HEK293 (d) cells. In the left graph for both cell types, LAMP1+ diameter was assessed under endogenous conditions (first column), TMEM106B overexpression (second column), TMEM106B overexpression with C9orf72 knockdown (third column), and TMEM106B overexpression with control siRNA knockdown (fourth column). In the right graph, LAMP1+ diameter is quantified under endogenous conditions (first column), C9orf72 overexpression (second column), C9orf72 knockdown alone (third column), TMEM106B overexpression alone (fourth column), and TMEM106B and C9orf72 concomitant overexpression (fifth column). All values are normalized to the endogenous condition (first column) and means \pm SEM from nine replicates performed on three separate days are shown. In both HeLa (c) and HEK293 (d) cells, TMEM106B overexpression significantly increased LAMP1+ organelle size ($p < 0.0001$, left graph, compare first and second columns). In both cell types, however, knockdown of C9orf72 abrogated the effects of TMEM106B overexpression, resulting in a return of LAMP1+ organelle size towards that of the endogenous baseline ($p < 0.001$, left graph, comparing second and third columns).

*** $p < 0.001$, **** $p < 0.0001$. TMEM106B is detected by N2077 (Ck). Scale bars = 10 μ m.

Experiments conducted with Travis L. Unger and Nimansha Jain.

Figure 3.13:

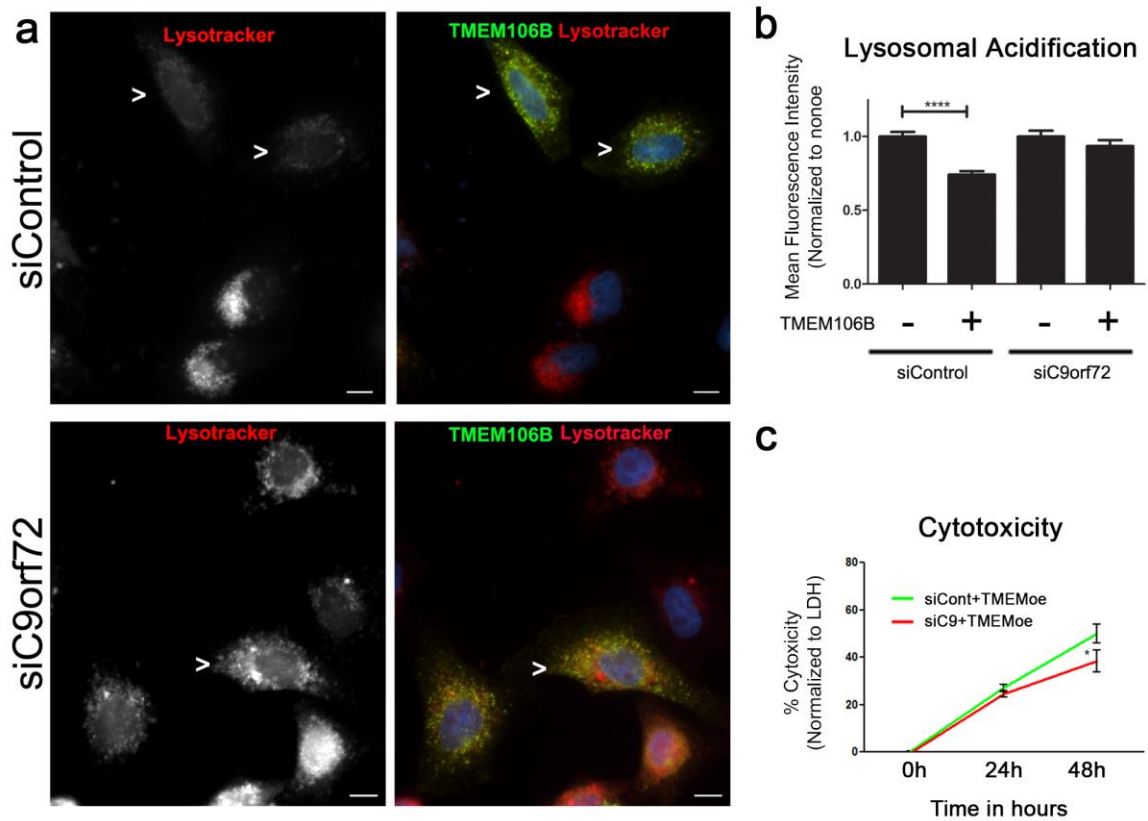


Figure 3.13: Knockdown of C9orf72 mitigates TMEM106B-induced acidification defects and cytotoxicity

(a, b) Knockdown of C9orf72 abrogates the acidification defect seen with TMEM106B overexpression. (c) HeLa cells were transfected with control siRNA + TMEM106B or with C9orf72 siRNA + TMEM106B and incubated with Lysotracker. (b) In each of these transfection conditions, the MFI was quantified for cells over-expressing TMEM106B and neighboring non-expressing cells. TMEM106B overexpression in the context of control siRNA yielded the previously described impairment in acidification in TMEM106B over-expressers compared to neighboring non-over-expressers. However, TMEM106B overexpression in the context of C9orf72 knockdown resulted in no significant difference in MFI between TMEM106B over-expressers and non-over-expressers.

(c) TMEM106B overexpression induces cytotoxicity in HeLa cells, as quantified by LDH release over a 48 hour time-course. Concomitant siRNA knockdown of C9orf72 abrogates cytotoxicity, whereas treatment with control siRNA does not. Means +/- SEM for >12 replicates performed on three days shown, and cytotoxicity compared by two-way ANOVA.

* $p < 0.05$, **** $p < 0.0001$. TMEM106B is detected by N2077 (Ck). Scale bars = 10 μ m.

Experiments conducted with Travis L. Unger and Nimansha Jain.

Figure 3.14:

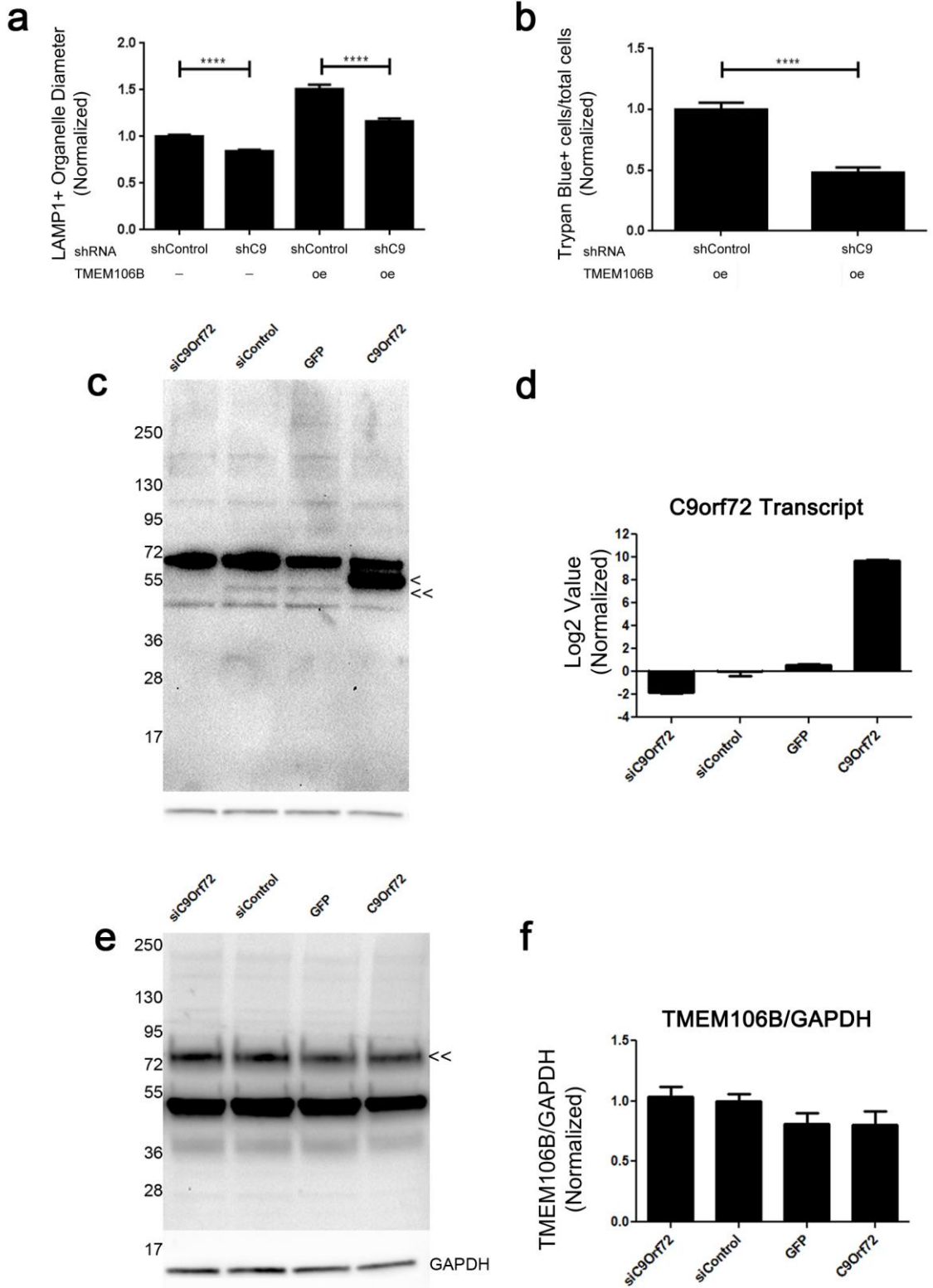


Figure 3.14: Overexpression and knockdown of C9orf72

(a) Knockdown of C9orf72 with shRNA (fourth column) demonstrates abrogation of the vacuolar phenotype associated with TMEM106B overexpression, relative to what is seen with control shRNA knockdown (third column). Results are quantified from nine replicates performed on three different days in HEK293 cells (mean \pm SEM; **** $p < 0.0001$), corroborating results seen with siRNA-mediated knockdown of C9orf72. Additionally, shRNA knockdown of C9orf72 in the context of endogenous levels of TMEM106B also led to a smaller LAMP1+ vesicle diameter size, similar to results from siRNA experiments (first and second columns). Data is normalized to the TMEM106B endogenous condition (shControl RNA and endogenous TMEM106B).

(b) Trypan Blue dye exclusion assay demonstrates that shRNA-mediated knockdown of C9orf72 rescues TMEM106B-overexpression-induced cell toxicity by ~50% in HEK293 cells. Data from nine replicates performed on three different days are depicted (mean \pm SEM; **** $p < 0.0001$); data are normalized to the shControl plus TMEM106B overexpression condition.

(c) Immunoblot with anti-C9orf72 (Sigma #HPA023873) demonstrates nearly complete knockdown of the endogenous C9orf72 band in HEK293 cells transfected with C9orf72 siRNA as compared to control siRNA (compare first and second columns, endogenous C9orf72 band indicated by double arrowhead). In contrast, HEK293 cells transiently transfected with FLAG-C9orf72 demonstrated a dark band slightly above the endogenous band, reflecting the slight increase in size introduced by the tag (fourth column, single arrowhead).

(d) Quantitative PCR corroborates the efficient knockdown (~70% knockdown, note that a base 2 logarithmic scale is used) and level of overexpression of C9orf72 at the mRNA level.

(e, f) Knockdown and overexpression of C9orf72 does not significantly alter protein levels of TMEM106B. Representative immunoblot (e) for TMEM106B demonstrates that TMEM106B protein levels are not altered by C9orf72 knockdown (compare left two columns) or overexpression (compare right two columns) in transiently transfected HEK293 cells. Both the 40 kDa and 70 kDa TMEM106B bands, probed with the N2077 TMEM106B antibody, are indicated by the double arrowheads. Quantification of nine replicates performed on three different days (f) demonstrates that knockdown (compare left two columns) or overexpression of C9orf72 (compare right two columns) does not significantly alter TMEM106B protein levels relative to control knockdown, or to overexpression of a control GFP construct.

**** $p < 0.0001$

c-f conducted by Travis L. Unger.

3.3 DISCUSSION

Genotypes at *TMEM106B* linked to increased risk for FTL-D-TDP are associated with increased expression of *TMEM106B* (Chen-Plotkin et al., 2012). Moreover, in human FTL-D-TDP brain, *TMEM106B* expression is also increased (Chen-Plotkin et al., 2012), with an altered subcellular distribution (Busch et al., 2013). Here we explore the cell biological consequences of this disease-associated increase in *TMEM106B* expression, demonstrating that it results in multiple perturbations to endolysosomal and autophagosomal pathways, and that these changes are dependent on the presence of *C9orf72*.

We and others have previously shown that *TMEM106B* overexpression results in enlargement of LAMP1+ organelles (Chen-Plotkin et al., 2012; Stagi et al., 2014; Schwenk et al., 2014). We corroborate and expand this result here with ultrastructural characterization in neurons, as well as demonstrate that the lysosomal acidification defect extends to neurons. We note that the ultrastructural characteristics of these organelles – single-membrane-bound, electron-lucent, containing possible degradation products – suggests that they may be late autophagic vacuoles (amphisomes and autolysosomes). Indeed, many LAMP1+ organelles co-localize with the autophagosomal marker LC3 in immunofluorescent labeling. Notably, overexpression of ENQLVAAA *TMEM106B*, a mutant version of *TMEM106B* that exhibits decreased LAMP1+ co-localization, results in only a minimal increase in the number of LC3+ organelles despite expressing at much higher levels than wild-type *TMEM106B*. This suggests a specific effect that is dependent on both the identity of *TMEM106B* and its localization to the lysosomal membrane.

Notably, the observed increase in the number of LC3+ organelles upon *TMEM106B* overexpression is also accompanied by a significant decrease in the number of LAMP1+ organelles. Moreover, the LAMP1+ organelles that remain are poorly acidified and demonstrate impairment in lysosomal degradation. Taken together, these results suggest that elevated *TMEM106B* levels skew the endolysosomal pathway towards an increase in downstream fusion products such as ALs, at the expense of maintaining a normal, functional lysosomal pool. This

phenomenon of lysosomal exhaustion and consumption has been previously described in starvation- as well as rapamycin-induced autophagy (Settembre et al., 2011; Yu et al., 2010). As such, further investigation of the role of TMEM106B in autophagy pathways may be a valuable addition to the data presented here. In support of an impact of TMEM106B on autophagy, it has been recently reported that increased expression of TMEM106B results in increased nuclear translocation of Transcription Factor EB (TFEB) (Stagi et al., 2014). Because TFEB has been proposed as a master regulator of lysosomal and autophagosomal gene expression (Settembre et al., 2011; Sardiello et al., 2009), our current findings may also support a potential interaction between TMEM106B and TFEB, although how direct this interaction might be remains to be seen. However, we note that the relationship is likely not straightforward, as while increased TFEB translocation would be expected to increase the number of autophagosomes and promote lysosome-autophagosome fusion, it would also be expected to increase lysosomal biogenesis and enhance the cell's ability to degrade (Sardiello et al., 2009; Ma et al., 2012).

Additionally, we identify for the first time here a possible lysosomal sorting motif for TMEM106B, demonstrating that point mutations to a potential extended dileucine motif (Letourneur and Klausner, 1992; Pond et al., 1995) abrogate lysosomal localization. The elucidation of this lysosomal sorting motif is important for two reasons. First, it provides domain-level detail for a protein that was virtually uncharacterized prior to 2010. Second, it provides a valuable tool for mechanistic exploration of TMEM106B function. We exploit the latter use in the current study as an important control, demonstrating that the effects seen with overexpression of TMEM106B depend on both the identity of the overexpressed protein (since they are not seen with LAMP1 or GFP overexpression) and on the proper subcellular localization of TMEM106B.

The abrogation of TMEM106B-induced effects by concomitant knockdown of *C9orf72* also supports the assumption that the vacuolar phenotype, lysosomal acidification defect, and cytotoxicity described here are disease-relevant effects of TMEM106B overexpression. Indeed, these findings provide the first mechanistic evidence for a link between the two FTLD-TDP associated genes *TMEM106B* and *C9orf72*. Hexanucleotide repeat expansions in *C9orf72* are

the most common Mendelian cause of both FTD and ALS (DeJesus-Hernandez et al., 2011; Renton et al., 2011; Beck et al., 2013). *C9orf72*-associated FTD and ALS cases demonstrate large expansions (800-4,400 repeats), while healthy controls have <33 repeats (van Blitterswijk et al., 2013; Beck et al., 2013). The effects of the *C9orf72* repeat expansion are an area of active research, with evidence for multiple mechanisms playing a role in disease. In particular, proposed pathophysiological mechanisms for *C9orf72* repeat expansions include toxic repeat RNA species (Fratta et al., 2012; Gendron et al., 2013; Lee et al., 2013; Mizielska et al., 2013), toxic dipeptide repeats resulting from repeat-associated, non-ATG (RAN) translation (Ash et al., 2013; Mizielska et al., 2014; Mori et al., 2013), and reduced levels/loss of function of the normal *C9orf72* protein (Ciura et al., 2013; DeJesus-Hernandez et al., 2011; Gijselinck et al., 2012; Renton et al., 2011).

We and others have previously demonstrated a genetic interaction between *TMEM106B* and *C9orf72* (Gallagher et al., 2014; van Blitterswijk et al., 2014), with *TMEM106B* genotypes associated with increased risk for FTLT-DTP in non-*C9orf72*-expansion cases paradoxically correlating with later age at death and age at onset in *C9orf72*-expansion-associated FTLT. This sign epistatic effect has been described in other contexts before, and in these other contexts, the protein products of the two genes involved have been shown to mechanistically interact (Schenk et al., 2013; Silva et al., 2011). Our present study implicates *TMEM106B* and *C9orf72* in the same mechanistic pathways as well, since knockdown of *C9orf72* mitigates most lysosomal effects of *TMEM106B* overexpression.

While the normal function of *C9orf72* protein is yet unknown, it is predicted by structural analysis to be a DENN protein (Zhang et al., 2010; Levine et al., 2013a). DENN proteins function as GDP-GTP exchange factors (GEFs) for Rab GTPases and, as such, they play a role in regulating autophagy, vesicular trafficking and fusion, and membrane trafficking events. Proper regulation of Rab GTPase activity is known to be important for neuronal function; furthermore, dysregulation of Rabs by DENN proteins or other protein families with similar GEF activity has previously been linked to neurodegeneration (Azzedine et al., 2003; Del Villar and Miller, 2004;

Hadano et al., 2010). Thus, it is possible that many of the effects of increased TMEM106B expression are mediated through alterations to one or more Rab GTPases, which are in turn regulated by C9orf72. Such a model of pathogenesis implies that C9orf72 loss-of-function mechanisms may play a role in development of disease.

We note that C9orf72 knockdown in the context of TMEM106B overexpression here has a phenotype rescue effect. While this result may be counter-intuitive to straightforward assumptions about loss-of-function mechanisms in disease, it is congruent with the sign epistatic genetic modifier effect we previously reported for *TMEM106B* and *C9orf72* in a 30-site international cohort of *C9orf72* expansion-associated FTL-D-TDP cases (Gallagher et al., 2014). That is, in human FTL-D-TDP and in cell culture, increased TMEM106B expression (proxied by *TMEM106B* risk genotype or manipulated by transient transfection) appears deleterious in most cases, but is rescued in the specific context of reduced C9orf72 (proxied by *C9orf72* expansion carrier state or manipulated by C9orf72 knockdown). We further note that C9orf72 knockdown, without concomitant TMEM106B overexpression, results in a small, but significant, decrease in the size of LAMP1+ organelles. These data also support the notion that C9orf72 and TMEM106B may function in the same cell biological pathways regulating the biogenesis, size, trafficking, or turnover of these organelles.

Several limitations of our study deserve consideration. First, because many common variant correlates of disease risk may act through *cis*-regulatory effects on expression of specific genes (Gilad et al., 2008), we modeled these effects in our specific FTL-D-TDP case by overexpression of *TMEM106B*. Such a strategy is not without its dangers, since overexpression may cause cellular artifacts. We guarded against such a possibility in several important ways. First, we evaluated levels of TMEM106B overexpression by immunoblot in all experiments, allowing us to verify that the observed cellular phenotypes occurred reliably at TMEM106B overexpression levels ranging from ~2-10X (**Figure 3.7b, c**). In addition, we employed as controls both overexpression of a different lysosomal protein (LAMP1) and overexpression ENQLVAAA TMEM106B, in each case confirming that expression levels of control were equivalent to or

greater than wild-type TMEM106B overexpression levels. Finally, we demonstrated that effects of TMEM106B overexpression on organelle morphology, acidification, and toxicity could be rescued by manipulation of a second disease-relevant protein, C9orf72. Taken together, these control measures greatly decrease the possibility that the observed effects of increased TMEM106B expression are non-specific overexpression artifacts.

A second limitation of our study is that we have modeled effects of TMEM106B overexpression by transient transfection. While the advantage of such an approach is that it allows for comparisons of cells overexpressing vs. not overexpressing TMEM106B within the same field, longer-term effects of alterations in expression might not be captured.

Third, our study focused on the effects of disease-relevant increases in TMEM106B expression on lysosomes, finding, in the process, that observed phenomena are dependent on the presence of C9orf72. We note here that previous work by our group (Chen-Plotkin et al., 2012) and others (Cruchaga et al., 2011; Brady et al., 2013; Lang et al., 2012) also suggests a potential connection between TMEM106B and progranulin based on genetic and cell-based analyses. Since progranulin localizes to lysosomes (Brady et al., 2013), and humans without functional progranulin manifest with a lysosomal storage disorder (Smith et al., 2012), the potential for TMEM106B-induced effects on lysosomes to affect progranulin pathways as well, either in neurons themselves or in other support cells in which progranulin expression is very high (e.g. microglia), is also an area worthy of further investigation.

In summary, since the discovery of the *TMEM106B* locus as a genetic risk factor for FTLT-DTP in 2010 (Van Deerlin et al., 2010), multiple groups have worked to understand the significance of TMEM106B in disease pathophysiology (Brady et al., 2013; Chen-Plotkin et al., 2012; Lang et al., 2012; Nicholson et al., 2013; Stagi et al., 2014; Schwenk et al., 2014). Here we dissect at a cell biological level the effects of disease-associated increases in TMEM106B expression, demonstrating significant effects on lysosomal morphology and impairment in lysosomal acidification, with associated cytotoxicity. We moreover demonstrate that these effects may depend on the presence of a second FTLT-DTP-associated protein, C9orf72. Our study thus

establishes the importance of lysosomal pathways to the development of FTLD-TDP and suggests a mechanistic interaction between TMEM106B and C9orf72.

3.4 MATERIALS AND METHODS

Constructs:

C9orf72 constructs – FLAG-C9orf72: open reading frame of human C9orf72 (transcript variant 2 NM_018325.3) in pCMV6 vector (Origene); this construct is dual-tagged with myc-FLAG inserted after the C-terminus; however, because only the FLAG was used for antibody detection, we hereinafter refer to this construct as FLAG-C9orf72.

Control constructs – 5TO: pcDNA/5TO backbone vector (Invitrogen). GFP: GFP was cloned into the pcDNA/5TO vector (Invitrogen). GFP-LAMP1: gift from L. Volpicelli-Daley (University of Alabama, Birmingham, AL). LAMP1: human LAMP1 in pCMV6-XL5 (Origene).

TMEM106B constructs – (1) FLAG-TMEM106B: the 5' untranslated region and open reading frame of TMEM106B and a C-terminal FLAG tag were cloned into pcDNA 3.0 vector (Life Technologies). (2) GFP-TMEM106B: cloned into pEGFP-C3 vector (Clontech) by F. Hu (Cornell University, Ithaca, NY) as previously described (Brady et al., 2013). (3) myc-TMEM106B: the 5' untranslated region and open reading frame of *TMEM106B* and an N-terminal myc tag were cloned into pcDNA 3.0 (Life Technologies).

Lysosomal motif mutants

Point mutations were introduced to putative lysosomal sorting motifs in the parent FLAG-TMEM106B construct (see previous section). Mutations to the tyrosine and dileucine-based motifs were created using the QuikChange II Site-Directed Mutagenesis Kit and primer design software (Agilent Technologies). The primer used to mutate YVEF → AVEF was tctgtaaattccacagctggaaactgagagacatctccatttctcc, YDGV → ADGV was gatgtgactccatcagcagcatcttcttgctgaatgcaaagg, and ENQLVALI → ENQLVAAA was tctctgatcactatatggagccgctgccaccagttggttttctgcccc.

Cell culture, transfection, and nucleofection:

Primary cortical and hippocampal mouse neurons were prepared from embryonic day 18 (E18) to E20 C57BL/6 mice. For each nucleofection, 5 million neurons in suspension were spun down at 80xg and resuspended in 100 μ l Mirus BioLingenio Electroporation Solution (Mirus #50111). To introduce expression constructs into neurons, neurons were then transferred to an Eppendorf containing 10 μ g of the construct in question, gently mixed, and transferred to an Amaxa aluminum electrode cuvette (Lonza). Mouse cortical and hippocampal neurons were nucleofected on program O-005 on a Nucleofector 2b machine (Lonza). After nucleofection, 500 μ l RPMI media (Corning #1040-CM) was gently added to the cuvette; media and cells were transferred to an Eppendorf tube and incubated in a tissue culture incubator at 37°C for 5-10 minutes to allow cells to recover. Neurons were then aliquoted at 80-100 μ l per well of a 12-well plate containing poly-L-lysine coated coverslips and 1 ml of Neurobasal media (Gibco #21103-031) supplemented with B27 (Gibco #17504-010) and Glutamax (Gibco #35050-061) per well. The following day, half of the volume of media was exchanged with fresh media.

Cos7, HEK293, HeLa, and U2OS cells were also used for experiments and maintained in complete DMEM medium (supplemented with 10% FBS (Gemini #900-108), 1% Pen-Strep (Gibco #15410), and 1% L-Glutamine (Gibco #25030)). U2OS cells stably expressing mCherry-GFP-LC3 were a gift from C. Coyne (University of Pittsburgh, Pittsburgh, PA) and have been previously described (Moy et al, 2014). For transient transfections, cells were plated the day prior to transfection; cells were transfected at 60-90% confluency using Lipofectamine 2000 (Invitrogen). Transfections were conducted in serum-free DMEM media (Gibco #19965) according to manufacturer's instructions; after 5-6 hours, serum-free medium was replaced with complete DMEM medium.

Immunoblotting:

Immunoblots were performed as previously described (Neumann et al., 2006). The following antibodies and conditions were used: N2077 rabbit TMEM106B antibody at 1 μ g/ml (Chen-Plotkin et al., 2012); EGFR (Cell Signaling #2232) at 1:1000; LC3: rabbit anti-human

(MBL) at 1:750; LAMP1 H4A3 at 0.5 µg/ml; alpha tubulin: mouse monoclonal DM1A (abcam #ab7291) at 0.1333 µg/ml (1:7500); C9orf72: rabbit anti-human at 1:500 (Sigma #023873).

Live and immunofluorescence microscopy:

Live images were taken with the EVOS FL Cell Imaging System (Life Technologies) at 40x or 60x magnification.

Double- and triple-label immunofluorescence labeling experiments were performed as previously described (Chen-Plotkin et al., 2012). The following primary antibodies and conditions were used: C9orf72: anti-human rabbit C9orf72 (Sigma #HPA023873) at 0.8 µg/ml (1:250); EEA-1: rat anti-mouse EEA-1 (BD #610456) at 1:100; GFP: goat polyclonal anti-GFP (abcam #6673) at 0.98 µg/ml (1:1000); LAMP1 1D4B: rat anti-mouse 1D4B (DSHB) at 1 µg/mL; LAMP1 H4A3: mouse anti-human H4A3 (DSHB) at 1 µg/ml; SV-2 mouse anti-mouse SV-2 (DSHB #SV2) at 1:3000. TMEM106B: custom rabbit anti-human, anti-mouse N2077 polyclonal antibody raised against amino acids 4-19 of TMEM106B at 1 µg/ml; custom chicken anti-human N2077 serum raised against the same peptide at 1:2000. TMEM106B antibody characterization has been previously reported (Chen-Plotkin et al., 2012). Secondary antibodies: goat anti-rabbit Alexa Fluor 488 (Life Technologies #A-11008); goat anti-rabbit Alexa Fluor 594 (Life Technologies #A-11037); goat anti-chicken Alexa Fluor 488 (Life Technologies #A-11039) all used at 1:1000. AMCA anti-mouse (Vector Laboratories #CI-2000) at 1:100. LysoTracker DND-99 (Life Technologies #L-7528) was used as previously described (Chen-Plotkin et al., 2012). Images were taken on a Nikon 80i upright fluorescence microscope and analyzed with Nikon NIS-Elements AR Imaging Software.

BODIPY 493/503 (Life #D-3922) was used per manufacturer's instructions. Briefly, cells grown on coverslips were washed with PBS and fixed with 2% paraformaldehyde. BODIPY stock (1 mg/ml in 100% EtOH) was freshly diluted at 1:500 in DPBS and incubated on the coverslips in the dark at room temperature for 15 minutes. Coverslips were then rinsed with DPBS three times,

then counterstained with DAPI and mounted with ProLong Gold mounting medium (Life #P36930).

Quantification of LAMP1+ organelle diameter:

The maximum diameter of the ten largest LAMP1+ organelles (by visual inspection) within each cell analyzed was measured using the Nikon NIS-Elements AR Imaging Software, with >150 LAMP1+ organelles (>15 cells) measured for each condition from images captured at 40X.

In the C9orf72 knockdown experiments, HeLa and HEK293 cells were transiently transfected with TMEM106B plus one other transfectant, which could be: (1) siRNA targeting C9orf72, (2) nontargeting siRNA control, (3) C9orf72 construct, for overexpression, or (4) nothing, as indicated in the text. Within each transiently transfected well, there are cells that over-express TMEM106B as well as neighboring cells that do not. These are readily distinguishable by staining with antibodies against the TMEM106B construct. Raw data were scored for TMEM106B over-expressing cells vs. TMEM106B non-over-expressing cells, in these various transiently-transfected conditions. These raw data were then normalized to the control condition (cells that have no additional transfectant – condition #4 above -- and are deemed not to over-express TMEM106B by immunofluorescence microscopy).

Quantification of LC3 puncta, LAMP1 organelles, LysoTracker mean fluorescence intensity:

LC3 puncta quantification: LC3 puncta were quantified in HeLa cells as well as U2OS cells stably expressing mCherry-GFP-LC3. For HeLas, cells were transfected with TMEM106B or GFP control constructs and stained with N2077 or anti-GFP antibodies to identify the cells expressing each construct. Anti-LC3 antibody was used to stain autophagosomes. 20 fields were captured at 40x magnification using Nikon NIS-Elements AR Imaging Software. LC3+ puncta were then counted in >75 cells for each condition – GFP-expressing, TMEM106B-expressing and no-

construct-expressing cells for two independent experiments. mCherry-GFP-LC3 U2OS cells were similarly transfected with TMEM106B or LAMP1 (Origene) and stained with N2077 and anti-LAMP1 H4A3 antibody, respectively. 50 fields were imaged at 60x magnification for each condition. The number of red and yellow LC3 puncta per cell was then counted for >50 cells for each condition. The average number of yellow dots (autophagosomes) and red dots (autolysosomes) per cell was calculated (\pm SEM). The % autophagosomes was calculated as yellow dot/total red dot x 100 (Lu 2013). Data from two identical replicates were combined and graphed.

LAMP1 quantification: Cells transfected with GFP or TMEM106B were stained for GFP or TMEM106B respectively, as well as LAMP1. For each transfection condition, 12 fields were captured at 60x magnification. The total number of LAMP1+ organelles per cell was then counted for 25 GFP- and TMEM106B-overexpressing cells and 10 no-construct-expressing cells, and the average number per cell was calculated (\pm SEM). Graph displays data from three replicate experiments performed by two independent operators.

LysoTracker mean fluorescence intensity (MFI): Primary mouse hippocampal neurons were nucleofected with either GFP-TMEM106B or GFP-LAMP1. At DIV4, LysoTracker Red DND-99 (Life Technologies) was administered according to manufacturer's instructions and coverslips were stained for DAPI and mounted onto slides. The average cytosolic MFI was determined as previously described (Chen-Plotkin et al., 2012) for GFP-LAMP1-expressing, GFP-TMEM106B-expressing and no-construct-expressing cells. >180 neurons were counted for each condition. Data from four identical experiments were compiled and graphed.

EGF-R degradation and EGF trafficking assays:

EGF-R degradation assays: HeLa cells were transfected with FLAG-TMEM106B, GFP or 5TO (vector) constructs. The next day, media was replaced with serum-free DMEM media. After 24h starvation, 25 mg/ml cycloheximide (Sigma #C1988) was added to the wells; cells were then stimulated with 100 ng/ml recombinant EGF (Invitrogen # PHG0311). At each timepoint, cells

were lysed and harvested into 1x RIPA on ice and immunoblots were performed with anti-EGFR antibody at 1:1000. Densitometry was used to quantify the amount of EGFR as normalized to alpha tubulin for four replicate experiments.

EGF trafficking assays: A previously published protocol was adapted (Urwin et al., 2010). In brief, HeLa cells were transfected with TMEM106B; 24-hours later, media was changed to serum-free media containing 1 μ M leupeptin in DMSO (Sigma #L2023) and 1 μ M pepstatin in DMSO (Sigma #P4265). EGF-488 (Invitrogen #E-13345) was then added at 50 ng/ml or 400 ng/ml. The 0h timepoint was immediately fixed and immunofluorescently labeled with anti-LAMP1 H4A3 and N2077. For subsequent timepoints, after 20 minutes of pulsing with EGF-488, media was removed, cells were washed, and media containing unlabeled recombinant EGF, leupeptin, and pepstatin was added to the cells. Coverslips were fixed at each timepoint and immunofluorescently labeled. Z-stack images were taken at 100x and deconvolved using Nikon NIS-Elements AR Imaging Software. For each timepoint, ~8 fields were taken; non-over-expressing and over-expressing cells (>12 each) were outlined using the region-of-interest tool and Mander's overlap was determined between the LAMP1- and EGF channels with the Nikon NIS-Elements AR Imaging Software, comparing neighboring cells with vs. without TMEM106B overexpression.

Cytotoxicity (LDH) assays:

The Clontech lactate dehydrogenase (LDH) assay #630117, an LDH-based colorimetric kit, was used for quantitation of cytotoxicity. LDH release is indicative of compromise of cell membrane integrity. HeLa cells were transfected as described above with FLAG-TMEM106B, LAMP1, ENQLVAAA TMEM106B or 5TO vector backbone constructs. At 0 hours, 24 hours, and 48 hours after transfection, 150 μ l media was removed from each condition and centrifuged at 800xg for 5 minutes. 100 μ l of supernatant was then gently transferred into a clear 96-well plate; 100 μ l of LDH Reaction Mixture (Clontech LDH assay #630117) was then added to each well. The plate was incubated at room temperature in the dark for ten minutes, then read at 492 nm

with a 620 nm reference wavelength. The percent cytotoxicity was calculated as indicated by the manufacturer: $(\text{Absorbance} - \text{Low control}) / (\text{High control} - \text{low control})$, with “low control” being media collected from untransfected cells and “high control” being media collected from cells treated with Triton-X to release maximal LDH. Trypan Blue assays were also used to assess cytotoxicity. 48 hours after transfection, media was collected, adherent cells were trypsinized and added to the collected media, and cells were spun down at 800xg for 5 minutes. Media was then removed and a 50/50 mix of DMEM and 0.4% Trypan Blue were used to resuspend the cells. The number of blue and total cells were counted using a hemacytometer.

Terminal deoxynucleotidyl transferase dUTP nick end labeling (TUNEL) assays were used to assess for cells with apoptosis-induced DNA damage. HeLa cells were transfected with FLAG-TMEM106B or control empty vector. At 24 hours after transfection, staurosporine (Sigma #S6942-200) was added to a final concentration of 1 μM to positive control wells and cells were returned to the incubator for an additional 4 hours. Coverslips were then removed from the wells for immunofluorescent labelling, with TMEM106B over-expressing cells identified by staining against the FLAG tag. The TUNEL assay was then performed according to manufacturer's protocol (Roche #11 684 795 910), with the TUNEL fluorescein reaction mixture incorporated into the secondary antibody step of immunofluorescent labelling. Images were taken on a Nikon 80i upright fluorescence microscope and analyzed with Nikon NIS-Elements AR Imaging Software.

Electron microscopy:

Tissues for electron microscopic examination were fixed with 2.5% glutaraldehyde, 2.0% paraformaldehyde in 0.1M sodium cacodylate buffer, pH 7.4, overnight at 4°C. After subsequent buffer washes, the samples were post-fixed in 2.0% osmium tetroxide for 1 hour at room temperature, and rinsed in dH₂O. After dehydration through a graded ethanol series, the samples were infiltrated and embedded in EMBED-812 (Electron Microscopy Sciences, Fort Washington, PA). The glass cover slips were dissolved with hydrofluoric acid, and thin sections were taken and stained with uranyl acetate and lead citrate prior to examination with a JEOL 1010 electron

microscope fitted with a Hamamatsu digital camera and AMT Advantage image capture software. For analysis, grids with cells or neurons nucleofected with either control or TMEM106B expression constructs were then scanned systematically; non-dividing, non-apoptotic cells were imaged in an unbiased manner

C9orf72 knockdown:

Two rounds of knockdown with 120 pg of siRNA against C9orf72 (GE Healthcare ON-TARGETplus SMARTpool #L-013341-01 Human C9orf72) or 120 pg of siControl (GE Healthcare ON-TARGETplus Non-targeting Pool #D-001810-10-05) were performed at 24 hours and 48 hours after cell plating. For experiments that required concomitant overexpression of another construct, the overexpression construct was transfected in parallel with the siRNA during the second round of knockdown.

As a second method to confirm specificity of C9orf72 knockdown effects, we used 4 µg of shRNA against C9orf72 (Origene pRS construct # TR305711 construct C) or 4 µg of an shRNA to GFP as a negative control (Origene pRS construct # TR30003). Transfections were performed 24 hours and 48 hours after plating, with overexpression of TMEM106B occurring at the same time as the 48-hour knockdown transfection.

Statistical tests:

Two-tailed nonparametric (Mann-Whitney) tests were used except for time-course experiments, for which two-way ANOVAs were used instead. Fisher exact tests were used for electron microscopy analysis given low event counts in some control categories. Calculations were performed using GraphPad Prism 5.

Quantitative PCR:

qPCR was performed per standard protocols. Relative quantification was performed (delta–delta method) using the geomean of *ACTB* and *PPIA* as our reference housekeeping genes.

CHAPTER 4: DISCUSSION

PREFACE:

In this work, I have focused on the role of TMEM106B, a previously uncharacterized gene/protein implicated in risk for FTLD-TDP through genome-wide association of SNPs at this locus (Van Deerlin et al., 2003). I have demonstrated that TMEM106B is an endolysosomal protein in multiple cell types, including neurons, and that changing expression levels of TMEM106B perturbs endolysosomal/autophagosomal pathways. The latter result is significant because we and others (Van Deerlin et al., 2010; Yu et al., 2015; Nicholson et al., 2013; Chen-Plotkin et al., 2012) have shown that SNPs associated with increased risk for FTLD-TDP at the *TMEM106B* locus also correlate with increased expression of *TMEM106B*. My work adds to the growing body of evidence implicating dysfunction in the endolysosomal/autophagosomal pathway in the pathogenesis of FTLD.

In Chapter 2, I provide the first characterization of TMEM106B expression in human brain, demonstrating that in neurologically normal controls, TMEM106B is expressed in the cytoplasm of neurons, glia, and perivascular cells (endothelial cells or pericytes) and is found in a polarized, perikaryal distribution in neurons through all layers of the neocortex. In addition, I also find that TMEM106B exhibits a much more disorganized pattern in frontal cortical neurons from *GRN*-associated FTLD-TDP brain as compared to FTLD-tau, FTLD-TDP cases lacking *GRN* mutations, Alzheimer's disease, and neurologically normal controls. This is likely indicative of underlying endolysosomal dysfunction in *GRN*-associated FTLD-TDP, as subsequent LAMP1+ immunostaining recapitulated the TMEM106B immunostaining results with increased LAMP1+ disorganization seen primarily in *GRN*-associated FTLD-TDP specimens (Gotzl et al., 2014). As discussed below, whether this perturbation in endolysosomal pathways is due to progranulin deficiency, increased levels of TMEM106B, or a combination of both remains to be determined.

In Chapter 3, I investigate the cellular effects of disease-relevant, increased levels of TMEM106B. I find that increased TMEM106B expression decreases cell viability and results in

major perturbations of the endolysosomal/autophagosomal pathway. Increased TMEM106B levels also result in strikingly enlarged organelles positive for late endosomal/lysosomal markers, marked impairment of lysosomal acidification and degradation, and increased cellular toxicity. These biological effects of TMEM106B are dependent on its lysosomal localization, as point mutations in a potential lysosomal sorting motif abrogated these effects. Lastly, knockdown of *C9orf72* mitigated the effects of elevated TMEM106B expression. Coupled with our previous finding that *TMEM106B* acts as a genetic modifier affecting age at death in *C9orf72*-associated FTLT-DTP, this suggests that TMEM106B and *C9orf72* may interact, contributing to the pathophysiology of FTLT-DTP.

In the following sections, I will discuss important implications of these results in the context of existing literature on TMEM106B and on FTLT. I will highlight themes emerging from my own findings, as well as those of others, considering them in aggregate. Specifically, I will discuss the cell biological effects of TMEM106B overexpression and suggest two potential models that might underlie these effects. I then will discuss the relationship between TMEM106B and progranulin as well as *C9orf72*. Progranulin and *C9orf72* have two things in common which are pertinent here. First, genetic changes in each (*GRN* and *C9orf72*) are major autosomal dominant causes of FTLT-DTP. Second, both progranulin (Ghoshal et al., 2012; Petkau et al., 2010; Wils et al., 2012; Ahmed et al., 2007; Smith et al., 2012) and *C9orf72* (Farg et al., 2014; Levine et al., 2013b; O'Rourke et al., 2016) have been linked to endolysosomal/autophagosomal pathways in previous literature. Finally, I will consider the role of endolysosomal/autophagosomal dysfunction as a major disease mechanism underlying FTLT, pointing to specific roles that TMEM106B, *C9orf72*, progranulin may play in this over-arching pathophysiological cascade.

4.1 Changes in TMEM106B expression levels result in alterations to the endolysosomal/autophagosomal pathway

4.1.1 Increased levels of TMEM106B result in enlarged LAMP1 organelle size

Our laboratory and multiple investigators have shown that endogenous TMEM106B co-localizes with late endosomal/lysosomal markers, such as LAMP1, LAMP2, and Rab7 in a variety

of immortalized cell lines as well as mouse and rat primary cortical and hippocampal neurons (Lang et al., 2012; Schwenk et al., 2014; Stagi et al., 2014; Brady et al., 2013). Furthermore, TMEM106B does not appear to co-localize with synaptic vesicle markers or early or recycling endosomal markers (Schwenk et al., 2014; Brady et al., 2013; Chen-Plotkin et al., 2012). Additionally, we and others demonstrate that increased TMEM106B levels result in a striking phenotype of enlarged organelles, which maintain late endosomal/lysosomal marker immunoreactivity (Stagi et al., 2014; Brady et al., 2013; Lang et al., 2012), with my work extending this to primary murine neurons as well.

A question that remains is what are these enlarged organelles? They appear to be lysosome derived – N2A cells preloaded with dextran and transfected with TMEM106B demonstrate that many of these enlarged organelles are positive for dextran. In this experiment, cells are incubated with dextran, washed, then chased with growth medium such that dextran accumulates in and marks lysosomes (Ohkuma, 1989; Brady et al., 2013). The enlarged TMEM106B+ organelles were positive for dextran, suggesting they are likely derived from lysosomes. In addition, in a parallel experiment, TMEM106B was first transfected, then subsequently loaded with dextran and chased; these pre-existing TMEM106B overexpression-induced organelles were found to be accessible to administered dextran, suggesting no significant blockades between these organelles and incoming endosomes (Brady et al., 2013). My data also suggests that many of the enlarged organelles demonstrate immunoreactivity, and at times co-localization, for TMEM106B, LC3 and LAMP1 by immunofluorescence, suggesting that these organelles are additionally capable of fusing with LC3+ autophagosomes. The ultrastructure of these organelles also reveals them to be primarily single-membrane organelles which appear empty or contain cytoplasmic debris, multilamellar structures, and organelles in varying states of degradation. In some instances, we visualized a second membrane, suggestive of the inner membrane of an autophagosome being degraded following the fusion of a lysosome. Taken together, the morphological and immunofluorescence labeling data suggest that these enlarged organelles may be an aberrant entity with characteristics of late endosomes/lysosomes

or autolysosomes/amphisomes that demonstrate intact fusion capabilities but may fail to degrade effectively.

4.1.2 Increased levels of TMEM106B results in lysosomal acidification and degradative defects

In line with this, we also found that increased expression of TMEM106B, but not LAMP1 as a control, decreases the fluorescence of LysoTracker, as well as LysoSensor, in immortalized cells (Chen-Plotkin et al., 2012) as well as in primary neurons, indicative of an increase in intraluminal pH. This acidification defect was accompanied by delayed degradation of endocytic cargo; specifically, the lysosomal degradation of EGFR was impaired. Similar results were reported by Brady and colleagues – expression of GFP-TMEM106B in T98G cells, a glioblastoma cell line, resulted in impaired lysosomal degradation of EGFR compared to vector control (Brady et al., 2013). Additionally, I found that cells in which TMEM106B overexpression is established exhibit delayed targeting of endocytosed EGF to LAMP1+ organelles. However, whether this is a primary effect of TMEM106B overexpression itself or a secondary effect has yet to be determined – for example, TMEM106B levels could directly affect mechanisms of internalization or membrane trafficking to lysosomes; alternatively, the delay in EGF internalization itself may be a downstream consequence of TMEM106B's primary effect on another aspect of endolysosomal function, such as lysosomal acidification itself – accumulation of undigested material can slow down membrane trafficking and sorting (Parkinson-Lawrence et al., 2010; Luzio et al., 2007).

Impaired lysosomal acidification has previously been shown to play a role in other neurodegenerative diseases – for example, Alzheimer's-associated mutations in *PSEN1* may impair lysosomal acidification by impairing the trafficking of a vATPase subunit (Lee et al., 2010). Additionally, mutations in ATPase type 13A2 (*ATP13A2*), a component of the lysosomal acidification machinery, have been found in patients with hereditary parkinsonism (Williams et al., 2005; Dehay et al., 2012). Moreover, mutations in *LRRK2* are the most common known genetic cause of Parkinson's disease (Hedrich et al., 2006) and LRRK2 kinase activity has been

proposed to activate a Ca^{2+} -dependent pathway that results in alkalization of lysosomes as well as increased autophagosome formation (Gomez-Suaga et al., 2012).

Late endosomal/lysosomal acidification is maintained primarily by the vATPase, with ClC transporters (which mediate Cl^- transport) and Na^+/K^+ channels providing the counter-ions to uphold this 100-1000x H^+ gradient. Maintenance of this gradient is vital to lysosomal trafficking, maintenance, and generation of the membrane potential, as well as content condensation during membrane fusion (Luzio et al., 2007). The vATPase consists of V_0 and V_1 domains and operates through an incompletely understood mechanism in which each cycle of ATP hydrolysis by the V_1 domain results in rotation of the V_0 rotor domain (Forgac, 2007). This coordinated rotation results in the translocation of H^+ ions into the lysosomal lumen.

I note in this context our preliminary data from an initial immunoprecipitation-mass spectrometry experiment. I expressed FLAG-TMEM106B in HEK293 cells, immunoprecipitated against the FLAG tag, and subjected the immunoprecipitated material for peptide identification of potential TMEM106B binding partners by mass spectrometry. Intriguingly, my initial data demonstrate that TMEM106B may interact with several vacuolar ATPase (vATPase) subunits: **1) subunit a**, part of the integral domain V_0 which is involved in fusion between lysosomes and phagosomes as well as in the acidification of synaptic vesicles in neurons as well (Nishi and Forgac, 2000; Hiesinger et al., 2005); **2) subunit A**, part of the cytosolic domain V_1 which plays a role in ATP binding and hydrolysis (Forgac, 1998); and **3) subunit B2 (brain isoform)**, part of the V_1 domain, shown to bind to actin and aid in vATPase recycling (Bernasconi et al., 1990). The interaction of TMEM106B and the vATPase was also found in a repetition of this experiment by others in the lab.

It is possible that our preliminary findings are artifactual, as the vATPase can appear as a non-specific hit in immunoprecipitation-mass spectrometry experiments; we minimized this possibility as much as possible by comparing TMEM106B overexpression hits to hits from a GFP overexpression control, subtracting non-specific hits and hits obtained from a TMEM106B knockdown condition control, to enrich for true interactions. I will next attempt to confirm these

interactions through co-immunoprecipitation or pulldown experiments between TMEM106B and individual subunits. If confirmed, a direct interaction between TMEM106B and elements of the vATPase raises the possibility that increased TMEM106B may disrupt the assembly or function of the vATPase, perhaps by binding to and sequestering critical subunits, ultimately resulting in downstream failure to acidify organelles. Additionally, future experiments should be aimed at further elucidating the acidification defect on lysosomal function, such as assessing if it impairs the maturation and thus activation of lysosomal enzymes, such as Cathepsin D. This would further support my hypothesis that increased levels of TMEM106B result in significant lysosomal dysfunction.

4.1.3 Increased levels of TMEM106B may impact autophagy pathways

As discussed above, our LC3 immunofluorescent experiments and ultrastructural analysis suggested the increased TMEM106B levels may impact autophagy pathways. As preliminary experiments, we enumerated the number of LC3+ organelles/cell, and found that they significantly increased upon TMEM106B overexpression, but not with GFP overexpression control. Additionally, expression of ENQLVAAA TMEM106B resulted in only a minimal increase in LC3 puncta, despite much higher expression levels than wild-type TMEM106B. This suggests that the significant increase in LC3+ organelles seen upon TMEM106B expression is dependent on the localization of TMEM106B to the lysosomal membrane.

The observed apparent increase in LC3 may be the result of 1) an increase in autophagosome formation 2) a block in downstream autophagic flux, such as due to the lysosomal acidification defect or 3) a combination of both (Mizushima et al., 2010; Klionsky et al., 2012). The third scenario is seen in a subset of lysosomal storage diseases – primary defects in lysosomal function as seen in murine models of Niemann-Pick type C disease as well as Gaucher's are also associated with a maladaptive increase in basal autophagy (Lieberman et al., 2012). Indeed, my preliminary data, discussed below, suggest mTORC1 is inhibited upon TMEM106B expression, linking TMEM106B expression to autophagic induction. Consistent with this, Stagi et al. report that TMEM106B overexpression results in increased TFEB translocation to

the nucleus (Stagi et al., 2014); TFEB translocates to the nucleus upon mTORC1 inhibition, as mTORC1 inhibition releases TFEB from mTORC1-mediated phosphorylation and inactivation (Zhou et al., 2013). To help clarify the effect of TMEM106B on autophagic flux, future experiments will include monitoring the degradation of long-lived proteins, autophagic substrates such as p62, and TDP-43 itself (which has been shown to be degraded by autophagy as well as the ubiquitin proteasome system (Brady et al., 2011) over extended periods of carefully controlled levels of TMEM106B expression.

4.1.4 TMEM106B overexpression may skew the endolysosomal/autophagosomal pathway towards a net increase in fusion products

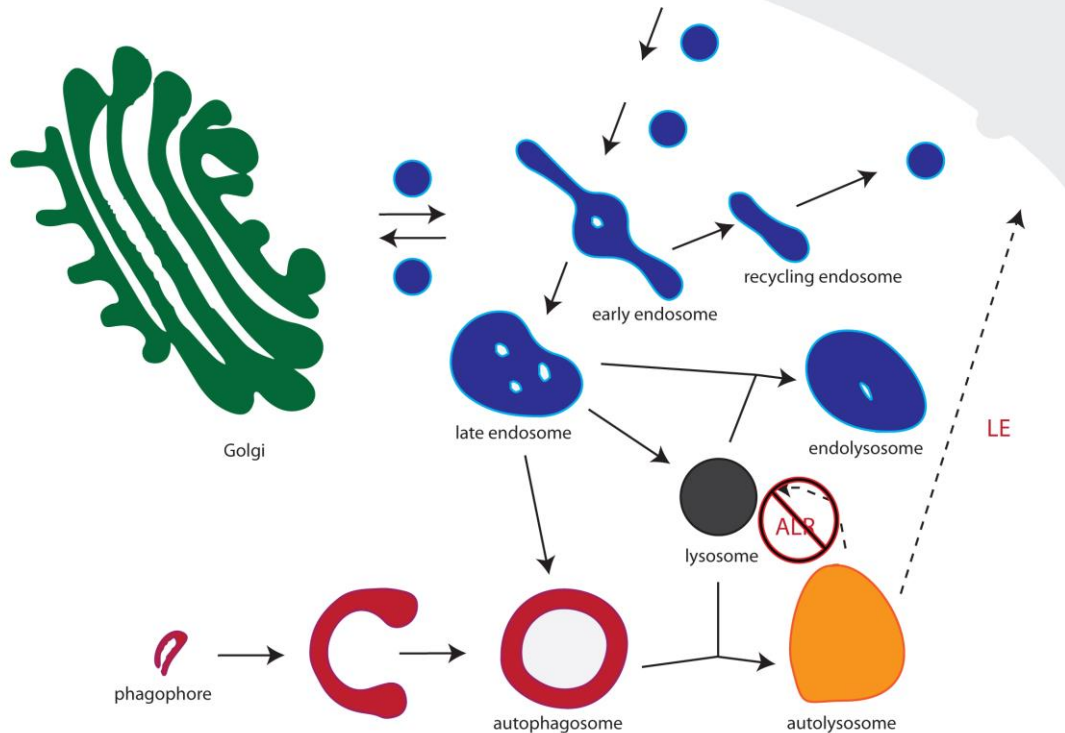
While the effects of TMEM106B overexpression on autophagy pathways await further clarification, I note that the increase in the number of LC3+ structures upon wild-type TMEM106B expression was accompanied by a significant *decrease* in the number of LAMP1+ organelles in HeLa cells and primary mouse hippocampal neurons. Non-overexpressing cells display many small, punctate LAMP1+, LysoTracker-^{bright} organelles, while TMEM106B overexpressing cells display a marked absence of this punctate population and instead are predominated by fewer, enlarged LAMP1+ LysoTracker-^{dim} organelles. Taken together, I hypothesize these data suggest that elevated TMEM106B levels bias the endolysosomal/autophagosomal pathway towards a net increase in secondary lysosomes (such as endolysosomes, amphisomes, and autolysosomes) and that this is accompanied by depletion of the normal lysosomal pool.

In response to physiologic changes in cellular status, membrane fusion/fission events trigger short-lived increases in lysosomal size and the genesis of larger (>0.5 μ m) LAMP1+ secondary lysosomes (such as endolysosomes (ELs), autolysosomes (ALs), and amphisomes). (Yu et al., 2010). These secondary lysosomes are usually transient species which return to normal-sized primary lysosomes via lysosomal reformation or fission (Luzio et al., 2007; Xu and Ren, 2015; Yu et al., 2010). However, changes in trafficking flux, or the accumulation of undegraded material such as seen in lysosomal storage diseases may result in vesicle enlargement (Walkley and Vanier, 2009). For instance, defective lysosomal reformation (leading

to persistent ALs), or, impaired autophagosome-lysosome fusion (leading to ELs via increased endosome-lysosome fusion), can increase the lifespan of these typically transient enlarged species. This increase in the lifespan of these secondary lysosomes results in disequilibrium between input and output along the endolysosomal/autophagosomal pathway (Lieberman et al., 2012). Moreover, the incompletely digested materials within these enlarged species can result in their further enlargement, ultimately causing escalating disruption of the endolysosomal/autophagosomal pathway (Xu and Ren, 2015; Walkley and Vanier, 2009).

What then is the mechanism by which TMEM106B overexpression results in the observed skew towards the predominance and persistence of secondary lysosomes? A number of possibilities exist, but they may be considered in the form of two general models: TMEM106B overexpression may skew the endolysosomal/autophagosomal pathway towards secondary lysosomes (autolysosomes, amphisomes, endolysosomes), either by (1) decreasing their dissolution, or (2) increasing their formation.

Figure 4.1: Model 1



Model 1: TMEM106B overexpression results in persistent secondary lysosomes through inhibition of autophagic lysosomal reformation.

ALR = autophagic lysosomal reformation. LE= lysosomal exocytosis.

Adapted from (Tooze and Yoshimori, 2010).

Our data suggests elevated levels of TMEM106B may result in a defect in the resolution of secondary lysosomes; given the observed co-localization with LC3, I posit these secondary lysosomes may comprise primarily amphisomes/autolysosomes. Persistent amphisomes/autolysosomes can result from impairment in several major processes, including: 1) autolysosomal exocytosis or 2) autophagic lysosomal reformation. In autolysosomal exocytosis, autolysosomes fuse with the plasma membrane, and their contents are expelled (Reddy et al., 2001; Samie and Xu, 2014). However, impaired lysosomal acidification and TFEB overexpression are typically associated with *increased* autolysosomal exocytosis (Ejlervskov et al., 2013; Martina

et al., 2014; Medina et al., 2011; Spampanato et al., 2013). Thus, although it is possible that increased TMEM106B overexpression may interfere with the autolysosomal exocytic machinery (Heuser, 1989; Pryor et al., 2000) or impair the Ca^{+2} influx required for lysosomal fusion with the plasma membrane (Jahn and Scheller, 2006), decreased autolysosomal exocytosis seems less likely given that TMEM106B overexpression is associated with lysosomal acidification defects and potentially increased TFEB translocation to the nucleus (Stagi et al., 2014).

It is more likely that the persistent amphisomes/autolysosomes represent impairment in the process of autophagic lysosomal reformation (ALR). This hypothesis is consistent with: 1) the enlarged persistent LC3+ organelles we see by immunofluorescence 2) the lysosomal acidification and degradation defects observed and 3) the associated loss in lysosomal number seen with TMEM106B overexpression.

ALR was first characterized as an evolutionarily conserved mechanism that coordinates nutrient sensing and lysosomal homeostasis in starvation-induced autophagy (Yu et al., 2010). Starvation typically results in the inhibition of mTORC1 and the induction of autophagy. However, after this initial period of inhibition, mTORC1 is reactivated and ALR commences. This reactivation is associated with the budding off of protolysosomes from autolysosomes/amphisomes, resulting in the restoration of the lysosomal population and the disappearance of autolysosomes/amphisomes (Yu et al., 2010; Chen and Yu, 2013; Rong et al., 2012). An impairment in ALR results in “stalled” autolysosomes which continue to fuse with existing lysosomes but do not resolve, depleting the lysosomal pool.

Importantly, ALR and the reactivation of mTORC1 have been shown to be dependent on the ability of the lysosome to degrade (Rong et al., 2012), suggesting that the impaired lysosomal acidification and degradation defects associated with increased TMEM106B may have significant consequences on ALR and exhibit sustained mTORC1 inhibition. Indeed, my preliminary experiments assessing mTORC1 activity via phosphoS6K immunoblots (active mTORC1 phosphorylates S6K) show that while normal HEK293s reactivate mTORC1 9 hours after an initial starvation-induced inhibition, cells expressing TMEM106B at expression levels ranging from 2-5x

over endogenous levels do not reactivate mTORC1 and remain in a state of mTORC1 inhibition even 24h later (data not shown).

Notably, starvation-induced mTORC1 inhibition increases autophagosome formation; it also increases intracellular pH, clustering of lysosomes near the microtubule organizing center, autophagosome-lysosome fusion (Korolchuk et al., 2011), and TFEB translocation (Settembre et al., 2012; Roczniak-Ferguson et al., 2012; Martina et al., 2014). TMEM106B overexpression is similarly associated with increased autophagosome formation, increased intracellular pH, and the appearance of enlarged LC3+ LAMP1+ organelles, alterations in lysosomal trafficking and positioning, and TFEB translocation (Chen-Plotkin et al., 2012; Schwenk et al., 2014; Stagi et al., 2014), possibly representing a state of sustained impaired ALR. TMEM106B overexpression would thus be expected to result in impaired autolysosomal clearance accompanied by a decrease in the number of available lysosomes.

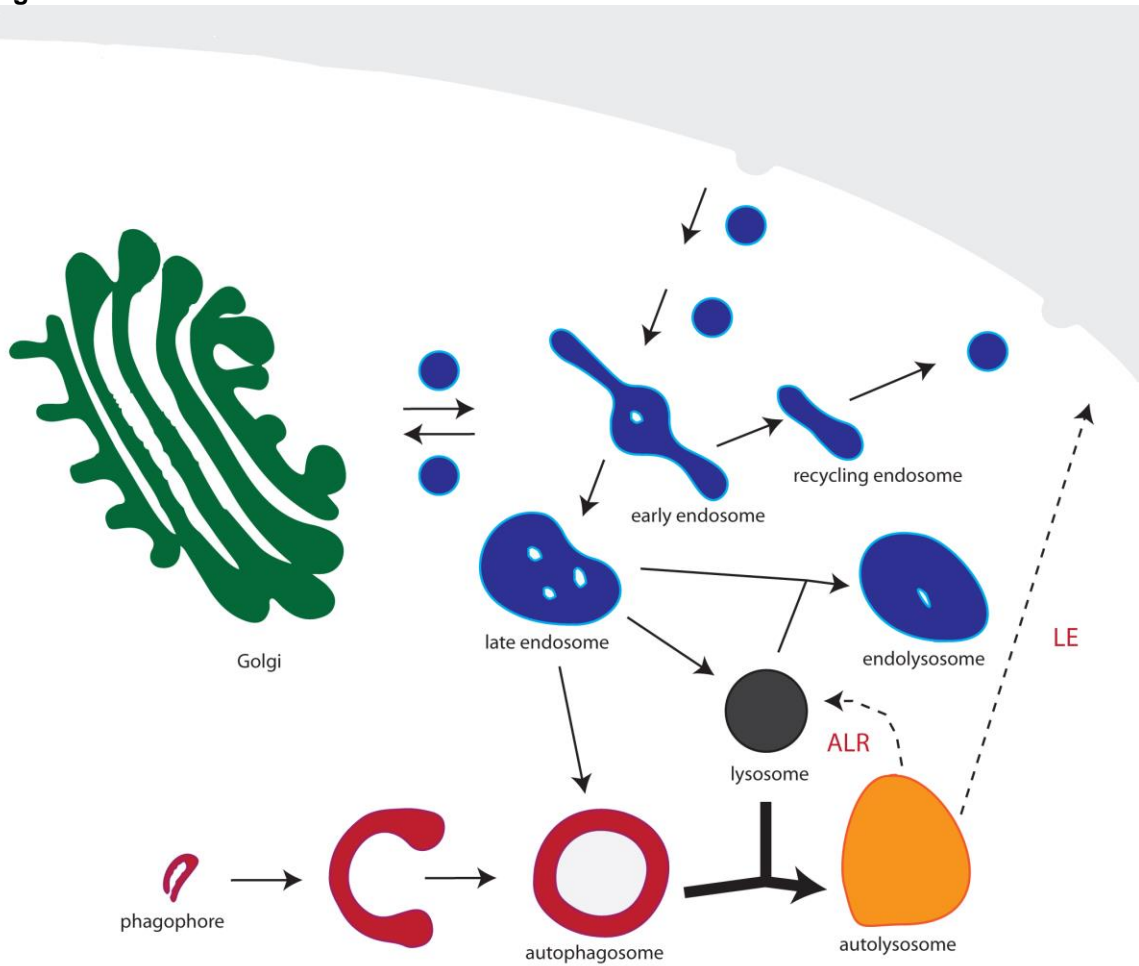
An important next step would be to confirm the dynamics and efficiency of autolysosomal clearance. As one example, the fluorescent lysosomal substrate DQ-BSA can be monitored in control versus TMEM106B overexpressing cells over time to assess for defects in lysosomal degradation. DQ-BSA is a self-quenched dye conjugated to BSA which, when digested by lysosomal proteases, is dequenched releasing highly fluorescent protein fragments (Voss et al., 1996). In addition, to assess if the formation of the enlarged LAMP1+ organelles is indeed autophagy dependent (as would be expected in ALR), we have begun experiments knocking down essential autophagy genes in the context of TMEM106B overexpression. We can also assess if restoring mTORC1 activity, in the context of TMEM106B overexpression, such as with 3-benzyl-5-((2-nitrophenoxy) methyl)-dihydrofuran-2(3H)-one (Ge et al., 2014), abrogates the vacuolar phenotype.

One possible mechanism as to why increased TMEM106B may impair ALR is via perturbation of the vATPase/mTOR/Ragulator axis, which is important for coordinating lysosomal responses to cellular stressors and nutrient states (Settembre et al., 2013). The effect of TMEM106B overexpression on the vATPase/mTORC1/Ragulator axis could be indirect, such as

by altering lysosomal membrane integrity or lysosomal size (via changes in ion content, osmolarity (Bandyopadhyay et al., 2014), decreases or increases in trafficking and membrane fusion and fission events (Settembre et al., 2013), or impaired lysosomal degradative capacity (Lieberman et al., 2012). Another possibility is via TMEM106B's proposed interaction with the vATPase subunits. ATP hydrolysis by the vATPase is necessary for the vATPase to mediate amino-acid sensitive interactions between Ragulator and RAG GTPases which recruit mTORC1 to and, together with RHEB (Ras homologue enriched in brain), activate it at the lysosomal membrane (Zoncu et al., 2011; Settembre et al., 2012). Elevated levels of TMEM106B may interfere with the proper assembly and function of the vATPase at the lysosomal membrane, thereby impairing the ability of vATPase to interact with Ragulator and Rag GTPases to recruit mTORC1 to the lysosomal membrane. In any case, we could assess the effect of TMEM106B levels on the localization of these players to the lysosomal membrane, especially mTORC1 localization, expecting that TMEM106B overexpression will correlate with decreased localization of mTORC1 at the lysosomal membrane.

One potentially puzzling observation is that TMEM106B overexpression has been shown by one group to result in increased TFEB translocation to the nucleus (Stagi et al., 2014), which might be expected at face value to *activate* lysosomal function through transcription of the CLEAR lysosomal and autophagosomal gene network. However, I note that TFEB translocation to the nucleus 1) is necessary but not sufficient to coordinate transcription of the CLEAR network (Zhou et al., 2013) and 2) increased expression of autophagosomal and lysosomal genes does not necessarily translate to enhanced lysosomal function – for example, in many lysosomal storage diseases, expression levels of lysosomal genes are increased in what is proposed to be compensatory response to reduced degradative capacity (Gotzl et al., 2014; Ballabio and Gieselmann, 2009; Lieberman et al., 2012). Confirmation of the TFEB translocation, as well as further identification of specific lysosomal and autophagosomal genes affected by TMEM106B overexpression, will be needed to further investigate these data.

Figure 4.2: Model 2



Model 2: TMEM106B overexpression results increases the production of secondary lysosomes via modulation of endolysosomal/autophagosomal Rab GTPase activity.
ALR = autophagic lysosomal reformation. LE = lysosomal exocytosis.

Adapted from (Tooze and Yoshimori, 2010).

As a second model, I propose that TMEM106B overexpression may primarily increase the production and enlargement of secondary lysosomes, primarily amphisomes/autolysosomes, via modulation of endolysosomal/autophagosomal Rab GTPase activity. This hypothesis stems from 1) my data demonstrating that TMEM106B overexpression effects are abrogated by C9orf72 knockdown 2) growing evidence that C9orf72 may function, potentially as a GEF as predicted, within the endolysosomal pathway (O'Rourke et al., 2016; Farg et al., 2014; Zhang et al., 2012). Taken together this would implicate TMEM106B in Rab GTPase-modulated pathways. Thus, I

hypothesize that TMEM106B modulates Rab GTPase activity to exert its effects on the endolysosomal pathway.

To assess this hypothesis, I would determine if TMEM106B modulates Rab GTPase activity by acting as an effector by using a panel of dominant negative and constitutively active forms of candidate Rab GTPases. While there are >60 mammalian Rabs, I would prioritize Rab GTPases that are known to be involved in endocytic and lysosomal trafficking as well as those shown to co-localize with C9orf72 (Farg et al., 2014). These would include Rab5, Rab7, Rab 11, as well as Rab38, noting the recent GWAS demonstrating it may be a genetic risk factor for frontotemporal dementia and its role in trafficking to lysosomal-related organelles and maturation of phagosomes (Ferrari et al., 2014; Bultema et al., 2012). Notably, constitutively active Rab7 has been reported to impair ALR, resulting in the accumulation of enlarged autolysosomes, with the dissociation of Rab7 a requirement for ALR to proceed (Yu et al., 2010). If TMEM106B is a Rab effector, we would also expect it to reverse or prevent the effects of dominant negative forms of Rabs when co-expressed with them. Additionally, I would assess the ability of TMEM106B to bind efficiently to GTP-bound constitutively active forms of Rabs and weakly if at all to dominant negative forms.

It is also possible that TMEM106B may not function as a Rab effector directly, but may modulate Rab GTPases via other avenues. For example, rather than exhibit effector activity itself, TMEM106B might interact with specific Rab effectors or alter the recruitment of a GEF or GTPase-activating protein (GAP) (GAPs are the counterparts to GEFs, and activate hydrolysis of GTP (Bos et al., 2007)). Alternatively, increased TMEM106B could impact Rab recruitment in general, increasing or decreasing recruitment to target membranes. This would follow a similar paradigm as one proposed to explain *CHMP2B*-associated FTL, in which *CHMP2B*-associated FTL mutant cells were defective in their ability to recruit Rab7 to late endosomal membranes, resulting in enlarged late endosomes and amphisomes (Urwin et al., 2010). If TMEM106B expression levels affect Rab recruitment, we would expect TMEM106B overexpression and knockdown to result in reciprocal changes in the candidate Rab's colocalization with its

associated endosomal/lysosomal membranes. This could be assessed by co-transfection of labeled Rab7, for example, with either TMEM106B overexpression or knockdown constructs followed by immunofluorescent staining for LAMP1+ and subsequent quantification of the level of co-localization between Rab7 and LAMP1.

4.1.5 Point mutations in an extended dileucine lysosomal sorting motif abrogates TMEM106B overexpression phenotypes

Our data demonstrate the effects of increased TMEM106B expression (the appearance of enlarged organelles, acidification defect, and cytotoxicity) are abrogated by point mutations to a potential extended dileucine lysosomal sorting motif in TMEM106B (ENQLVALI → ENQLVAAA). This provided a valuable overexpression control to my experiments and suggested that it is unlikely that the observed cell biological effects of TMEM106B overexpression are non-specific artifacts of protein overexpression, since they are not seen with the even higher levels of expression of ENQLVAAA TMEM106B, and are dependent on TMEM106B targeting to the lysosome. In addition, this provides domain-level detail for a protein that was uncharacterized prior to 2010.

The ENQLVAAA TMEM106B mutant will be useful in the future to identify and investigate the adaptor protein(s) and other proteins with which wild-type TMEM106B interacts. ENQLVALI may be an extended classical dileucine lysosomal targeting motif of the general consensus of [DE]XXXL[LI] (Letourneur and Klausner, 1992; Bonifacino and Traub, 2003). This demonstrates the importance of the [LI] in lysosomal targeting of TMEM106B, although other signals may contribute as well. Substitution of either of the critical leucines/iso-leucines by alanine has been shown to abrogate activities of [DE]XXXL[LI] signals (Letourneur and Klausner, 1992; Pond et al., 1995). [DE]XXXL[LI] motifs interact with heterotetrameric adaptor proteins, AP-1, AP-2, and AP-3 (Ohno et al., 1997; Braulke and Bonifacino, 2009; Hirst et al., 2011). Briefly, AP-1 regulates delivery of proteins from the trans-Golgi network to the endolysosomal system and back (Braulke and Bonifacino, 2009). AP-2 regulates clathrin-mediated endocytosis from the plasma membrane (Pearse and Robinson, 1990). AP-3 is found in endosomes and is thought to regulate

the transport of select proteins in the endolysosomal pathway (Le Borgne et al., 1998; Dell'Angelica et al., 2000).

I would expect that wild-type TMEM106B would interact with AP-1, AP-2, or AP-3 given the abrogation of its lysosomal localization by mutation of the [LI] in the potential dileucine motif, although ultimately, the adaptor protein with which a motif interacts must be experimentally determined. Initial yeast-two hybrid results from by Stagi et al. using the cytoplasmic domain of TMEM106B as bait and a prey library derived from human adult brain report that TMEM106B interacts with the μ 2 subunit AP-2 as well as with CLTC (clathrin heavy chain) (Stagi et al., 2014), both of which play a major role in the formation of coated vesicles (Kirchhausen, 2000; Pawlowski, 2010). Intriguingly, AP-2 has been shown to complex with other proteins to act as an autophagic cargo receptor for the amyloid precursor protein cleaved C-terminal fragment, linking the endocytic pathway to the autophagic degradation pathway in neurodegenerative disease (Tian et al., 2013). AP-2 has also been shown to be essential for autophagic lysosomal reformation (ALR), along with clathrin and PtdIns(4,5)P2 (Rong et al., 2012). Stagi et al.'s data is the first suggesting a potential interaction with AP-2 and will need to be confirmed by other investigators; notably, affinity for sorting adaptors is low and methods such as yeast two-hybrid, yeast-three hybrid, and GST-pulldown experiments will be required to explore potential interactions between TMEM106B and adaptor proteins.

However, understanding the molecular mechanisms underlying the effects of TMEM106B overexpression will require identification of other key binding partners. This will require the above methods as well as immunoprecipitation-mass spectrometry. The ENQLVAAA TMEM106B mutant may serve as a useful comparator in these experiments.

4.1.6 The endolysosomal/autophagosomal disturbances caused by increased TMEM106B are cytotoxic to cells

We began our work with the observation that specific genotypes in TMEM106B are associated with both increased TMEM106B expression and increased risk for neurodegeneration. This, in addition to the striking endolysosomal disruption we observed, led us to hypothesize that

increased levels of TMEM106B might have cytotoxic effects. Indeed, in HeLa cells, TMEM106B expression, but not LAMP1 expression, resulted in a significant increase in cell death. In parallel to these data, we observed that GFP-tagged TMEM106B-overexpressing cells “disappear” from culture within 72h after transfection, whereas cells transfected with GFP-tagged LAMP1 or the ENQLVAAA TMEM106B mutant remain.

Initial investigations into specific cell death pathways responsible for the observed cytotoxicity have been negative. Specifically, we and others (Brady et al., 2013) have shown that TMEM106B overexpressing cells are negative for TUNEL staining, suggesting that apoptotic cell death pathways do not play a major role in the observed cytotoxicity. However, I note that compromised lysosomal function results in a deficiency of precursors for biosynthetic pathways and cellular starvation, which may ultimately have deleterious effects on viability (Schulze and Sandhoff, 2011). To compensate for impaired degradative capacity, cells have been shown to initially maladaptively increase basal levels of autophagy (Ballabio and Gieselmann, 2009; Cang et al., 2014). These compensatory changes may initially help, but may ultimately result in cytotoxicity. While autophagy is often viewed as beneficial, mediating cellular homeostasis during stress conditions, inappropriate sustained autophagy has also been shown to induce cell death (Yu et al., 2004a; Yu et al., 2004b; Yu et al., 2008; Levine and Yuan, 2005). Thus, future investigations of other cell death pathways which exhibit autophagic vacuolization, including necroptosis (Basit et al., 2013; Bonapace et al., 2010; Bray et al., 2012) and autosis (Liu and Levine, 2015; Liu et al., 2013), may be a valuable addition here.

4.1.7 TMEM106B knockdown may alter lysosomal size and trafficking

While my data has focused mainly on the effects on increased TMEM106B, others have in parallel investigated the effects of TMEM106B knockdown. Notably, knockdown does not result in changes in expression levels in FTLD-associated proteins TDP-43, progranulin, FUS, or tau (Schwenk et al., 2014; Brady et al., 2013), and TMEM106B knockdown does not appear to have neurotoxic effects in primary rat cortical neurons (Schwenk et al., 2014). Investigations into the role of TMEM106B knockdown on lysosomal positioning and trafficking has yielded some results

that are concordant and some that are not. The data are concordant in that several groups demonstrate that TMEM106B knockdown results in changes in lysosomal positioning and movement within the dendrites of murine neurons. The data are discordant in that one group report that TMEM106B knockdown results in an increase in retrograde dendritic lysosomes (Schwenk et al., 2014), while another group find that TMEM106B knockdown results in overall distally distributed lysosomes, suggesting net anterograde movement (Stagi et al., 2014). Differences in neuronal populations assessed (mouse cortical versus rat hippocampal) and lysosomal markers used in live imaging (Rab7 versus LAMP1, which may identify different subsets of endolysosomal populations) may account for these discordant results.

These data are preliminary as the molecular players responsible for these events still need to be confirmed; however, they suggest an important role for TMEM106B levels in lysosomal motility and placement. With respect to my own findings, these data suggest that the real-time effects of aberrant lysosomal motility and placement might moreover explain the disorganized lysosomal staining pattern I observed by immunohistochemistry in the soma and dendrites of cortical neurons from *GRN*-associated FTL-D-TDP postmortem brain samples (Busch et al., 2013).

Whether this effect on lysosomal position is due to a direct interaction of TMEM106B with the lysosomal trafficking machinery and motor proteins or is a downstream consequence of TMEM106B's effects remains to be fully determined. For example, lysosomal positioning has been shown to be determined by luminal pH and mTORC1 activity (Johnson et al., 2016; Korolchuk et al., 2011); thus, the primary defect induced by TMEM106B overexpression could be due to altered pH, which then in turn affects lysosomal trafficking.

4.2 TMEM106B and C9orf72

I next place into context our discovery that many of the effects of TMEM106B overexpression can be rescued by concomitant knockdown of C9orf72. Much of the field has focused on toxic *C9orf72* RNA and dipeptide repeats. However, evidence is accumulating that C9orf72 may normally play a role in the endolysosomal pathway and that reduced levels and/or

loss of function of *C9orf72* may contribute to disease pathogenesis (DeJesus-Hernandez et al., 2011; Farg et al., 2014; Renton et al., 2011; Ciura et al., 2013; Gijssels et al., 2012; O'Rourke et al., 2016).

Homology analyses predict *C9orf72* to be a homologue of DENN proteins, which function as GEFs that activate Rab GTPases (Levine et al., 2013b). In one study, endogenous *C9orf72* was reported to co-localize and co-immunoprecipitate with several Rab GTPases involved in endolysosomal and autophagic transport (Rab1, Rab5, Rab7, and Rab11) in primary cortical neurons and human spinal cord motor neurons (Farg et al., 2014). While these data are intriguing as they are the first to link *C9orf72* to Rab GTPases, these data imply that *C9orf72* co-localizes with diverse Rabs which are localized to different compartments – Rab1 is involved in endoplasmic reticulum to Golgi trafficking; Rab5 in endocytic and early endosomal trafficking (Zerial and McBride, 2001; van der Bliek, 2005) and Rab11 in recycling endosomes as well as vesicle exocytosis (Takahashi et al., 2012). The authors suggest that it is via interactions with different sets of protein partners that *C9orf72* localizes to these compartments; while this is possible, this seems unlikely. Thus, the proposed interaction with these Rab GTPases awaits confirmation by other investigators. Indeed, in contrast to Farg et al.'s findings, Xiao et al. did not see co-localization of *C9orf72* with endosomal, lysosomal, or autophagosomal markers using house-made and validated *C9orf72* antibodies, as compared to the commercial antibodies used by Farg et al. (Farg et al., 2014; Xiao et al., 2015). Further investigation into *C9orf72* must proceed with caution and attention to validation of antibodies.

However, with regards to evidence for a role for *C9orf72* in endolysosomal pathways, new data from *C9orf72* null mice adds to the evidence for this and additionally highlights a heretofore underappreciated role for its loss in microglia in promoting pro-inflammatory states in disease pathogenesis. Macrophages and microglia from *C9orf72* null mice harbored enlarged LysoTracker+ and LAMP1+ structures (O'Rourke et al., 2016). Accumulations of LAMP1+ material were also found in microglia from spinal cord and motor cortex tissue from *C9orf72*-associated, but not sporadic, ALS cases. The authors suggest that *C9orf72* may function in late

endosomal to lysosomal trafficking. Specifically, in myeloid cells, *C9orf72* may play a role in phagosome to lysosome maturation, as bone marrow-derived macrophages from *C9orf72* null mice showed enhanced production of reactive oxygen species after feeding of zymosan particles, indicative of defective fusion of phagosomes to lysosomes (Ma et al., 2014).

Given data suggesting a role for *C9orf72* in endolysosomal pathways, as well as the finding that *TMEM106B* acts as a genetic modifier in *C9orf72*-associated FTLD-TDP cases (Gallagher et al., 2014; van Blitterswijk et al., 2014), we investigated the potential for manipulation of *C9orf72* to rescue or exacerbate the phenotypes associated with *TMEM106B* overexpression. We found that knockdown of *C9orf72* mitigated the vacuolar phenotype, lysosomal acidification defect, and cytotoxicity induced by *TMEM106B* overexpression independent of an effect on *TMEM106B* expression levels. These data suggest an interaction between *TMEM106B* and *C9orf72*. The interaction may be direct, or *C9orf72* may exert its countereffects on *TMEM106B* phenotypes through its predicted GEF function. For the former possibility, identification of both *TMEM106B* and *C9orf72*'s binding partners by previously discussed methods (co-immunoprecipitation, GST-pulldown, yeast-two hybrid assays) could shed light on whether the two proteins interact, and domain-mutation experiments as well as use of our ENQLVAAA *TMEM106B* mutant could refine our understanding of potential interactions. Alternatively, the mechanistic basis for the observed rescue of *TMEM106B*-induced phenotypes by knockdown of *C9orf72* may be through the predicted GEF function of *C9orf72*. To investigate this possibility, the first step would be to determine if *C9orf72* exhibits GEF functionality. I would test a panel of Rab GTPases in a GDP-releasing assay (Yoshimura et al., 2010), prioritizing candidate Rab GTPases as previously discussed. I would then assess their GTP binding, as GTP binding rapidly follows GDP release for true GEFs, using radioactive GTP γ S (a non-hydrolyzable analog of GTP). As an alternative to these classical radioactive approaches, recently developed fluorescent analogs of guanine nucleotides, such as mant (N-methylanthraniloyl) fluorophores, which analogs exhibit spectroscopic differences when bound or unbound. This would allow for real time analysis of GEF activity, including kinetic and thermodynamic properties (Cheng et al., 2002; Rossman et

al., 2002). I would then modulate the activity of any identified GTPases, expecting knockdown of candidate Rabs or expression of dominant negative Rab GDP-bound versions to exert similar effects as C9orf72 knockdown, such as smaller LAMP1+ organelles and rescue of TMEM106B overexpression phenotypes.

One interesting question in the field has been why the *C9orf72*-expansion disease state appears to be *mitigated* by the presence of the TMEM106B major allele (associated with increased risk for FTD in non-*C9orf72*-carriers) as opposed to the minor allele (associated with protection from FTD in non-*C9orf72*-carriers), resulting in later age at disease onset and death (van Blitterswijk et al., 2014; Gallagher et al., 2014). Now, the evidence seems to be growing that loss of the normal C9orf72 may impair endolysosomal trafficking, with detrimental effects that contribute to disease pathogenesis. This might suggest that elevated levels of TMEM106B, as associated with the major allele, may work to counterbalance the effects of C9orf72 deficiency through its effects in the endolysosomal pathway, initially mitigating the onset of disease in the *C9orf72*-expansion context. However, increased levels of TMEM106B are, as I have shown, detrimental to endolysosomal/autophagosomal pathways themselves and disease ultimately progresses. Taken together, these data highlight the importance of proper balance within the endolysosomal pathway in the health of neurons and their supporting cells.

We note that implicit in these scenarios discussed above is the assumption that C9orf72's normal function matters. Accordingly, our data and the experiments outlined above fall into the general category of assuming that haploinsufficiency of C9orf72 from repeat expansions may be a pathogenic mechanism. We have not addressed other major putative mechanisms of disease, such as the contribution of gain-of-toxicity from the expanded hexanucleotide repeat. However, we are struck by the fact that two proteins implicated in FTLD-TDP – TMEM106B and C9orf72 – appear to both act in the same pathways and that knockdown of C9orf72 can rescue effects of TMEM106B overexpression. If *C9orf72* repeat expansions act exclusively by gain-of-function mechanisms through the generation of RNA foci or dipeptide repeats, then the

interaction of TMEM106B and C9orf72 observed here is simply due to chance. While not impossible, this seems highly unlikely.

4.3 TMEM106B and progranulin

A third major emerging theme is the relationship between TMEM106B and progranulin. I have found that TMEM106B expression patterns in *GRN*-associated FTLT-TDP human frontal cortex exhibit a much more cytoplasmically dispersed TMEM106B staining pattern, with TMEM106B immunoreactivity extending into the processes of these neurons, as compared to the perikaryal pattern found in both neurologically normal controls and FTLT-TDP without *GRN* mutations.

The finding of altered TMEM106B expression in this Mendelian subgroup of FLTD-TDP taken at face value might suggest that *GRN* haploinsufficiency results in downstream effects on TMEM106B. However, the answer is likely not this straightforward. Consider, for example, the genetic modifier study reported by Cruchaga et al. in 2011. In a study of 50 patients with FTLT-TDP due to mutations in *GRN* (*GRN*-associated FTLT-TDP), the authors found that homozygous carriers of the risk allele of *TMEM106B* at rs1990622 showed a mean decrease of the age at onset of 13 years ($p=9.9 \times 10^{-7}$), compared to heterozygotes or homozygous carriers of the protective allele. Additionally, the risk allele associated with lower plasma progranulin levels in both healthy older adults ($p=4 \times 10^{-4}$) and *GRN* mutation carriers ($p=.0027$) (Cruchaga et al., 2011). Since *TMEM106B* genotypes (and therefore expression levels) were found to modify age at onset for *GRN*-associated FTLT-TDP, as well as correlating with circulating levels of progranulin protein, this study suggests that TMEM106B may modulate progranulin effects, possibly via altered endolysosomal pathways.

A second line of evidence supporting an effect of TMEM106B on progranulin (as opposed to vice-versa) lies in our direct manipulation of TMEM106B expression in cell culture. We found that increasing TMEM106B expression results in an increase in the intracellular:extracellular ratio of progranulin (Chen-Plotkin et al., 2012). Brady et al. saw a similar increase in intracellular progranulin upon TMEM106B overexpression in N2A cells (a mouse neuroblastoma cell line).

These data support a relationship between TMEM106B and progranulin. Moreover, growing evidence supports a major role of progranulin in lysosomal biology. The strongest evidence comes from the finding that the complete loss of progranulin, as discovered in a human sibling pair with homozygous c.813_816del (p.Thr272Serfs*10) mutations results in adult-onset neuronal ceroid lipofuscinosis (NCL) (Smith et al., 2012), implicating the function of the normal progranulin protein in lysosomal biology. Notably, some *Grn*^{-/-} mouse models have been found to exhibit pathological hallmarks of lysosomal dysregulation often found in lysosomal storage diseases (Ghoshal et al., 2012; Petkau et al., 2010; Wils et al., 2012; Ahmed et al., 2007). Similarly, *GRN*-associated FTLN-TDP brain also exhibit many of the pathological findings seen in tissue derived from NCL brain: increased levels of LAMP1 and LAMP2, the accumulation of saposin D, and subunit c of mitochondria ATP synthase (SCMAS) (Gotzl et al., 2014).

Progranulin deficiency thus results in significant lysosomal derangements, although why complete loss of progranulin results in NCL, whereas partial loss results in FTLN is still unclear. I posit the *TMEM106B* risk genotype can compound the negative effects of progranulin haploinsufficiency via several possible scenarios. First, *TMEM106B* overexpression may impact the development of disease by specific effects on progranulin and progranulin signaling, impairing the known neuroprotective effects and lysosomal functions of progranulin (Van Damme et al., 2008). Second, *TMEM106B* overexpression-induced endolysosomal/autophagosomal alterations may further exacerbate existing lysosomal derangements and neurotoxic effects caused by progranulin deficiency, together resulting in earlier onset of disease.

4.3.1 TMEM106B overexpression may disrupt neuroprotective progranulin pathways

I posit that the endolysosomal/autophagosomal disturbances caused by *TMEM106B* overexpression may have direct or indirect effects on progranulin internalization, sorting, and trafficking. This may impair progranulin's normal neuroprotective signaling pathway, i.e., the network of interconnected endosomes and lysosomes which executes spatiotemporal control over signaling events, delivering the appropriate amount of neurotrophic progranulin "signal" to different regions of the cell (Sadowski et al., 2009). Proper regulation of this network pathway is

critical in long and polarized neurons. An example of a pathway that relies heavily on the integrity of a signaling endosome network is the EGF/EGFR signaling pathway. Endocytosis of EGF/EGFR activates the EGFR/MAPK signaling pathway, which remains activated until EGFR is inwardly budded into the intraluminal vesicles of the late endosome, removing the catalytic domain of EGFR from the cytoplasm (Sorkin and Duex, 2010; Eden et al., 2009). The neurotrophic effects of progranulin are likely to be similarly dependent on the regulated internalization of progranulin, with downstream signaling cascades and ultimate termination of signal through degradation of progranulin in the lysosome. As a consequence, TMEM106B's effects on the endolysosomal network could affect the ability to appropriately internalize progranulin, signal through progranulin, or terminate progranulin signaling appropriately. Intriguingly, progranulin has been shown to activate signaling pathways known to be dependent on proper spatial-temporal function of signaling endosome networks (e.g., MAPK, PI3K) (He et al., 2002; Zanocco-Marani et al., 1999).

As we and others have shown, increased TMEM106B significantly disrupts the endolysosomal network and lysosomal trafficking in neurons, with knockdown of TMEM106B increasing and overexpression decreasing lysosomal trafficking in mouse cortical cultures (Stagi et al., 2014; Schwenk et al., 2014). Thus, perturbations in the endolysosomal pathway as induced by varying levels of TMEM106B could exacerbate the negative effects of progranulin deficiency by disturbing the spatio-temporal relationship of signaling endosomes and lysosomes involved in progranulin signaling pathways, thus disrupting progranulin's neurotrophic effects. While the progranulin pathway responsible for its neurotrophic effects has yet to be determined, I note that progranulin deficiency has been shown to result in decreased mTORC1 activity in frontal cortex in a *Gpn-/-* mouse model (Tanaka et al., 2013); thus, an intriguing possibility is that the pathway that TMEM106B overexpression negatively impacts may be mTORC1 itself.

4.4 The endolysosomal/autophagosomal pathway in disease pathogenesis

Overall, emerging data on TMEM106B, progranulin, and C9orf72 highlight a role for all three of these disease-associated proteins in endolysosomal trafficking and function. In addition,

rarer, Mendelian forms of FTLD also point to disturbances in the endolysosomal/autophagosomal pathway and altered trafficking dynamics as a central theme in FTLD.

As shown in **Figure 4.3**, FTLD-TDP-associated mutations in *CHMP2B* may impair fusion of endosomes with autophagosomes and lysosomes; (Urwin et al., 2010; Filimonenko et al., 2007; Lee et al., 2007); disease-associated mutations in *VCP* may impair autophagosomal maturation and transport of ubiquitinated cargo to lysosomes (Ju et al., 2009; Ritz et al., 2011); moreover, new evidence suggests that *C9orf72* expansions may result in impaired endosomal to lysosomal trafficking due to loss of *C9orf72*'s normal function (O'Rourke et al., 2016). In addition, progranulin deficiency has indeed been associated with significant disturbances to lysosomal and autophagosomal pathways (Petkau et al., 2010; Shacka, 2012; Gotzl et al., 2014). Thus, impairments in lysosomal function, altered fusion dynamics, and altered vesicular trafficking emerge as common themes in FTLD. I further note that endolysosomal/autophagosomal dysfunction may play an important role in other neurodegenerative diseases such as Parkinson's, Alzheimer's, and Huntington's disease, as discussed in the Introduction (Wong and Cuervo, 2010).

How does TMEM106B fit within this contextual framework? I posit that disease-associated increases in TMEM106B result in altered dynamics within the endolysosomal/autophagosomal pathway. TMEM106B overexpression may do this by impairing dissolution of the secondary lysosomes (such as autolysosomes/amphisomes), potentially via impairment of autophagic lysosomal reformation. Alternatively, TMEM106B levels may modulate one or more Rab GTPases or effectors, increasing trafficking and membrane fusion dynamics to result in an increase in secondary lysosomes.

The effects of increased TMEM106B may perturb progranulin pathways that are vital to lysosomal and cellular homeostasis. In addition, TMEM106B may interact with endogenous *C9orf72*, and elevated levels of TMEM106B may counterbalance the loss of *C9orf72* within the endolysosomal pathway.

Figure 4.3:

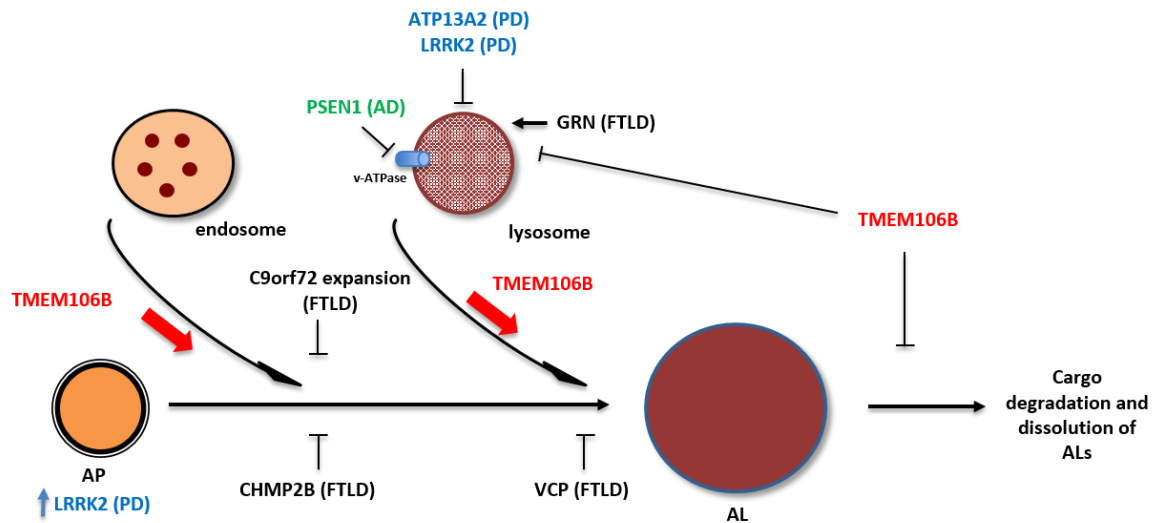


Figure 4.3: Endolysosomal/autophagosomal dysfunction in neurodegeneration

Mutations in multiple genes involved in the endolysosomal/autophagosomal pathway are implicated in neurodegeneration and are shown where they have been implicated to impact. **Black text:** mutations associated with FTLN. Disease-associated mutations in CHMP2B have been shown to impair endolysosome-lysosome fusion. Mutations in VCP have been shown to impair lysosomal fusion with autophagosomes. C9orf72 has been implicated in late endosomal to lysosomal trafficking, with the disease-associated hexanucleotide expansion resulting in reduced levels of functional C9orf72 protein. **Green text:** Alzheimer's mutations in PSEN1 impair lysosomal acidification by impairing proper trafficking of a vATPase subunit. **Blue text:** Parkinson's-associated mutations in ATP13A2, a lysosomal P-type ATPase, results in impaired lysosomal acidification. Mutations in LRRK2 activate a Ca²⁺-dependent pathway that results in lysosomal acidification defects and increased autophagosome formation. Against this backdrop of endolysosomal/autophagosomal disruption, **TMEM106B** may exert its effects on the endolysosomal pathway by 1) impairing the dissolution of secondary lysosomes (such as ALs depicted) 2) increasing secondary lysosomal formation by modulation of endolysosomal Rab GTPase activity.

AL= autolysosome. AP=autophagosome.

Recent data highlight the important roles of both progranulin and C9orf72 in microglia, with *C9orf72* deficient mice and *Grn* deficient mice exhibiting pro-inflammatory microglial cytokine profiles and neurotoxic effects (Tanaka et al., 2013; O'Rourke et al., 2016). These studies emphasize the growing importance of considering the microglia-neuron interaction in the pathogenesis of disease. Manipulation of TMEM106B within microglia, and assessment of how this influences microglial cytokine profiles as well as neuronal toxicity, should be a major focus of study in future studies attempting to unravel the relationship between TMEM106B and

progranulin, and TMEM106B and C9orf72.

Finally, an as-yet-unanswered question within the field of FTLD-TDP concerns the relationship between TDP-43, the major protein forming the pathognomonic inclusions of the disease, and the various proteins implicated by the genetics in FTLD-TDP. Despite both being linked to FTLD-TDP ten years ago, a mechanistic link between progranulin and TDP-43 has yet to emerge. Similarly, few mechanistic connections have been found between TDP-43 and C9orf72. Our findings suggest one way that TDP-43 may be linked to these various genetic causes of FTLD-TDP is through endolysosomal/autophagosomal pathway dysfunction. Aggregates of TDP-43 are reported to be degraded by autophagy as well as by the ubiquitin proteasome system (Wang et al., 2010; Brady et al., 2011). Thus, if degradative pathways are affected by, for example TMEM106B expression levels, one major route for the cell to rid itself of TDP-43 aggregates would be impaired. I note in this context that in addition to the genes mentioned above, other ALS/FTLD-associated mutations have recently emerged in genes that are all to various extents related to autophagy. The protein products of *UBQLN2*, *SQSTM1*, *OPTN* – ubiquilin2, p62, and optineurin respectively – have all been shown to function in autophagy as autophagy receptors, binding ubiquitinated protein aggregates and directing them to autophagosomes for degradation (Wagner 2008, Wild 2011).

In the case of these specific, rare, Mendelian causes of ALS/FTLD, the existing evidence points to defects in autophagic proteins or related proteins that compromise the neuron's ability to adequately degrade these protein aggregates, with subsequent toxic effects that cause neurodegeneration. Increases in TMEM106B expression may similarly compromise degradation of protein aggregates, to a lesser degree, through impairments to endolysosomal/autophagosomal function, thus contributing to increased risk for FTLD.

4.5 Future Directions

While the field has made great strides in the preliminary characterization of a protein otherwise unknown prior to 2010, much is still left to be learned about TMEM106B. Identification and confirmation of TMEM106B's binding partners will be vital in fully establishing its function.

Currently, potential non-overlapping interacting proteins have been reported by two separate groups. Schwenk et al. identified MAP6 as the only common hit in three independent immunoprecipitation-mass spectrometry experiments from P15 rat brain, linking TMEM106B to microtubule-dependent processes. Another group (Stagi et al., 2014) has reported, via yeast two-hybrid assays, that TMEM106B can bind to AP-2, CLTC, VPS11, and VPS13D; the latter two proteins play roles in late endosome to lysosome trafficking (Velayos-Baeza et al., 2004; Bankaitis et al., 1986). Our preliminary immunoprecipitation-mass spectrometry experiments demonstrate a potential interaction with vATPase subunits, but our hits do not overlap with these previously identified proteins. Thus, consensus and independent confirmation are needed for these and other future potential partners of TMEM106B, and future co-immunoprecipitation experiments should be ideally performed in frontal and temporal cortex to help elucidate TMEM106B's binding partners within disease-relevant tissue.

Notably, TMEM106C was also identified as a potential binding partner of TMEM106B, in a yeast two-hybrid screen; TMEM106C has 47% amino acid identity and 63% amino acid similarity with TMEM106B (Stagi et al., 2014). The role of oligomerization of TMEM106B with family members TMEM106A and TMEM106C, or self-dimerization/oligomerization is also an area that may be fruitful for future study, especially within the context of how various homo- and hetero-dimerization events might affect lysosomal pathways, trafficking dynamics, and binding to other protein partners.

It will also be important to translate the role of TMEM106B from cell culture models into more clinically relevant patient-derived cells and tissue as well as *in vivo* models. To that end, the availability of fibroblasts from patients with *GRN*-associated FTLD-TDP, *C9orf72*-associated FTLD-TDP, FTLD-TDP without either genetic mutation, and FTLD-tau offers potential for investigation of lysosomal readouts in these cells as well as potential derivatives (e.g. iPSC-derived neurons) of these cells. A key aspect of the work described in this thesis is the fact that effects of *TMEM106B* manipulation in specific genetic contexts have been explored. With the advent of genome editing, it is increasingly feasible to create isogenic controls from patient-

derived cell lines that differ only in whether a mutation (e.g. *C9orf72* expansion) is present or whether a specific gene is silenced. Thus, one can pinpoint with molecular precision, in patient-derived cells, what the effects of specific mutations or gene silencing would be. As just one example, experiments investigating the effect of presence vs. absence of *C9orf72* (or *C9orf72* expansions) in otherwise isogenic iPSC-derived neurons on the phenotypes triggered by TMEM106B overexpression (lysosomal morphology and function, cell viability) are feasible and would add greatly to the clinical relevance of the work described here.

Lastly, the generation and characterization of *TMEM106B* mouse models may add to our understanding of TMEM106B. To date, no knockout mouse model for TMEM106B has been reported, and such a model may help elucidate the function of endogenous TMEM106B. Notably, Schwenk et al. found that knockdown of TMEM106B in rat cortical neurons results in a striking loss of dendritic arborization and decreased pre- and post-synaptic marker proteins, suggesting that a neurological phenotype may likely result from loss of TMEM106B in an animal (Schwenk et al., 2014). TMEM106B overexpression can also be modeled in an *in vivo* animal context, which may allow us to parse the whole organism consequences of the cell biological phenotypes described in this thesis. Because of the genetic modifier effects reported by us and others for *TMEM106B* on phenotype in carriers of *C9orf72* expansions (Gallagher et al., 2014; van Blitterswijk et al., 2014) and *GRN* mutations (Finch et al., 2011; Cruchaga et al., 2011; Van Deerlin et al., 2010), crosses between *TMEM106B* overexpression or *TMEM106B* null animals and *C9orf72* expansion, *C9orf72* null, or *GRN* null animals may be of interest. Indeed, *C9orf72* expansion (Peters et al., 2015), *C9orf72* null (Koppers et al., 2015), and *Grn* null mice (Kayasuga et al., 2007; Yin et al., 2010; Filiano et al., 2013) have already been generated and reported and many are striking for the general lack of a clear neurodegenerative phenotype. Should the manipulation of *TMEM106B* as a second locus in these existing mouse models bring out a clear neurodegenerative phenotype, this would strongly support the mechanistic interactions hinted at in this work and faithfully model the genetic modifier effects observed in human disease.

4.6 Conclusion

Our work and the work of others demonstrates that TMEM106B is important in endolysosomal/autophagosomal trafficking and function, that increased levels of TMEM106B may have toxic effects on cells, and that TMEM106B may interact with C9orf72, which is also implicated as functioning within the endolysosomal/autophagosomal pathway. Furthermore, we see that elevated levels of TMEM106B alter progranulin intracellular:extracellular partitioning, suggesting that disruption of progranulin signaling pathways may also contribute to disease. In addition to these effects on progranulin, elevated levels of TMEM106B, as seen in carriers of FTLD-TDP risk genotypes, may result in small alterations in the dynamics of lysosomal or autolysosomal degradation. These changes may over the lifetime of an individual ultimately result in failure to clear toxic aggregates from neurons. A relative impairment in the ability to clear toxic aggregates may then result in increased neuronal toxicity, leading to the neurodegeneration seen in FTLD-TDP as well as other neurodegenerative diseases.

BIBLIOGRAPHY

Abramzon Y, Johnson JO, Scholz SW, Taylor JP, Brunetti M, Calvo A, Mandrioli J, Benatar M, Mora G, Restagno G, Chio A, Traynor BJ (2012) Valosin-containing protein (VCP) mutations in sporadic amyotrophic lateral sclerosis. *Neurobiol Aging (United States)* 33:2231.e1-2231.e6.

Ahmed Z, Mackenzie IR, Hutton ML, Dickson DW (2007) Progranulin in frontotemporal lobar degeneration and neuroinflammation. *J Neuroinflammation (England)* 4:7.

Almeida S, Zhou L, Gao FB (2011) Progranulin, a glycoprotein deficient in frontotemporal dementia, is a novel substrate of several protein disulfide isomerase family proteins. *PLoS One (United States)* 6:e26454.

Arai T, Hasegawa M, Akiyama H, Ikeda K, Nonaka T, Mori H, Mann D, Tsuchiya K, Yoshida M, Hashizume Y, Oda T (2006) TDP-43 is a component of ubiquitin-positive tau-negative inclusions in frontotemporal lobar degeneration and amyotrophic lateral sclerosis. *Biochem Biophys Res Commun (United States)* 351:602-611.

Ash PE, Bieniek KF, Gendron TF, Caulfield T, Lin WL, DeJesus-Hernandez M, van Blitterswijk MM, Jansen-West K, Paul JW, 3rd, Rademakers R, Boylan KB, Dickson DW, Petrucelli L (2013) Unconventional translation of C9ORF72 GGGGCC expansion generates insoluble polypeptides specific to c9FTD/ALS. *Neuron (United States)* 77:639-646.

Avrahami L, Farfara D, Shaham-Kol M, Vassar R, Frenkel D, Eldar-Finkelman H (2013) Inhibition of glycogen synthase kinase-3 ameliorates beta-amyloid pathology and restores lysosomal acidification and mammalian target of rapamycin activity in the alzheimer disease mouse model: In vivo and in vitro studies. *J Biol Chem (United States)* 288:1295-1306.

Axe EL, Walker SA, Manifava M, Chandra P, Roderick HL, Habermann A, Griffiths G, Ktistakis NT (2008) Autophagosome formation from membrane compartments enriched in

phosphatidylinositol 3-phosphate and dynamically connected to the endoplasmic reticulum. *J Cell Biol (United States)* 182:685-701.

Azzedine H, Bolino A, Taieb T, Birouk N, Di Duca M, Bouhouche A, Benamou S, Mrabet A, Hammadouche T, Chkili T, Gouider R, Ravazzolo R, Brice A, Laporte J, LeGuern E (2003) Mutations in MTMR13, a new pseudophosphatase homologue of MTMR2 and Sbf1, in two families with an autosomal recessive demyelinating form of charcot-marie-tooth disease associated with early-onset glaucoma. *Am J Hum Genet (United States)* 72:1141-1153.

Baborie A, Griffiths TD, Jaros E, McKeith IG, Burn DJ, Richardson A, Ferrari R, Moreno J, Momeni P, Duplessis D, Pal P, Rollinson S, Pickering-Brown S, Thompson JC, Neary D, Snowden JS, Perry R, Mann DM (2011) Pathological correlates of frontotemporal lobar degeneration in the elderly. *Acta Neuropathol (Germany)* 121:365-371.

Baker M et al (2006) Mutations in progranulin cause tau-negative frontotemporal dementia linked to chromosome 17. *Nature (England)* 442:916-919.

Ballabio A, Gieselmann V (2009) Lysosomal disorders: From storage to cellular damage. *Biochim Biophys Acta (Netherlands)* 1793:684-696.

Bankaitis VA, Johnson LM, Emr SD (1986) Isolation of yeast mutants defective in protein targeting to the vacuole. *Proc Natl Acad Sci U S A (UNITED STATES)* 83:9075-9079.

Basit F, Cristofanon S, Fulda S (2013) Obatoclax (GX15-070) triggers necroptosis by promoting the assembly of the necrosome on autophagosomal membranes. *Cell Death Differ (England)* 20:1161-1173.

BasuRay S, Mukherjee S, Romero E, Wilson MC, Wandinger-Ness A (2010) Rab7 mutants associated with charcot-marie-tooth disease exhibit enhanced NGF-stimulated signaling. *PLoS One (United States)* 5:e15351.

Bayer N, Schober D, Prchla E, Murphy RF, Blaas D, Fuchs R (1998) Effect of bafilomycin A1 and nocodazole on endocytic transport in HeLa cells: Implications for viral uncoating and infection. *J Virol (UNITED STATES)* 72:9645-9655.

Beck J et al (2013) Large C9orf72 hexanucleotide repeat expansions are seen in multiple neurodegenerative syndromes and are more frequent than expected in the UK population. *Am J Hum Genet (United States)* 92:345-353.

Behnia R, Munro S (2005) Organelle identity and the signposts for membrane traffic. *Nature (England)* 438:597-604.

Bennion Callister J, Pickering-Brown SM (2014) Pathogenesis/genetics of frontotemporal dementia and how it relates to ALS. *Exp Neurol* .

Bernasconi P, Rausch T, Struve I, Morgan L, Taiz L (1990) An mRNA from human brain encodes an isoform of the B subunit of the vacuolar H(+)-ATPase. *J Biol Chem (UNITED STATES)* 265:17428-17431.

Bock JB, Matern HT, Peden AA, Scheller RH (2001) A genomic perspective on membrane compartment organization. *Nature (England)* 409:839-841.

Boeynaems S, Bogaert E, Michiels E, Gijssels I, Sieben A, Jovicic A, De Baets G, Scheveneels W, Steyaert J, Cuijt I, Verstrepen KJ, Callaerts P, Rousseau F, Schymkowitz J, Cruts M, Van Broeckhoven C, Van Damme P, Gitler AD, Robberecht W, Van Den Bosch L (2016) Drosophila screen connects nuclear transport genes to DPR pathology in c9ALS/FTD. *Sci Rep (England)* 6:20877.

Bonapace L, Bornhauser BC, Schmitz M, Cario G, Ziegler U, Niggli FK, Schafer BW, Schrappe M, Stanulla M, Bourquin JP (2010) Induction of autophagy-dependent necroptosis is required for

childhood acute lymphoblastic leukemia cells to overcome glucocorticoid resistance. *J Clin Invest* (United States) 120:1310-1323.

Bonifacino JS, Traub LM (2003) Signals for sorting of transmembrane proteins to endosomes and lysosomes. *Annu Rev Biochem* (United States) 72:395-447.

Borroni B, Bonvicini C, Alberici A, Buratti E, Agosti C, Archetti S, Papetti A, Stuani C, Di Luca M, Gennarelli M, Padovani A (2009) Mutation within TARDBP leads to frontotemporal dementia without motor neuron disease. *Hum Mutat* (United States) 30:E974-83.

Bos JL, Rehmann H, Wittinghofer A (2007) GEFs and GAPs: Critical elements in the control of small G proteins. *Cell* (United States) 129:865-877.

Brady OA, Zheng Y, Murphy K, Huang M, Hu F (2013) The frontotemporal lobar degeneration risk factor, TMEM106B, regulates lysosomal morphology and function. *Hum Mol Genet* (England) 22:685-695.

Brady OA, Meng P, Zheng Y, Mao Y, Hu F (2011) Regulation of TDP-43 aggregation by phosphorylation and p62/SQSTM1. *J Neurochem* (England) 116:248-259.

Braulke T, Bonifacino JS (2009) Sorting of lysosomal proteins. *Biochim Biophys Acta* (Netherlands) 1793:605-614.

Braun S, Matuschewski K, Rape M, Thoms S, Jentsch S (2002) Role of the ubiquitin-selective CDC48(UFD1/NPL4) chaperone (segregase) in ERAD of OLE1 and other substrates. *Embo J* (England) 21:615-621.

Bray K, Mathew R, Lau A, Kamphorst JJ, Fan J, Chen J, Chen HY, Ghavami A, Stein M, DiPaola RS, Zhang D, Rabinowitz JD, White E (2012) Autophagy suppresses RIP kinase-dependent necrosis enabling survival to mTOR inhibition. *PLoS One* (United States) 7:e41831.

Brettschneider J, Van Deerlin VM, Robinson JL, Kwong L, Lee EB, Ali YO, Safren N, Monteiro MJ, Toledo JB, Elman L, McCluskey L, Irwin DJ, Grossman M, Molina-Porcel L, Lee VM, Trojanowski JQ (2012) Pattern of ubiquilin pathology in ALS and FTLN indicates presence of C9ORF72 hexanucleotide expansion. *Acta Neuropathol (Germany)* 123:825-839.

Bright NA, Gratian MJ, Luzio JP (2005) Endocytic delivery to lysosomes mediated by concurrent fusion and kissing events in living cells. *Curr Biol (England)* 15:360-365.

Bucci C, Thomsen P, Nicoziani P, McCarthy J, van Deurs B (2000) Rab7: A key to lysosome biogenesis. *Mol Biol Cell (UNITED STATES)* 11:467-480.

Bultema JJ, Ambrosio AL, Burek CL, Di Pietro SM (2012) BLOC-2, AP-3, and AP-1 proteins function in concert with Rab38 and Rab32 proteins to mediate protein trafficking to lysosome-related organelles. *J Biol Chem (United States)* 287:19550-19563.

Buratti E, De Conti L, Stuani C, Romano M, Baralle M, Baralle F (2010) Nuclear factor TDP-43 can affect selected microRNA levels. *Febs J (England)* 277:2268-2281.

Burrell JR, Hodges JR (2010) From FUS to fibs: What's new in frontotemporal dementia? *J Alzheimers Dis (Netherlands)* 21:349-360.

Busch JI, Martinez-Lage M, Ashbridge E, Grossman M, Van Deerlin VM, Hu F, Lee VM, Trojanowski JQ, Chen-Plotkin AS (2013) Expression of TMEM106B, the frontotemporal lobar degeneration-associated protein, in normal and diseased human brain. *Acta Neuropathol Commun (England)* 1:36-5960-1-36.

Butler GS, Dean RA, Tam EM, Overall CM (2008) Pharmacoproteomics of a metalloproteinase hydroxamate inhibitor in breast cancer cells: Dynamics of membrane type 1 matrix metalloproteinase-mediated membrane protein shedding. *Mol Cell Biol (United States)* 28:4896-4914.

Cang C, Bekele B, Ren D (2014) The voltage-gated sodium channel TPC1 confers endolysosomal excitability. *Nat Chem Biol (United States)* 10:463-469.

Chan EY, Longatti A, McKnight NC, Tooze SA (2009) Kinase-inactivated ULK proteins inhibit autophagy via their conserved C-terminal domains using an Atg13-independent mechanism. *Mol Cell Biol (United States)* 29:157-171.

Chartier-Harlin MC et al (2011) Translation initiator EIF4G1 mutations in familial parkinson disease. *Am J Hum Genet (United States)* 89:398-406.

Chen Y, Yu L (2013) Autophagic lysosome reformation. *Exp Cell Res (United States)* 319:142-146.

Cheng L, Rossman KL, Mahon GM, Worthylake DK, Korus M, Sondel J, Whitehead IP (2002) RhoGEF specificity mutants implicate RhoA as a target for *src* transforming activity. *Mol Cell Biol (United States)* 22:6895-6905.

Chen-Plotkin AS, Lee VM, Trojanowski JQ (2010) TAR DNA-binding protein 43 in neurodegenerative disease. *Nat Rev Neurol (England)* 6:211-220.

Chen-Plotkin AS, Geser F, Plotkin JB, Clark CM, Kwong LK, Yuan W, Grossman M, Van Deerlin VM, Trojanowski JQ, Lee VM (2008) Variations in the progranulin gene affect global gene expression in frontotemporal lobar degeneration. *Hum Mol Genet (England)* 17:1349-1362.

Chen-Plotkin AS, Unger TL, Gallagher MD, Bill E, Kwong LK, Volpicelli-Daley L, Busch JI, Akle S, Grossman M, Van Deerlin V, Trojanowski JQ, Lee VM (2012) TMEM106B, the risk gene for frontotemporal dementia, is regulated by the microRNA-132/212 cluster and affects progranulin pathways. *J Neurosci (United States)* 32:11213-11227.

Chew J et al (2015) Neurodegeneration. C9ORF72 repeat expansions in mice cause TDP-43 pathology, neuronal loss, and behavioral deficits. *Science (United States)* 348:1151-1154.

Ciura S, Lattante S, Le Ber I, Latouche M, Tostivint H, Brice A, Kabashi E (2013) Loss of function of C9orf72 causes motor deficits in a zebrafish model of amyotrophic lateral sclerosis. *Ann Neurol (United States)* 74:180-187.

Clark LN, Poorkaj P, Wszolek Z, Geschwind DH, Nasreddine ZS, Miller B, Li D, Payami H, Awert F, Markopoulou K, Andreadis A, D'Souza I, Lee VM, Reed L, Trojanowski JQ, Zhukareva V, Bird T, Schellenberg G, Wilhelmsen KC (1998) Pathogenic implications of mutations in the tau gene in pallido-ponto-nigral degeneration and related neurodegenerative disorders linked to chromosome 17. *Proc Natl Acad Sci U S A (UNITED STATES)* 95:13103-13107.

Colombrita C, Onesto E, Megiorni F, Pizzuti A, Baralle FE, Buratti E, Silani V, Ratti A (2012) TDP-43 and FUS RNA-binding proteins bind distinct sets of cytoplasmic messenger RNAs and differently regulate their post-transcriptional fate in motoneuron-like cells. *J Biol Chem (United States)* 287:15635-15647.

Conner SD, Schmid SL (2003) Regulated portals of entry into the cell. *Nature (England)* 422:37-44.

Cooper-Knock J, Shaw PJ, Kirby J (2014) The widening spectrum of C9ORF72-related disease; genotype/phenotype correlations and potential modifiers of clinical phenotype. *Acta Neuropathol (Germany)* 127:333-345.

Cruchaga C, Graff C, Chiang HH, Wang J, Hinrichs AL, Spiegel N, Bertelsen S, Mayo K, Norton JB, Morris JC, Goate A (2011) Association of TMEM106B gene polymorphism with age at onset in granulin mutation carriers and plasma granulin protein levels. *Arch Neurol (United States)* 68:581-586.

Cruts M, Theuns J, Van Broeckhoven C (2012) Locus-specific mutation databases for neurodegenerative brain diseases. *Hum Mutat (United States)* 33:1340-1344.

Cruts M et al (2006) Null mutations in progranulin cause ubiquitin-positive frontotemporal dementia linked to chromosome 17q21. *Nature (England)* 442:920-924.

Cuervo AM, Dice JF (2000) Regulation of lamp2a levels in the lysosomal membrane. *Traffic (Denmark)* 1:570-583.

Da Cruz S, Cleveland DW (2011) Understanding the role of TDP-43 and FUS/TLS in ALS and beyond. *Curr Opin Neurobiol (England)* 21:904-919.

Daniel R, He Z, Carmichael KP, Halper J, Bateman A (2000) Cellular localization of gene expression for progranulin. *J Histochem Cytochem (UNITED STATES)* 48:999-1009.

De Muynck L, Herdewyn S, Beel S, Scheveneels W, Van Den Bosch L, Robberecht W, Van Damme P (2013) The neurotrophic properties of progranulin depend on the granulin E domain but do not require sortilin binding. *Neurobiol Aging (United States)* 34:2541-2547.

Dehay B, Ramirez A, Martinez-Vicente M, Perier C, Canron MH, Doudnikoff E, Vital A, Vila M, Klein C, Bezdard E (2012) Loss of P-type ATPase ATP13A2/PARK9 function induces general lysosomal deficiency and leads to parkinson disease neurodegeneration. *Proc Natl Acad Sci U S A (United States)* 109:9611-9616.

DeJesus-Hernandez M et al (2011) Expanded GGGGCC hexanucleotide repeat in noncoding region of C9ORF72 causes chromosome 9p-linked FTD and ALS. *Neuron (United States)* 72:245-256.

del Toro D, Alberch J, Lazaro-Dieguez F, Martin-Ibanez R, Xifro X, Egea G, Canals JM (2009) Mutant huntingtin impairs post-golgi trafficking to lysosomes by delocalizing optineurin/Rab8 complex from the golgi apparatus. *Mol Biol Cell (United States)* 20:1478-1492.

Del Villar K, Miller CA (2004) Down-regulation of DENN/MADD, a TNF receptor binding protein, correlates with neuronal cell death in alzheimer's disease brain and hippocampal neurons. *Proc Natl Acad Sci U S A (United States)* 101:4210-4215.

Dell'Angelica EC, Puertollano R, Mullins C, Aguilar RC, Vargas JD, Hartnell LM, Bonifacino JS (2000) GGAs: A family of ADP ribosylation factor-binding proteins related to adaptors and associated with the golgi complex. *J Cell Biol (UNITED STATES)* 149:81-94.

Deming Y, Cruchaga C (2014) TMEM106B: A strong FTLN disease modifier. *Acta Neuropathol (Germany)* 127:419-422.

Deretic V, Delgado M, Vergne I, Master S, De Haro S, Ponpuak M, Singh S (2009) Autophagy in immunity against mycobacterium tuberculosis: A model system to dissect immunological roles of autophagy. *Curr Top Microbiol Immunol (Germany)* 335:169-188.

Di Bartolomeo S, Corazzari M, Nazio F, Oliverio S, Lisi G, Antonioli M, Pagliarini V, Matteoni S, Fuoco C, Giunta L, D'Amelio M, Nardacci R, Romagnoli A, Piacentini M, Cecconi F, Fimia GM (2010) The dynamic interaction of AMBRA1 with the dynein motor complex regulates mammalian autophagy. *J Cell Biol (United States)* 191:155-168.

Di Carlo V, Grossi E, Laneve P, Morlando M, Dini Modigliani S, Ballarino M, Bozzoni I, Caffarelli E (2013) TDP-43 regulates the microprocessor complex activity during in vitro neuronal differentiation. *Mol Neurobiol (United States)* 48:952-963.

Dixon AL, Liang L, Moffatt MF, Chen W, Heath S, Wong KC, Taylor J, Burnett E, Gut I, Farrall M, Lathrop GM, Abecasis GR, Cookson WO (2007) A genome-wide association study of global gene expression. *Nat Genet (United States)* 39:1202-1207.

Dobrowolski R, Vick P, Ploper D, Gumper I, Snitkin H, Sabatini DD, De Robertis EM (2012) Presenilin deficiency or lysosomal inhibition enhances wnt signaling through relocalization of GSK3 to the late-endosomal compartment. *Cell Rep (United States)* 2:1316-1328.

Donnelly CJ, Zhang PW, Pham JT, Haeusler AR, Mistry NA, Vidensky S, Daley EL, Poth EM, Hoover B, Fines DM, Maragakis N, Tienari PJ, Petrucelli L, Traynor BJ, Wang J, Rigo F, Bennett CF, Blackshaw S, Sattler R, Rothstein JD (2013) RNA toxicity from the ALS/FTD C9ORF72 expansion is mitigated by antisense intervention. *Neuron (United States)* 80:415-428.

Dooley HC, Razi M, Polson HE, Girardin SE, Wilson MI, Tooze SA (2014) WIPI2 links LC3 conjugation with PI3P, autophagosome formation, and pathogen clearance by recruiting Atg12-5-16L1. *Mol Cell (United States)* 55:238-252.

Ebneth A, Godemann R, Stamer K, Illenberger S, Trinczek B, Mandelkow E (1998) Overexpression of tau protein inhibits kinesin-dependent trafficking of vesicles, mitochondria, and endoplasmic reticulum: Implications for alzheimer's disease. *J Cell Biol (UNITED STATES)* 143:777-794.

Eden ER, White IJ, Futter CE (2009) Down-regulation of epidermal growth factor receptor signalling within multivesicular bodies. *Biochem Soc Trans (England)* 37:173-177.

Ejlertskov P, Rasmussen I, Nielsen TT, Bergstrom AL, Tohyama Y, Jensen PH, Vilhardt F (2013) Tubulin polymerization-promoting protein (TPPP/p25alpha) promotes unconventional secretion of alpha-synuclein through exophagy by impairing autophagosome-lysosome fusion. *J Biol Chem (United States)* 288:17313-17335.

Falguieres T, Luyet PP, Bissig C, Scott CC, Velluz MC, Gruenberg J (2008) In vitro budding of intraluminal vesicles into late endosomes is regulated by alix and Tsg101. *Mol Biol Cell (United States)* 19:4942-4955.

Farg MA, Sundaramoorthy V, Sultana JM, Yang S, Atkinson RA, Levina V, Halloran MA, Gleeson PA, Blair IP, Soo KY, King AE, Atkin JD (2014) C9ORF72, implicated in amyotrophic lateral sclerosis and frontotemporal dementia, regulates endosomal trafficking. *Hum Mol Genet (England)* 23:3579-3595.

Fernandez-Saiz V, Buchberger A (2010) Imbalances in p97 co-factor interactions in human proteinopathy. *EMBO Rep (England)* 11:479-485.

Ferrari R et al (2014) Frontotemporal dementia and its subtypes: A genome-wide association study. *Lancet Neurol (England)* 13:686-699.

Filiano AJ, Martens LH, Young AH, Warmus BA, Zhou P, Diaz-Ramirez G, Jiao J, Zhang Z, Huang EJ, Gao FB, Farese RV, Jr, Roberson ED (2013) Dissociation of frontotemporal dementia-related deficits and neuroinflammation in progranulin haploinsufficient mice. *J Neurosci (United States)* 33:5352-5361.

Filimonenko M, Stuffers S, Raiborg C, Yamamoto A, Malerod L, Fisher EM, Isaacs A, Brech A, Stenmark H, Simonsen A (2007) Functional multivesicular bodies are required for autophagic clearance of protein aggregates associated with neurodegenerative disease. *J Cell Biol (United States)* 179:485-500.

Fimia GM, Stoykova A, Romagnoli A, Giunta L, Di Bartolomeo S, Nardacci R, Corazzari M, Fuoco C, Ucar A, Schwartz P, Gruss P, Piacentini M, Chowdhury K, Cecconi F (2007) Ambra1 regulates autophagy and development of the nervous system. *Nature (England)* 447:1121-1125.

Finch N, Baker M, Crook R, Swanson K, Kuntz K, Surtees R, Bisceglia G, Rovelet-Lecrux A, Boeve B, Petersen RC, Dickson DW, Younkin SG, Deramecourt V, Crook J, Graff-Radford NR, Rademakers R (2009) Plasma progranulin levels predict progranulin mutation status in frontotemporal dementia patients and asymptomatic family members. *Brain (England)* 132:583-591.

Finch N et al (2011) TMEM106B regulates progranulin levels and the penetrance of FTLD in GRN mutation carriers. *Neurology (United States)* 76:467-474.

Forgac M (2007) Vacuolar ATPases: Rotary proton pumps in physiology and pathophysiology. *Nat Rev Mol Cell Biol (England)* 8:917-929.

Forgac M (1998) Structure, function and regulation of the vacuolar (H⁺)-ATPases. *FEBS Lett (NETHERLANDS)* 440:258-263.

Fratia P, Mizielinska S, Nicoll AJ, Zloh M, Fisher EM, Parkinson G, Isaacs AM (2012) C9orf72 hexanucleotide repeat associated with amyotrophic lateral sclerosis and frontotemporal dementia forms RNA G-quadruplexes. *Sci Rep (England)* 2:1016.

Freibaum BD, Lu Y, Lopez-Gonzalez R, Kim NC, Almeida S, Lee KH, Badders N, Valentine M, Miller BL, Wong PC, Petrucelli L, Kim HJ, Gao FB, Taylor JP (2015) GGGGCC repeat expansion in C9orf72 compromises nucleocytoplasmic transport. *Nature (England)* 525:129-133.

Fujita N, Saitoh T, Kageyama S, Akira S, Noda T, Yoshimori T (2009) Differential involvement of Atg16L1 in crohn disease and canonical autophagy: Analysis of the organization of the Atg16L1 complex in fibroblasts. *J Biol Chem (United States)* 284:32602-32609.

Gallagher MD et al (2014) TMEM106B is a genetic modifier of frontotemporal lobar degeneration with C9orf72 hexanucleotide repeat expansions. *Acta Neuropathol (Germany)* 127:407-418.

Gao X, Joselin AP, Wang L, Kar A, Ray P, Bateman A, Goate AM, Wu JY (2010) Progranulin promotes neurite outgrowth and neuronal differentiation by regulating GSK-3beta. *Protein Cell (Germany)* 1:552-562.

Garcin B, Lillo P, Hornberger M, Piguet O, Dawson K, Nestor PJ, Hodges JR (2009) Determinants of survival in behavioral variant frontotemporal dementia. *Neurology (United States)* 73:1656-1661.

Gass J et al (2006) Mutations in progranulin are a major cause of ubiquitin-positive frontotemporal lobar degeneration. *Hum Mol Genet (England)* 15:2988-3001.

Ge D, Han L, Huang S, Peng N, Wang P, Jiang Z, Zhao J, Su L, Zhang S, Zhang Y, Kung H, Zhao B, Miao J (2014) Identification of a novel MTOR activator and discovery of a competing endogenous RNA regulating autophagy in vascular endothelial cells. *Autophagy (United States)* 10:957-971.

Geisler S, Holmstrom KM, Skujat D, Fiesel FC, Rothfuss OC, Kahle PJ, Springer W (2010) PINK1/parkin-mediated mitophagy is dependent on VDAC1 and p62/SQSTM1. *Nat Cell Biol (England)* 12:119-131.

Gendron TF, Bieniek KF, Zhang YJ, Jansen-West K, Ash PE, Caulfield T, Daugherty L, Dunmore JH, Castanedes-Casey M, Chew J, Cosio DM, van Blitterswijk M, Lee WC, Rademakers R, Boylan KB, Dickson DW, Petrucelli L (2013) Antisense transcripts of the expanded C9ORF72 hexanucleotide repeat form nuclear RNA foci and undergo repeat-associated non-ATG translation in c9FTD/ALS. *Acta Neuropathol (Germany)* 126:829-844.

Geser F, Martinez-Lage M, Robinson J, Uryu K, Neumann M, Brandmeir NJ, Xie SX, Kwong LK, Elman L, McCluskey L, Clark CM, Malunda J, Miller BL, Zimmerman EA, Qian J, Van Deerlin V,

Grossman M, Lee VM, Trojanowski JQ (2009) Clinical and pathological continuum of multisystem TDP-43 proteinopathies. *Arch Neurol (United States)* 66:180-189.

Ghidoni R, Benussi L, Glionna M, Franzoni M, Binetti G (2008) Low plasma progranulin levels predict progranulin mutations in frontotemporal lobar degeneration. *Neurology (United States)* 71:1235-1239.

Ghosh P, Dahms NM, Kornfeld S (2003) Mannose 6-phosphate receptors: New twists in the tale. *Nat Rev Mol Cell Biol (England)* 4:202-212.

Ghoshal N, Dearborn JT, Wozniak DF, Cairns NJ (2012) Core features of frontotemporal dementia recapitulated in progranulin knockout mice. *Neurobiol Dis (United States)* 45:395-408.

Gijssels I, Van Broeckhoven C, Cruts M (2008) Granulin mutations associated with frontotemporal lobar degeneration and related disorders: An update. *Hum Mutat (United States)* 29:1373-1386.

Gijssels I et al (2012) A C9orf72 promoter repeat expansion in a flanders-belgian cohort with disorders of the frontotemporal lobar degeneration-amyotrophic lateral sclerosis spectrum: A gene identification study. *Lancet Neurol (England)* 11:54-65.

Gilad Y, Rifkin SA, Pritchard JK (2008) Revealing the architecture of gene regulation: The promise of eQTL studies. *Trends Genet (England)* 24:408-415.

Ginsberg SD, Mufson EJ, Counts SE, Wu J, Alldred MJ, Nixon RA, Che S (2010) Regional selectivity of rab5 and rab7 protein upregulation in mild cognitive impairment and alzheimer's disease. *J Alzheimers Dis (Netherlands)* 22:631-639.

Goedert M, Spillantini MG, Jakes R, Rutherford D, Crowther RA (1989) Multiple isoforms of human microtubule-associated protein tau: Sequences and localization in neurofibrillary tangles of alzheimer's disease. *Neuron (UNITED STATES)* 3:519-526.

Goldman JS, Farmer JM, Wood EM, Johnson JK, Boxer A, Neuhaus J, Lomen-Hoerth C, Wilhelmsen KC, Lee VM, Grossman M, Miller BL (2005) Comparison of family histories in FTL D subtypes and related tauopathies. *Neurology (United States)* 65:1817-1819.

Gomez-Deza J, Lee YB, Troakes C, Nolan M, Al-Sarraj S, Gallo JM, Shaw CE (2015) Dipeptide repeat protein inclusions are rare in the spinal cord and almost absent from motor neurons in C9ORF72 mutant amyotrophic lateral sclerosis and are unlikely to cause their degeneration. *Acta Neuropathol Commun (England)* 3:38-015-0218-y.

Gomez-Suaga P, Churchill GC, Patel S, Hilfiker S (2012) A link between LRRK2, autophagy and NAADP-mediated endolysosomal calcium signalling. *Biochem Soc Trans (England)* 40:1140-1146.

Gotzl JK, Mori K, Damme M, Fellerer K, Tahirovic S, Kleinberger G, Janssens J, van der Zee J, Lang CM, Kremmer E, Martin JJ, Engelborghs S, Kretzschmar HA, Arzberger T, Van Broeckhoven C, Haass C, Capell A (2014) Common pathobiochemical hallmarks of progranulin-associated frontotemporal lobar degeneration and neuronal ceroid lipofuscinosis. *Acta Neuropathol (Germany)* 127:845-860.

Gregory RI, Yan KP, Amuthan G, Chendrimada T, Doratotaj B, Cooch N, Shiekhattar R (2004) The microprocessor complex mediates the genesis of microRNAs. *Nature (England)* 432:235-240.

Guerreiro R, Bras J, Hardy J (2015) SnapShot: Genetics of ALS and FTD. *Cell (United States)* 160:798.e1.

Guo A, Tapia L, Bamji SX, Cynader MS, Jia W (2010) Progranulin deficiency leads to enhanced cell vulnerability and TDP-43 translocation in primary neuronal cultures. *Brain Res (Netherlands)* 1366:1-8.

Gustke N, Trinczek B, Biernat J, Mandelkow EM, Mandelkow E (1994) Domains of tau protein and interactions with microtubules. *Biochemistry (UNITED STATES)* 33:9511-9522.

Gutierrez MG, Munafo DB, Beron W, Colombo MI (2004) Rab7 is required for the normal progression of the autophagic pathway in mammalian cells. *J Cell Sci (England)* 117:2687-2697.

Hadano S, Otomo A, Kunita R, Suzuki-Utsunomiya K, Akatsuka A, Koike M, Aoki M, Uchiyama Y, Itoyama Y, Ikeda JE (2010) Loss of ALS2/alsin exacerbates motor dysfunction in a SOD1-expressing mouse ALS model by disturbing endolysosomal trafficking. *PLoS One (United States)* 5:e9805.

Hanada T, Noda NN, Satomi Y, Ichimura Y, Fujioka Y, Takao T, Inagaki F, Ohsumi Y (2007) The Atg12-Atg5 conjugate has a novel E3-like activity for protein lipidation in autophagy. *J Biol Chem (United States)* 282:37298-37302.

Hara T, Nakamura K, Matsui M, Yamamoto A, Nakahara Y, Suzuki-Migishima R, Yokoyama M, Mishima K, Saito I, Okano H, Mizushima N (2006) Suppression of basal autophagy in neural cells causes neurodegenerative disease in mice. *Nature (England)* 441:885-889.

Harris H, Rubinsztein DC (2011) Control of autophagy as a therapy for neurodegenerative disease. *Nat Rev Neurol (England)* 8:108-117.

He C, Klionsky DJ (2009) Regulation mechanisms and signaling pathways of autophagy. *Annu Rev Genet (United States)* 43:67-93.

He Z, Ismail A, Kriazhev L, Sadvakassova G, Bateman A (2002) Progranulin (PC-cell-derived growth factor/acrogranin) regulates invasion and cell survival. *Cancer Res (United States)* 62:5590-5596.

Hedrich K, Winkler S, Hagenah J, Kabakci K, Kasten M, Schwinger E, Volkmann J, Pramstaller PP, Kostic V, Vieregge P, Klein C (2006) Recurrent LRRK2 (Park8) mutations in early-onset parkinson's disease. *Mov Disord (United States)* 21:1506-1510.

Hiesinger PR, Fayyazuddin A, Mehta SQ, Rosenmund T, Schulze KL, Zhai RG, Verstreken P, Cao Y, Zhou Y, Kunz J, Bellen HJ (2005) The v-ATPase V0 subunit a1 is required for a late step in synaptic vesicle exocytosis in drosophila. *Cell (United States)* 121:607-620.

Hirst J, Barlow LD, Francisco GC, Sahlender DA, Seaman MN, Dacks JB, Robinson MS (2011) The fifth adaptor protein complex. *PLoS Biol (United States)* 9:e1001170.

Hodges JR, Davies R, Xuereb J, Kril J, Halliday G (2003) Survival in frontotemporal dementia. *Neurology (United States)* 61:349-354.

Hollenbeck PJ (1993) Products of endocytosis and autophagy are retrieved from axons by regulated retrograde organelle transport. *J Cell Biol (UNITED STATES)* 121:305-315.

Hu F, Padukkavidana T, Vaegter CB, Brady OA, Zheng Y, Mackenzie IR, Feldman HH, Nykjaer A, Strittmatter SM (2010) Sortilin-mediated endocytosis determines levels of the frontotemporal dementia protein, progranulin. *Neuron (United States)* 68:654-667.

Huang J, Klionsky DJ (2007) Autophagy and human disease. *Cell Cycle (United States)* 6:1837-1849.

Huotari J, Helenius A (2011) Endosome maturation. *Embo J (England)* 30:3481-3500.

Hutton M et al (1998) Association of missense and 5'-splice-site mutations in tau with the inherited dementia FTDP-17. *Nature (ENGLAND)* 393:702-705.

Hyttinen JM, Niittykoski M, Salminen A, Kaarniranta K (2013) Maturation of autophagosomes and endosomes: A key role for Rab7. *Biochim Biophys Acta (Netherlands)* 1833:503-510.

Ingelsson M, Ramasamy K, Russ C, Freeman SH, Orne J, Raju S, Matsui T, Growdon JH, Frosch MP, Ghetti B, Brown RH, Irizarry MC, Hyman BT (2007) Increase in the relative expression of tau with four microtubule binding repeat regions in frontotemporal lobar degeneration and progressive supranuclear palsy brains. *Acta Neuropathol (Germany)* 114:471-479.

Itakura E, Mizushima N (2010) Characterization of autophagosome formation site by a hierarchical analysis of mammalian atg proteins. *Autophagy (United States)* 6:764-776.

Itakura E, Kishi-Itakura C, Mizushima N (2012) The hairpin-type tail-anchored SNARE syntaxin 17 targets to autophagosomes for fusion with endosomes/lysosomes. *Cell (United States)* 151:1256-1269.

Jager S, Bucci C, Tanida I, Ueno T, Kominami E, Saftig P, Eskelinen EL (2004) Role for Rab7 in maturation of late autophagic vacuoles. *J Cell Sci (England)* 117:4837-4848.

Jahn R, Scheller RH (2006) SNAREs--engines for membrane fusion. *Nat Rev Mol Cell Biol (England)* 7:631-643.

Johnson DE, Ostrowski P, Jaumouille V, Grinstein S (2016) The position of lysosomes within the cell determines their luminal pH. *J Cell Biol (United States)* 212:677-692.

Johnson JK, Diehl J, Mendez MF, Neuhaus J, Shapira JS, Forman M, Chute DJ, Roberson ED, Pace-Savitsky C, Neumann M, Chow TW, Rosen HJ, Forstl H, Kurz A, Miller BL (2005)

Frontotemporal lobar degeneration: Demographic characteristics of 353 patients. *Arch Neurol (United States)* 62:925-930.

Johnston C, Jiang W, Chu T, Levine B (2001) Identification of genes involved in the host response to neurovirulent alphavirus infection. *J Virol (United States)* 75:10431-10445.

Jovicic A, Mertens J, Boeynaems S, Bogaert E, Chai N, Yamada SB, Paul JW, 3rd, Sun S, Herdy JR, Bieri G, Kramer NJ, Gage FH, Van Den Bosch L, Robberecht W, Gitler AD (2015) Modifiers of C9orf72 dipeptide repeat toxicity connect nucleocytoplasmic transport defects to FTD/ALS. *Nat Neurosci (United States)* 18:1226-1229.

Ju JS, Fuentealba RA, Miller SE, Jackson E, Piwnicka-Worms D, Baloh RH, Weihl CC (2009) Valosin-containing protein (VCP) is required for autophagy and is disrupted in VCP disease. *J Cell Biol (United States)* 187:875-888.

Kabashi E, Valdmanis PN, Dion P, Spiegelman D, McConkey BJ, Vande Velde C, Bouchard JP, Lacomblez L, Pochigaeva K, Salachas F, Pradat PF, Camu W, Meininger V, Dupre N, Rouleau GA (2008) TARDBP mutations in individuals with sporadic and familial amyotrophic lateral sclerosis. *Nat Genet (United States)* 40:572-574.

Kanazawa M, Kawamura K, Takahashi T, Miura M, Tanaka Y, Koyama M, Toriyabe M, Igarashi H, Nakada T, Nishihara M, Nishizawa M, Shimohata T (2015) Multiple therapeutic effects of progranulin on experimental acute ischaemic stroke. *Brain* .

Katzmann DJ, Odorizzi G, Emr SD (2002) Receptor downregulation and multivesicular-body sorting. *Nat Rev Mol Cell Biol (England)* 3:893-905.

Katzmann DJ, Babst M, Emr SD (2001) Ubiquitin-dependent sorting into the multivesicular body pathway requires the function of a conserved endosomal protein sorting complex, ESCRT-I. *Cell (United States)* 106:145-155.

Kawahara Y, Mieda-Sato A (2012) TDP-43 promotes microRNA biogenesis as a component of the drosha and dicer complexes. *Proc Natl Acad Sci U S A (United States)* 109:3347-3352.

Kayasuga Y, Chiba S, Suzuki M, Kikusui T, Matsuwaki T, Yamanouchi K, Kotaki H, Horai R, Iwakura Y, Nishihara M (2007) Alteration of behavioural phenotype in mice by targeted disruption of the progranulin gene. *Behav Brain Res (Netherlands)* 185:110-118.

Kessenbrock K, Frohlich L, Sixt M, Lammermann T, Pfister H, Bateman A, Belaouaj A, Ring J, Ollert M, Fassler R, Jenne DE (2008) Proteinase 3 and neutrophil elastase enhance inflammation in mice by inactivating antiinflammatory progranulin. *J Clin Invest (United States)* 118:2438-2447.

Kirchhausen T (2000) Clathrin. *Annu Rev Biochem (UNITED STATES)* 69:699-727.

Kleinberger G, Wils H, Ponsaerts P, Joris G, Timmermans JP, Van Broeckhoven C, Kumar-Singh S (2010) Increased caspase activation and decreased TDP-43 solubility in progranulin knockout cortical cultures. *J Neurochem (England)* 115:735-747.

Klionsky DJ et al (2012) Guidelines for the use and interpretation of assays for monitoring autophagy. *Autophagy (United States)* 8:445-544.

Knibb JA, Xuereb JH, Patterson K, Hodges JR (2006) Clinical and pathological characterization of progressive aphasia. *Ann Neurol (United States)* 59:156-165.

Komatsu M, Waguri S, Chiba T, Murata S, Iwata J, Tanida I, Ueno T, Koike M, Uchiyama Y, Kominami E, Tanaka K (2006) Loss of autophagy in the central nervous system causes neurodegeneration in mice. *Nature (England)* 441:880-884.

Komatsu M, Waguri S, Ueno T, Iwata J, Murata S, Tanida I, Ezaki J, Mizushima N, Ohsumi Y, Uchiyama Y, Kominami E, Tanaka K, Chiba T (2005) Impairment of starvation-induced and constitutive autophagy in Atg7-deficient mice. *J Cell Biol (United States)* 169:425-434.

Kopito RR (2000) Aggresomes, inclusion bodies and protein aggregation. Trends Cell Biol (ENGLAND) 10:524-530.

Koppers M, Blokhuis AM, Westeneng HJ, Terpstra ML, Zundel CA, Vieira de Sa R, Schellevis RD, Waite AJ, Blake DJ, Veldink JH, van den Berg LH, Jeroen Pasterkamp R (2015) C9orf72 ablation in mice does not cause motor neuron degeneration or motor deficits. Ann Neurol .

Korolchuk VI, Saiki S, Lichtenberg M, Siddiqi FH, Roberts EA, Imarisio S, Jahreiss L, Sarkar S, Futter M, Menzies FM, O'Kane CJ, Deretic V, Rubinsztein DC (2011) Lysosomal positioning coordinates cellular nutrient responses. Nat Cell Biol (England) 13:453-460.

Kwon I, Xiang S, Kato M, Wu L, Theodoropoulos P, Wang T, Kim J, Yun J, Xie Y, McKnight SL (2014) Poly-dipeptides encoded by the C9orf72 repeats bind nucleoli, impede RNA biogenesis, and kill cells. Science (United States) 345:1139-1145.

Lagier-Tourenne C, Cleveland DW (2009) Rethinking ALS: The FUS about TDP-43. Cell (United States) 136:1001-1004.

Laird AS, Van Hoecke A, De Mynck L, Timmers M, Van den Bosch L, Van Damme P, Robberecht W (2010) Progranulin is neurotrophic in vivo and protects against a mutant TDP-43 induced axonopathy. PLoS One (United States) 5:e13368.

Lamb CA, Dooley HC, Tooze SA (2013) Endocytosis and autophagy: Shared machinery for degradation. Bioessays (United States) 35:34-45.

Lang CM, Fellerer K, Schwenk BM, Kuhn PH, Kremmer E, Edbauer D, Capell A, Haass C (2012) Membrane orientation and subcellular localization of transmembrane protein 106B (TMEM106B), a major risk factor for frontotemporal lobar degeneration. J Biol Chem (United States) 287:19355-19365.

Laplante M, Sabatini DM (2012) mTOR signaling in growth control and disease. *Cell (United States)* 149:274-293.

Larsen KE, Sulzer D (2002) Autophagy in neurons: A review. *Histol Histopathol (Spain)* 17:897-908.

Le Borgne R, Alconada A, Bauer U, Hoflack B (1998) The mammalian AP-3 adaptor-like complex mediates the intracellular transport of lysosomal membrane glycoproteins. *J Biol Chem (UNITED STATES)* 273:29451-29461.

Lee EB, Lee VM, Trojanowski JQ (2011a) Gains or losses: Molecular mechanisms of TDP43-mediated neurodegeneration. *Nat Rev Neurosci (England)* 13:38-50.

Lee JA, Gao FB (2009) Inhibition of autophagy induction delays neuronal cell loss caused by dysfunctional ESCRT-III in frontotemporal dementia. *J Neurosci (United States)* 29:8506-8511.

Lee JA, Beigneux A, Ahmad ST, Young SG, Gao FB (2007) ESCRT-III dysfunction causes autophagosome accumulation and neurodegeneration. *Curr Biol (England)* 17:1561-1567.

Lee JH, Yu WH, Kumar A, Lee S, Mohan PS, Peterhoff CM, Wolfe DM, Martinez-Vicente M, Massey AC, Sovak G, Uchiyama Y, Westaway D, Cuervo AM, Nixon RA (2010) Lysosomal proteolysis and autophagy require presenilin 1 and are disrupted by alzheimer-related PS1 mutations. *Cell (United States)* 141:1146-1158.

Lee S, Sato Y, Nixon RA (2011b) Lysosomal proteolysis inhibition selectively disrupts axonal transport of degradative organelles and causes an alzheimer's-like axonal dystrophy. *J Neurosci (United States)* 31:7817-7830.

Lee YB, Chen HJ, Peres JN, Gomez-Deza J, Attig J, Stalekar M, Troakes C, Nishimura AL, Scotter EL, Vance C, Adachi Y, Sardone V, Miller JW, Smith BN, Gallo JM, Ule J, Hirth F, Rogelj

B, Houart C, Shaw CE (2013) Hexanucleotide repeats in ALS/FTD form length-dependent RNA foci, sequester RNA binding proteins, and are neurotoxic. *Cell Rep (United States)* 5:1178-1186.

Letourneur F, Klausner RD (1992) A novel di-leucine motif and a tyrosine-based motif independently mediate lysosomal targeting and endocytosis of CD3 chains. *Cell (UNITED STATES)* 69:1143-1157.

Levine B, Yuan J (2005) Autophagy in cell death: An innocent convict? *J Clin Invest (United States)* 115:2679-2688.

Levine B, Mizushima N, Virgin HW (2011) Autophagy in immunity and inflammation. *Nature (England)* 469:323-335.

Levine TP, Daniels RD, Gatta AT, Wong LH, Hayes MJ (2013a) The product of C9orf72, a gene strongly implicated in neurodegeneration, is structurally related to DENN rab-GEFs. *Bioinformatics (England)* 29:499-503.

Levine TP, Daniels RD, Gatta AT, Wong LH, Hayes MJ (2013b) The product of C9orf72, a gene strongly implicated in neurodegeneration, is structurally related to DENN rab-GEFs. *Bioinformatics (England)* 29:499-503.

Liang XH, Kleeman LK, Jiang HH, Gordon G, Goldman JE, Berry G, Herman B, Levine B (1998) Protection against fatal sindbis virus encephalitis by beclin, a novel bcl-2-interacting protein. *J Virol (UNITED STATES)* 72:8586-8596.

Lieberman AP, Puertollano R, Raben N, Slaugenhaupt S, Walkley SU, Ballabio A (2012) Autophagy in lysosomal storage disorders. *Autophagy (United States)* 8:719-730.

Ling SC, Polymenidou M, Cleveland DW (2013) Converging mechanisms in ALS and FTD: Disrupted RNA and protein homeostasis. *Neuron (United States)* 79:416-438.

Ling SC, Albuquerque CP, Han JS, Lagier-Tourenne C, Tokunaga S, Zhou H, Cleveland DW (2010) ALS-associated mutations in TDP-43 increase its stability and promote TDP-43 complexes with FUS/TLS. *Proc Natl Acad Sci U S A (United States)* 107:13318-13323.

Lipinski MM, Zheng B, Lu T, Yan Z, Py BF, Ng A, Xavier RJ, Li C, Yankner BA, Scherzer CR, Yuan J (2010) Genome-wide analysis reveals mechanisms modulating autophagy in normal brain aging and in alzheimer's disease. *Proc Natl Acad Sci U S A (United States)* 107:14164-14169.

Liu Y, Levine B (2015) Autosis and autophagic cell death: The dark side of autophagy. *Cell Death Differ (England)* 22:367-376.

Liu Y, Shoji-Kawata S, Sumpter RM, Jr, Wei Y, Ginet V, Zhang L, Posner B, Tran KA, Green DR, Xavier RJ, Shaw SY, Clarke PG, Puyal J, Levine B (2013) Autosis is a Na^+ , K^+ -ATPase-regulated form of cell death triggered by autophagy-inducing peptides, starvation, and hypoxia-ischemia. *Proc Natl Acad Sci U S A (United States)* 110:20364-20371.

Lu Y, Hao BX, Graeff R, Wong CW, Wu WT, Yue J (2013) Two pore channel 2 (TPC2) inhibits autophagosomal-lysosomal fusion by alkalinizing lysosomal pH. *J Biol Chem (United States)* 288:24247-24263.

Luzio JP, Pryor PR, Bright NA (2007) Lysosomes: Fusion and function. *Nat Rev Mol Cell Biol (England)* 8:622-632.

Ma J, Becker C, Reyes C, Underhill DM (2014) Cutting edge: FYCO1 recruitment to dectin-1 phagosomes is accelerated by light chain 3 protein and regulates phagosome maturation and reactive oxygen production. *J Immunol (United States)* 192:1356-1360.

Ma X, Godar RJ, Liu H, Diwan A (2012) Enhancing lysosome biogenesis attenuates BNIP3-induced cardiomyocyte death. *Autophagy (United States)* 8:297-309.

Mackenzie IR, Feldman HH (2005) Ubiquitin immunohistochemistry suggests classic motor neuron disease, motor neuron disease with dementia, and frontotemporal dementia of the motor neuron disease type represent a clinicopathologic spectrum. *J Neuropathol Exp Neurol (United States)* 64:730-739.

Mackenzie IR, Rademakers R, Neumann M (2010) TDP-43 and FUS in amyotrophic lateral sclerosis and frontotemporal dementia. *Lancet Neurol (England)* 9:995-1007.

Mackenzie IR, Neumann M, Baborie A, Sampathu DM, Du Plessis D, Jaros E, Perry RH, Trojanowski JQ, Mann DM, Lee VM (2011) A harmonized classification system for FTLD-TDP pathology. *Acta Neuropathol (Germany)* 122:111-113.

Mackenzie IR, Baker M, Pickering-Brown S, Hsiung GY, Lindholm C, Dwosh E, Gass J, Cannon A, Rademakers R, Hutton M, Feldman HH (2006) The neuropathology of frontotemporal lobar degeneration caused by mutations in the progranulin gene. *Brain (England)* 129:3081-3090.

Mackenzie IR et al (2009) Nomenclature for neuropathologic subtypes of frontotemporal lobar degeneration: Consensus recommendations. *Acta Neuropathol (Germany)* 117:15-18.

MacLeod DA, Rhinn H, Kuwahara T, Zolin A, Di Paolo G, McCabe BD, Marder KS, Honig LS, Clark LN, Small SA, Abeliovich A (2013) RAB7L1 interacts with LRRK2 to modify intraneuronal protein sorting and parkinson's disease risk. *Neuron (United States)* 77:425-439.

Marcusson EG, Horazdovsky BF, Cereghino JL, Gharakhanian E, Emr SD (1994) The sorting receptor for yeast vacuolar carboxypeptidase Y is encoded by the VPS10 gene. *Cell (UNITED STATES)* 77:579-586.

Martens LH, Zhang J, Barmada SJ, Zhou P, Kamiya S, Sun B, Min SW, Gan L, Finkbeiner S, Huang EJ, Farese RV, Jr (2012) Progranulin deficiency promotes neuroinflammation and neuron loss following toxin-induced injury. *J Clin Invest (United States)* 122:3955-3959.

Martin I, Kim JW, Dawson VL, Dawson TM (2016) LRRK2 pathobiology in parkinson's disease - virtual inclusion. *J Neurochem* .

Martina JA, Diab HI, Lishu L, Jeong-A L, Patange S, Raben N, Puertollano R (2014) The nutrient-responsive transcription factor TFE3 promotes autophagy, lysosomal biogenesis, and clearance of cellular debris. *Sci Signal (United States)* 7:ra9.

Matsuda J, Yoneshige A, Suzuki K (2007) The function of sphingolipids in the nervous system: Lessons learnt from mouse models of specific sphingolipid activator protein deficiencies. *J Neurochem (England)* 103 Suppl 1:32-38.

Medina DL, Fraldi A, Bouche V, Annunziata F, Mansueto G, Spampanato C, Puri C, Pignata A, Martina JA, Sardiello M, Palmieri M, Polishchuk R, Puertollano R, Ballabio A (2011) Transcriptional activation of lysosomal exocytosis promotes cellular clearance. *Dev Cell (United States)* 21:421-430.

Melendez A, Talloczy Z, Seaman M, Eskelinen EL, Hall DH, Levine B (2003) Autophagy genes are essential for dauer development and life-span extension in *C. elegans*. *Science (United States)* 301:1387-1391.

Mercy L, Hodges JR, Dawson K, Barker RA, Brayne C (2008) Incidence of early-onset dementias in cambridgeshire, united kingdom. *Neurology (United States)* 71:1496-1499.

Meresse S, Gorvel JP, Chavrier P (1995) The rab7 GTPase resides on a vesicular compartment connected to lysosomes. *J Cell Sci (ENGLAND)* 108 (Pt 11):3349-3358.

Mijaljica D, Prescott M, Devenish RJ (2011) Microautophagy in mammalian cells: Revisiting a 40-year-old conundrum. *Autophagy (United States)* 7:673-682.

Minami SS, Min SW, Krabbe G, Wang C, Zhou Y, Asgarov R, Li Y, Martens LH, Elia LP, Ward ME, Mucke L, Farese RV, Jr, Gan L (2014) Progranulin protects against amyloid beta deposition and toxicity in Alzheimer's disease mouse models. *Nat Med (United States)* 20:1157-1164.

Mineo C, Gill GN, Anderson RG (1999) Regulated migration of epidermal growth factor receptor from caveolae. *J Biol Chem (UNITED STATES)* 274:30636-30643.

Mizielinska S, Lashley T, Norona FE, Clayton EL, Ridler CE, Fratta P, Isaacs AM (2013) C9orf72 frontotemporal lobar degeneration is characterised by frequent neuronal sense and antisense RNA foci. *Acta Neuropathol (Germany)* 126:845-857.

Mizielinska S, Gronke S, Niccoli T, Ridler CE, Clayton EL, Devoy A, Moens T, Norona FE, Woollacott IO, Pietrzyk J, Cleverley K, Nicoll AJ, Pickering-Brown S, Dols J, Cabecinha M, Hendrich O, Fratta P, Fisher EM, Partridge L, Isaacs AM (2014) C9orf72 repeat expansions cause neurodegeneration in *Drosophila* through arginine-rich proteins. *Science (United States)* 345:1192-1194.

Mizushima N, Yoshimori T, Levine B (2010) Methods in mammalian autophagy research. *Cell (United States)* 140:313-326.

Mizushima N, Noda T, Yoshimori T, Tanaka Y, Ishii T, George MD, Klionsky DJ, Ohsumi M, Ohsumi Y (1998) A protein conjugation system essential for autophagy. *Nature (ENGLAND)* 395:395-398.

Mori K, Arzberger T, Grasser FA, Gijssels I, May S, Rentzsch K, Weng SM, Schludi MH, van der Zee J, Cruts M, Van Broeckhoven C, Kremmer E, Kretschmar HA, Haass C, Edbauer D (2013) Bidirectional transcripts of the expanded C9orf72 hexanucleotide repeat are translated into aggregating dipeptide repeat proteins. *Acta Neuropathol (Germany)* 126:881-893.

Mukherjee O, Wang J, Gitcho M, Chakraverty S, Taylor-Reinwald L, Shears S, Kauwe JS, Norton J, Levitch D, Bigio EH, Hatanpaa KJ, White CL, Morris JC, Cairns NJ, Goate A (2008) Molecular characterization of novel progranulin (GRN) mutations in frontotemporal dementia. *Hum Mutat (United States)* 29:512-521.

Narendra D, Tanaka A, Suen DF, Youle RJ (2008) Parkin is recruited selectively to impaired mitochondria and promotes their autophagy. *J Cell Biol (United States)* 183:795-803.

Neary D, Snowden J, Mann D (2005) Frontotemporal dementia. *Lancet Neurol (England)* 4:771-780.

Neumann M, Sampathu DM, Kwong LK, Truax AC, Micsenyi MC, Chou TT, Bruce J, Schuck T, Grossman M, Clark CM, McCluskey LF, Miller BL, Masliah E, Mackenzie IR, Feldman H, Feiden W, Kretzschmar HA, Trojanowski JQ, Lee VM (2006) Ubiquitinated TDP-43 in frontotemporal lobar degeneration and amyotrophic lateral sclerosis. *Science (United States)* 314:130-133.

Nicholson AM, Finch NA, Wojtas A, Baker MC, Perkerson RB, Castanedes-Casey M, Rousseau L, Benussi L, Binetti G, Ghidoni R, Hsiung GY, Mackenzie IR, Finger E, Boeve BF, Ertekin-Taner N, Graff-Radford NR, Dickson DW, Rademakers R (2013) TMEM106B p.T185S regulates TMEM106B protein levels: Implications for frontotemporal dementia. *J Neurochem* .

Nishi T, Forgac M (2000) Molecular cloning and expression of three isoforms of the 100-kDa a subunit of the mouse vacuolar proton-translocating ATPase. *J Biol Chem (UNITED STATES)* 275:6824-6830.

Nixon RA, Yang DS (2011) Autophagy failure in alzheimer's disease--locating the primary defect. *Neurobiol Dis (United States)* 43:38-45.

O'Brien JS, Kishimoto Y (1991) Saposin proteins: Structure, function, and role in human lysosomal storage disorders. *Faseb J (UNITED STATES)* 5:301-308.

Ohkuma S (1989) Use of fluorescein isothiocyanate-dextran to measure proton pumping in lysosomes and related organelles. *Methods Enzymol (UNITED STATES)* 174:131-154.

Ohno H, Aguilar RC, Fournier MC, Hennecke S, Cosson P, Bonifacino JS (1997) Interaction of endocytic signals from the HIV-1 envelope glycoprotein complex with members of the adaptor medium chain family. *Virology (UNITED STATES)* 238:305-315.

Okura H, Yamashita S, Ohama T, Saga A, Yamamoto-Kakuta A, Hamada Y, Sougawa N, Ohyama R, Sawa Y, Matsuyama A (2010) HDL/apolipoprotein A-I binds to macrophage-derived progranulin and suppresses its conversion into proinflammatory granulins. *J Atheroscler Thromb (Japan)* 17:568-577.

O'Rourke JG, Bogdanik L, Yanez A, Lall D, Wolf AJ, Muhammad AK, Ho R, Carmona S, Vit JP, Zarrow J, Kim KJ, Bell S, Harms MB, Miller TM, Dangler CA, Underhill DM, Goodridge HS, Lutz CM, Baloh RH (2016) C9orf72 is required for proper macrophage and microglial function in mice. *Science (United States)* 351:1324-1329.

Ou SH, Wu F, Harrich D, Garcia-Martinez LF, Gaynor RB (1995) Cloning and characterization of a novel cellular protein, TDP-43, that binds to human immunodeficiency virus type 1 TAR DNA sequence motifs. *J Virol (UNITED STATES)* 69:3584-3596.

Palmieri M, Impey S, Kang H, di Ronza A, Pelz C, Sardiello M, Ballabio A (2011) Characterization of the CLEAR network reveals an integrated control of cellular clearance pathways. *Hum Mol Genet (England)* 20:3852-3866.

Parkinson-Lawrence EJ, Shandala T, Prodoehl M, Plew R, Borlace GN, Brooks DA (2010) Lysosomal storage disease: Revealing lysosomal function and physiology. *Physiology (Bethesda) (United States)* 25:102-115.

Pawlowski N (2010) Dynamin self-assembly and the vesicle scission mechanism: How dynamin oligomers cleave the membrane neck of clathrin-coated pits during endocytosis. *Bioessays* (United States) 32:1033-1039.

Pearse BM, Robinson MS (1990) Clathrin, adaptors, and sorting. *Annu Rev Cell Biol* (UNITED STATES) 6:151-171.

Pereson S, Wils H, Kleinberger G, McGowan E, Vandewoestyne M, Van Broeck B, Joris G, Cuijt I, Deforce D, Hutton M, Van Broeckhoven C, Kumar-Singh S (2009) Progranulin expression correlates with dense-core amyloid plaque burden in alzheimer disease mouse models. *J Pathol* (England) 219:173-181.

Peters OM et al (2015) Human C9ORF72 hexanucleotide expansion reproduces RNA foci and dipeptide repeat proteins but not neurodegeneration in BAC transgenic mice. *Neuron* (United States) 88:902-909.

Petersen CM, Nielsen MS, Nykjaer A, Jacobsen L, Tommerup N, Rasmussen HH, Roigaard H, Gliemann J, Madsen P, Moestrup SK (1997) Molecular identification of a novel candidate sorting receptor purified from human brain by receptor-associated protein affinity chromatography. *J Biol Chem* (UNITED STATES) 272:3599-3605.

Petkau TL, Neal SJ, Orban PC, MacDonald JL, Hill AM, Lu G, Feldman HH, Mackenzie IR, Leavitt BR (2010) Progranulin expression in the developing and adult murine brain. *J Comp Neurol* (United States) 518:3931-3947.

Pickford F, Masliah E, Britschgi M, Lucin K, Narasimhan R, Jaeger PA, Small S, Spencer B, Rockenstein E, Levine B, Wyss-Coray T (2008) The autophagy-related protein beclin 1 shows reduced expression in early alzheimer disease and regulates amyloid beta accumulation in mice. *J Clin Invest* (United States) 118:2190-2199.

Plowman GD, Green JM, Neubauer MG, Buckley SD, McDonald VL, Todaro GJ, Shoyab M (1992) The epithelin precursor encodes two proteins with opposing activities on epithelial cell growth. *J Biol Chem (UNITED STATES)* 267:13073-13078.

Polymenidou M, Lagier-Tourenne C, Hutt KR, Huelga SC, Moran J, Liang TY, Ling SC, Sun E, Wancewicz E, Mazur C, Kordasiewicz H, Sedaghat Y, Donohue JP, Shiue L, Bennett CF, Yeo GW, Cleveland DW (2011) Long pre-mRNA depletion and RNA missplicing contribute to neuronal vulnerability from loss of TDP-43. *Nat Neurosci (United States)* 14:459-468.

Pond L, Kuhn LA, Teyton L, Schutze MP, Tainer JA, Jackson MR, Peterson PA (1995) A role for acidic residues in di-leucine motif-based targeting to the endocytic pathway. *J Biol Chem (UNITED STATES)* 270:19989-19997.

Pryor PR, Mullock BM, Bright NA, Gray SR, Luzio JP (2000) The role of intraorganellar Ca^{2+} in late endosome-lysosome heterotypic fusion and in the reformation of lysosomes from hybrid organelles. *J Cell Biol (UNITED STATES)* 149:1053-1062.

Qi X, Grabowski GA (2001) Molecular and cell biology of acid beta-glucosidase and prosaposin. *Prog Nucleic Acid Res Mol Biol (UNITED STATES)* 66:203-239.

Raiborg C, Stenmark H (2009) The ESCRT machinery in endosomal sorting of ubiquitylated membrane proteins. *Nature (England)* 458:445-452.

Ramirez A, Heimbach A, Grundemann J, Stiller B, Hampshire D, Cid LP, Goebel I, Mubaidin AF, Wriekat AL, Roeper J, Al-Din A, Hillmer AM, Karsak M, Liss B, Woods CG, Behrens MI, Kubisch C (2006) Hereditary parkinsonism with dementia is caused by mutations in ATP13A2, encoding a lysosomal type 5 P-type ATPase. *Nat Genet (United States)* 38:1184-1191.

Ratnavalli E, Brayne C, Dawson K, Hodges JR (2002) The prevalence of frontotemporal dementia. *Neurology (United States)* 58:1615-1621.

Reddy A, Caler EV, Andrews NW (2001) Plasma membrane repair is mediated by Ca^{2+} -regulated exocytosis of lysosomes. *Cell (United States)* 106:157-169.

Renton AE et al (2011) A hexanucleotide repeat expansion in C9ORF72 is the cause of chromosome 9p21-linked ALS-FTD. *Neuron (United States)* 72:257-268.

Ringholz GM, Greene SR (2006) The relationship between amyotrophic lateral sclerosis and frontotemporal dementia. *Curr Neurol Neurosci Rep (United States)* 6:387-392.

Rink J, Ghigo E, Kalaidzidis Y, Zerial M (2005) Rab conversion as a mechanism of progression from early to late endosomes. *Cell (United States)* 122:735-749.

Ritz D, Vuk M, Kirchner P, Bug M, Schutz S, Hayer A, Bremer S, Lusk C, Baloh RH, Lee H, Glatter T, Gstaiger M, Aebersold R, Wehl CC, Meyer H (2011) Endolysosomal sorting of ubiquitylated caveolin-1 is regulated by VCP and UBXD1 and impaired by VCP disease mutations. *Nat Cell Biol (England)* 13:1116-1123.

Robberecht W, Philips T (2013) The changing scene of amyotrophic lateral sclerosis. *Nat Rev Neurosci (England)* 14:248-264.

Roberts VJ, Gorenstein C (1987) Examination of the transient distribution of lysosomes in neurons of developing rat brains. *Dev Neurosci (SWITZERLAND)* 9:255-264.

Roczniak-Ferguson A, Petit CS, Froehlich F, Qian S, Ky J, Angarola B, Walther TC, Ferguson SM (2012) The transcription factor TFEB links mTORC1 signaling to transcriptional control of lysosome homeostasis. *Sci Signal (United States)* 5:ra42.

Rong Y, Liu M, Ma L, Du W, Zhang H, Tian Y, Cao Z, Li Y, Ren H, Zhang C, Li L, Chen S, Xi J, Yu L (2012) Clathrin and phosphatidylinositol-4,5-bisphosphate regulate autophagic lysosome reformation. *Nat Cell Biol (England)* 14:924-934.

Rossmann KL, Worthylake DK, Snyder JT, Siderovski DP, Campbell SL, Sondek J (2002) A crystallographic view of interactions between dbpA and Cdc42: PH domain-assisted guanine nucleotide exchange. *Embo J (England)* 21:1315-1326.

Rosso SM, Donker Kaat L, Baks T, Joosse M, de Koning I, Pijnenburg Y, de Jong D, Dooijes D, Kamphorst W, Ravid R, Niermeijer MF, Verheij F, Kremer HP, Scheltens P, van Duijn CM, Heutink P, van Swieten JC (2003) Frontotemporal dementia in the Netherlands: Patient characteristics and prevalence estimates from a population-based study. *Brain (England)* 126:2016-2022.

Rusten TE, Stenmark H (2009) How do ESCRT proteins control autophagy? *J Cell Sci (England)* 122:2179-2183.

Rutherford NJ, Carrasquillo MM, Li M, Bisceglia G, Menke J, Josephs KA, Parisi JE, Petersen RC, Graff-Radford NR, Younkin SG, Dickson DW, Rademakers R (2012) TMEM106B risk variant is implicated in the pathologic presentation of Alzheimer disease. *Neurology (United States)* 79:717-718.

Sadowski L, Pilecka I, Miaczynska M (2009) Signaling from endosomes: Location makes a difference. *Exp Cell Res (United States)* 315:1601-1609.

Saftig P, Klumperman J (2009) Lysosome biogenesis and lysosomal membrane proteins: Trafficking meets function. *Nat Rev Mol Cell Biol (England)* 10:623-635.

Samie MA, Xu H (2014) Lysosomal exocytosis and lipid storage disorders. *J Lipid Res* 55:995-1009.

Sancak Y, Bar-Peled L, Zoncu R, Markhard AL, Nada S, Sabatini DM (2010) Ragulator-Rag complex targets mTORC1 to the lysosomal surface and is necessary for its activation by amino acids. *Cell (United States)* 141:290-303.

Sardi SP, Clarke J, Kinnecom C, Tamsett TJ, Li L, Stanek LM, Passini MA, Grabowski GA, Schlossmacher MG, Sidman RL, Cheng SH, Shihabuddin LS (2011) CNS expression of glucocerebrosidase corrects alpha-synuclein pathology and memory in a mouse model of gaucher-related synucleinopathy. *Proc Natl Acad Sci U S A (United States)* 108:12101-12106.

Sardiello M, Palmieri M, di Ronza A, Medina DL, Valenza M, Gennarino VA, Di Malta C, Donaudy F, Embrione V, Polishchuk RS, Banfi S, Parenti G, Cattaneo E, Ballabio A (2009) A gene network regulating lysosomal biogenesis and function. *Science (United States)* 325:473-477.

Sato-Harada R, Okabe S, Umeyama T, Kanai Y, Hirokawa N (1996) Microtubule-associated proteins regulate microtubule function as the track for intracellular membrane organelle transports. *Cell Struct Funct (JAPAN)* 21:283-295.

Schenk MF, Szendro IG, Salverda ML, Krug J, de Visser JA (2013) Patterns of epistasis between beneficial mutations in an antibiotic resistance gene. *Mol Biol Evol (United States)* 30:1779-1787.

Schu PV, Takegawa K, Fry MJ, Stack JH, Waterfield MD, Emr SD (1993) Phosphatidylinositol 3-kinase encoded by yeast VPS34 gene essential for protein sorting. *Science (UNITED STATES)* 260:88-91.

Schulze H, Sandhoff K (2011) Lysosomal lipid storage diseases. *Cold Spring Harb Perspect Biol (United States)* 3:10.1101/cshperspect.a004804.

Schwenk BM, Lang CM, Hogg S, Tahirovic S, Orozco D, Rentzsch K, Lichtenthaler SF, Hoogenraad CC, Capell A, Haass C, Edbauer D (2014) The FTLN risk factor TMEM106B and MAP6 control dendritic trafficking of lysosomes. *Embo J (England)* 33:450-467.

Schwenk JM, Lindberg J, Sundberg M, Uhlen M, Nilsson P (2007) Determination of binding specificities in highly multiplexed bead-based assays for antibody proteomics. *Mol Cell Proteomics (United States)* 6:125-132.

Seabra MC, Wasmeier C (2004) Controlling the location and activation of rab GTPases. *Curr Opin Cell Biol (United States)* 16:451-457.

Seelaar H, Rohrer JD, Pijnenburg YA, Fox NC, van Swieten JC (2011) Clinical, genetic and pathological heterogeneity of frontotemporal dementia: A review. *J Neurol Neurosurg Psychiatry (England)* 82:476-486.

Sephton CF, Cenik C, Kucukural A, Dammer EB, Cenik B, Han Y, Dewey CM, Roth FP, Herz J, Peng J, Moore MJ, Yu G (2011) Identification of neuronal RNA targets of TDP-43-containing ribonucleoprotein complexes. *J Biol Chem (United States)* 286:1204-1215.

Settembre C, Fraldi A, Medina DL, Ballabio A (2013) Signals from the lysosome: A control centre for cellular clearance and energy metabolism. *Nat Rev Mol Cell Biol (England)* 14:283-296.

Settembre C, Fraldi A, Jahreiss L, Spampinato C, Venturi C, Medina D, de Pablo R, Tacchetti C, Rubinsztein DC, Ballabio A (2008) A block of autophagy in lysosomal storage disorders. *Hum Mol Genet (England)* 17:119-129.

Settembre C, Zoncu R, Medina DL, Vetrini F, Erdin S, Erdin S, Huynh T, Ferron M, Karsenty G, Vellard MC, Facchinetti V, Sabatini DM, Ballabio A (2012) A lysosome-to-nucleus signalling mechanism senses and regulates the lysosome via mTOR and TFEB. *Embo J (England)* 31:1095-1108.

Settembre C, Di Malta C, Polito VA, Garcia Arencibia M, Vetrini F, Erdin S, Erdin SU, Huynh T, Medina D, Colella P, Sardiello M, Rubinsztein DC, Ballabio A (2011) TFEB links autophagy to lysosomal biogenesis. *Science (United States)* 332:1429-1433.

Shacka JJ (2012) Mouse models of neuronal ceroid lipofuscinoses: Useful pre-clinical tools to delineate disease pathophysiology and validate therapeutics. *Brain Res Bull (United States)* 88:43-57.

Shankaran SS, Capell A, Hruscha AT, Fellerer K, Neumann M, Schmid B, Haass C (2008) Missense mutations in the progranulin gene linked to frontotemporal lobar degeneration with ubiquitin-immunoreactive inclusions reduce progranulin production and secretion. *J Biol Chem (United States)* 283:1744-1753.

Shibutani ST, Yoshimori T (2014) A current perspective of autophagosome biogenesis. *Cell Res (England)* 24:58-68.

Shintani T, Klionsky DJ (2004) Autophagy in health and disease: A double-edged sword. *Science (United States)* 306:990-995.

Sieben A, Van Langenhove T, Engelborghs S, Martin JJ, Boon P, Cras P, De Deyn PP, Santens P, Van Broeckhoven C, Cruts M (2012) The genetics and neuropathology of frontotemporal lobar degeneration. *Acta Neuropathol (Germany)* 124:353-372.

Siintola E, Partanen S, Stromme P, Haapanen A, Haltia M, Maehlen J, Lehesjoki AE, Tyynela J (2006) Cathepsin D deficiency underlies congenital human neuronal ceroid-lipofuscinosis. *Brain (England)* 129:1438-1445.

Silva RF, Mendonca SC, Carvalho LM, Reis AM, Gordo I, Trindade S, Dionisio F (2011) Pervasive sign epistasis between conjugative plasmids and drug-resistance chromosomal mutations. *PLoS Genet (United States)* 7:e1002181.

Slegers K, Brouwers N, Van Damme P, Engelborghs S, Gijssels I, van der Zee J, Peeters K, Mattheijssens M, Cruts M, Vandenberghe R, De Deyn PP, Robberecht W, Van Broeckhoven C (2009) Serum biomarker for progranulin-associated frontotemporal lobar degeneration. *Ann Neurol (United States)* 65:603-609.

Smith KR, Damiano J, Franceschetti S, Carpenter S, Canafoglia L, Morbin M, Rossi G, Pareyson D, Mole SE, Staropoli JF, Sims KB, Lewis J, Lin WL, Dickson DW, Dahl HH, Bahlo M, Berkovic

SF (2012) Strikingly different clinicopathological phenotypes determined by progranulin-mutation dosage. *Am J Hum Genet (United States)* 90:1102-1107.

Sorkin A, Duex JE (2010) Quantitative analysis of endocytosis and turnover of epidermal growth factor (EGF) and EGF receptor. *Curr Protoc Cell Biol (United States)* Chapter 15:Unit 15.14.

Spampanato C, Feeney E, Li L, Cardone M, Lim JA, Annunziata F, Zare H, Polishchuk R, Puertollano R, Parenti G, Ballabio A, Raben N (2013) Transcription factor EB (TFEB) is a new therapeutic target for pompe disease. *EMBO Mol Med (England)* 5:691-706.

Spillantini MG, Crowther RA, Kamphorst W, Heutink P, van Swieten JC (1998) Tau pathology in two dutch families with mutations in the microtubule-binding region of tau. *Am J Pathol (UNITED STATES)* 153:1359-1363.

Spillantini MG, Murrell JR, Goedert M, Farlow M, Klug A, Ghetti B (2006) Mutations in the tau gene (MAPT) in FTDP-17: The family with multiple system tauopathy with presenile dementia (MSTD). *J Alzheimers Dis (Netherlands)* 9:373-380.

Sreedharan J, Blair IP, Tripathi VB, Hu X, Vance C, Rogelj B, Ackerley S, Durnall JC, Williams KL, Buratti E, Baralle F, de Belleruche J, Mitchell JD, Leigh PN, Al-Chalabi A, Miller CC, Nicholson G, Shaw CE (2008) TDP-43 mutations in familial and sporadic amyotrophic lateral sclerosis. *Science (United States)* 319:1668-1672.

Stagi M, Klein ZA, Gould TJ, Bewersdorf J, Strittmatter SM (2014) Lysosome size, motility and stress response regulated by fronto-temporal dementia modifier TMEM106B. *Mol Cell Neurosci (United States)* 61:226-240.

Suh HS, Choi N, Tarassishin L, Lee SC (2012) Regulation of progranulin expression in human microglia and proteolysis of progranulin by matrix metalloproteinase-12 (MMP-12). *PLoS One (United States)* 7:e35115.

Suzuki K, Kubota Y, Sekito T, Ohsumi Y (2007) Hierarchy of atg proteins in pre-autophagosomal structure organization. *Genes Cells (England)* 12:209-218.

Suzuki N, Maroof AM, Merkle FT, Koszka K, Intoh A, Armstrong I, Moccia R, Davis-Dusenbery BN, Eggan K (2013) The mouse C9ORF72 ortholog is enriched in neurons known to degenerate in ALS and FTD. *Nat Neurosci (United States)* 16:1725-1727.

Swinnen B, Robberecht W (2014) The phenotypic variability of amyotrophic lateral sclerosis. *Nat Rev Neurol* 10:661-670.

Takahashi S, Kubo K, Waguri S, Yabashi A, Shin HW, Katoh Y, Nakayama K (2012) Rab11 regulates exocytosis of recycling vesicles at the plasma membrane. *J Cell Sci (England)* 125:4049-4057.

Tanaka Y, Matsuwaki T, Yamanouchi K, Nishihara M (2013) Increased lysosomal biogenesis in activated microglia and exacerbated neuronal damage after traumatic brain injury in progranulin-deficient mice. *Neuroscience (United States)* 250:8-19.

Tang WK, Li D, Li CC, Esser L, Dai R, Guo L, Xia D (2010) A novel ATP-dependent conformation in p97 N-D1 fragment revealed by crystal structures of disease-related mutants. *Embo J (England)* 29:2217-2229.

Therrien M, Rouleau GA, Dion PA, Parker JA (2013) Deletion of C9ORF72 results in motor neuron degeneration and stress sensitivity in *C. elegans*. *PLoS One (United States)* 8:e83450.

Tian Y, Chang JC, Fan EY, Flajolet M, Greengard P (2013) Adaptor complex AP2/PICALM, through interaction with LC3, targets alzheimer's APP-CTF for terminal degradation via autophagy. *Proc Natl Acad Sci U S A (United States)* 110:17071-17076.

Tjelle TE, Brech A, Juvet LK, Griffiths G, Berg T (1996) Isolation and characterization of early endosomes, late endosomes and terminal lysosomes: Their role in protein degradation. *J Cell Sci (ENGLAND)* 109 (Pt 12):2905-2914.

Tollervey JR, Curk T, Rogelj B, Briese M, Cereda M, Kayikci M, Konig J, Hortobagyi T, Nishimura AL, Zupunski V, Patani R, Chandran S, Rot G, Zupan B, Shaw CE, Ule J (2011) Characterizing the RNA targets and position-dependent splicing regulation by TDP-43. *Nat Neurosci (United States)* 14:452-458.

Tooze SA, Yoshimori T (2010) The origin of the autophagosomal membrane. *Nat Cell Biol (England)* 12:831-835.

Tresse E, Salomons FA, Vesa J, Bott LC, Kimonis V, Yao TP, Dantuma NP, Taylor JP (2010) VCP/p97 is essential for maturation of ubiquitin-containing autophagosomes and this function is impaired by mutations that cause IBMPFD. *Autophagy (United States)* 6:217-227.

Trinczek B, Ebnet A, Mandelkow EM, Mandelkow E (1999) Tau regulates the attachment/detachment but not the speed of motors in microtubule-dependent transport of single vesicles and organelles. *J Cell Sci (ENGLAND)* 112 (Pt 14):2355-2367.

Urwin H, Authier A, Nielsen JE, Metcalf D, Powell C, Froud K, Malcolm DS, Holm I, Johannsen P, Brown J, Fisher EM, van der Zee J, Bruyland M, FReJA Consortium, Van Broeckhoven C, Collinge J, Brandner S, Fütter C, Isaacs AM (2010) Disruption of endocytic trafficking in frontotemporal dementia with CHMP2B mutations. *Hum Mol Genet (England)* 19:2228-2238.

Usenovic M, Tresse E, Mazzulli JR, Taylor JP, Krainc D (2012) Deficiency of ATP13A2 leads to lysosomal dysfunction, alpha-synuclein accumulation, and neurotoxicity. *J Neurosci (United States)* 32:4240-4246.

Valente EM et al (2004) Hereditary early-onset parkinson's disease caused by mutations in PINK1. *Science (United States)* 304:1158-1160.

van Blitterswijk M et al (2013) Association between repeat sizes and clinical and pathological characteristics in carriers of C9ORF72 repeat expansions (xpanse-72): A cross-sectional cohort study. *Lancet Neurol (England)* 12:978-988.

van Blitterswijk M et al (2014) TMEM106B protects C9ORF72 expansion carriers against frontotemporal dementia. *Acta Neuropathol (Germany)* 127:397-406.

Van Damme P, Van Hoecke A, Lambrechts D, Vanacker P, Bogaert E, van Swieten J, Carmeliet P, Van Den Bosch L, Robberecht W (2008) Progranulin functions as a neurotrophic factor to regulate neurite outgrowth and enhance neuronal survival. *J Cell Biol (United States)* 181:37-41.

Van Deerlin VM, Gill LH, Farmer JM, Trojanowski JQ, Lee VM (2003) Familial frontotemporal dementia: From gene discovery to clinical molecular diagnostics. *Clin Chem (United States)* 49:1717-1725.

Van Deerlin VM et al (2010) Common variants at 7p21 are associated with frontotemporal lobar degeneration with TDP-43 inclusions. *Nat Genet (United States)* 42:234-239.

van der Blik AM (2005) A sixth sense for Rab5. *Nat Cell Biol (England)* 7:548-550.

van der Zee J, Urwin H, Engelborghs S, Bruyland M, Vandenberghe R, Dermaut B, De Pooter T, Peeters K, Santens P, De Deyn PP, Fisher EM, Collinge J, Isaacs AM, Van Broeckhoven C (2008) CHMP2B C-truncating mutations in frontotemporal lobar degeneration are associated with an aberrant endosomal phenotype in vitro. *Hum Mol Genet (England)* 17:313-322.

van der Zee J, Van Langenhove T, Kleinberger G, Slegers K, Engelborghs S, Vandenberghe R, Santens P, Van den Broeck M, Joris G, Brys J, Mattheijssens M, Peeters K, Cras P, De Deyn PP,

Cruts M, Van Broeckhoven C (2011a) TMEM106B is associated with frontotemporal lobar degeneration in a clinically diagnosed patient cohort. *Brain (England)* 134:808-815.

van der Zee J, Van Langenhove T, Kleinberger G, Slegers K, Engelborghs S, Vandenberghe R, Santens P, Van den Broeck M, Joris G, Brys J, Mattheijssens M, Peeters K, Cras P, De Deyn PP, Cruts M, Van Broeckhoven C (2011b) TMEM106B is associated with frontotemporal lobar degeneration in a clinically diagnosed patient cohort. *Brain (England)* 134:808-815.

Vass R, Ashbridge E, Geser F, Hu WT, Grossman M, Clay-Falcone D, Elman L, McCluskey L, Lee VM, Van Deerlin VM, Trojanowski JQ, Chen-Plotkin AS (2011) Risk genotypes at TMEM106B are associated with cognitive impairment in amyotrophic lateral sclerosis. *Acta Neuropathol (Germany)* 121:373-380.

Velayos-Baeza A, Vettori A, Copley RR, Dobson-Stone C, Monaco AP (2004) Analysis of the human VPS13 gene family. *Genomics (United States)* 84:536-549.

Verhoeven K, De Jonghe P, Coen K, Verpoorten N, Auer-Grumbach M, Kwon JM, FitzPatrick D, Schmedding E, De Vriendt E, Jacobs A, Van Gerwen V, Wagner K, Hartung HP, Timmerman V (2003) Mutations in the small GTP-ase late endosomal protein RAB7 cause charcot-marie-tooth type 2B neuropathy. *Am J Hum Genet (United States)* 72:722-727.

Vitelli R, Santillo M, Lattero D, Chiariello M, Bifulco M, Bruni CB, Bucci C (1997) Role of the small GTPase Rab7 in the late endocytic pathway. *J Biol Chem (UNITED STATES)* 272:4391-4397.

Voss EW, Jr, Workman CJ, Mummert ME (1996) Detection of protease activity using a fluorescence-enhancement globular substrate. *BioTechniques (UNITED STATES)* 20:286-291.

Waite AJ, Baumer D, East S, Neal J, Morris HR, Ansorge O, Blake DJ (2014) Reduced C9orf72 protein levels in frontal cortex of amyotrophic lateral sclerosis and frontotemporal degeneration

brain with the C9ORF72 hexanucleotide repeat expansion. *Neurobiol Aging* (United States) 35:1779.e5-1779.e13.

Walkley SU, Vanier MT (2009) Secondary lipid accumulation in lysosomal disease. *Biochim Biophys Acta* (Netherlands) 1793:726-736.

Wang X, Fan H, Ying Z, Li B, Wang H, Wang G (2010) Degradation of TDP-43 and its pathogenic form by autophagy and the ubiquitin-proteasome system. *Neurosci Lett* (Ireland) 469:112-116.

Wen X, Tan W, Westergard T, Krishnamurthy K, Markandaiah SS, Shi Y, Lin S, Shneider NA, Monaghan J, Pandey UB, Pasinelli P, Ichida JK, Trotti D (2014) Antisense proline-arginine RAN dipeptides linked to C9ORF72-ALS/FTD form toxic nuclear aggregates that initiate in vitro and in vivo neuronal death. *Neuron* (United States) 84:1213-1225.

Wilhelmsen KC, Lynch T, Pavlou E, Higgins M, Nygaard TG (1994) Localization of disinhibition-dementia-parkinsonism-amyotrophy complex to 17q21-22. *Am J Hum Genet* (UNITED STATES) 55:1159-1165.

Williams DR, Hadeed A, al-Din AS, Wreikat AL, Lees AJ (2005) Kufor rakeb disease: Autosomal recessive, levodopa-responsive parkinsonism with pyramidal degeneration, supranuclear gaze palsy, and dementia. *Mov Disord* (United States) 20:1264-1271.

Wils H, Kleinberger G, Pereson S, Janssens J, Capell A, Van Dam D, Cuijt I, Joris G, De Deyn PP, Haass C, Van Broeckhoven C, Kumar-Singh S (2012) Cellular ageing, increased mortality and FTLTDP-associated neuropathology in progranulin knockout mice. *J Pathol* (England) 228:67-76.

Woerner AC, Frottin F, Hornburg D, Feng LR, Meissner F, Patra M, Tatzelt J, Mann M, Winklhofer KF, Hartl FU, Hipp MS (2016) Cytoplasmic protein aggregates interfere with nucleocytoplasmic transport of protein and RNA. *Science* (United States) 351:173-176.

Wong E, Cuervo AM (2010) Autophagy gone awry in neurodegenerative diseases. *Nat Neurosci (United States)* 13:805-811.

Xiao S, MacNair L, McGoldrick P, McKeever PM, McLean JR, Zhang M, Keith J, Zinman L, Rogaeva E, Robertson J (2015) Isoform-specific antibodies reveal distinct subcellular localizations of C9orf72 in amyotrophic lateral sclerosis. *Ann Neurol (United States)* 78:568-583.

Xiao S, Sanelli T, Dib S, Sheps D, Findlater J, Bilbao J, Keith J, Zinman L, Rogaeva E, Robertson J (2011) RNA targets of TDP-43 identified by UV-CLIP are deregulated in ALS. *Mol Cell Neurosci (United States)* 47:167-180.

Xie Z, Klionsky DJ (2007) Autophagosome formation: Core machinery and adaptations. *Nat Cell Biol (England)* 9:1102-1109.

Xu H, Ren D (2015) Lysosomal physiology. *Annu Rev Physiol (United States)* 77:57-80.

Xu Z, Poidevin M, Li X, Li Y, Shu L, Nelson DL, Li H, Hales CM, Gearing M, Wingo TS, Jin P (2013) Expanded GGGGCC repeat RNA associated with amyotrophic lateral sclerosis and frontotemporal dementia causes neurodegeneration. *Proc Natl Acad Sci U S A (United States)* 110:7778-7783.

Yamashiro DJ, Maxfield FR (1987) Acidification of morphologically distinct endosomes in mutant and wild-type chinese hamster ovary cells. *J Cell Biol (UNITED STATES)* 105:2723-2733.

Yin F, Dumont M, Banerjee R, Ma Y, Li H, Lin MT, Beal MF, Nathan C, Thomas B, Ding A (2010) Behavioral deficits and progressive neuropathology in progranulin-deficient mice: A mouse model of frontotemporal dementia. *Faseb J (United States)* 24:4639-4647.

Yoshimura S, Gerondopoulos A, Linford A, Rigden DJ, Barr FA (2010) Family-wide characterization of the DENN domain rab GDP-GTP exchange factors. *J Cell Biol* (United States) 191:367-381.

Yu L, Strandberg L, Lenardo MJ (2008) The selectivity of autophagy and its role in cell death and survival. *Autophagy* (United States) 4:567-573.

Yu L, Lenardo MJ, Baehrecke EH (2004a) Autophagy and caspases: A new cell death program. *Cell Cycle* (United States) 3:1124-1126.

Yu L, De Jager PL, Yang J, Trojanowski JQ, Bennett DA, Schneider JA (2015) The TMEM106B locus and TDP-43 pathology in older persons without FTL. *Neurology* (United States) 84:927-934.

Yu L, Alva A, Su H, Dutt P, Freundt E, Welsh S, Baehrecke EH, Lenardo MJ (2004b) Regulation of an ATG7-beclin 1 program of autophagic cell death by caspase-8. *Science* (United States) 304:1500-1502.

Yu L, McPhee CK, Zheng L, Mardones GA, Rong Y, Peng J, Mi N, Zhao Y, Liu Z, Wan F, Hailey DW, Oorschot V, Klumperman J, Baehrecke EH, Lenardo MJ (2010) Termination of autophagy and reformation of lysosomes regulated by mTOR. *Nature* (England) 465:942-946.

Zanocco-Marani T, Bateman A, Romano G, Valentinis B, He ZH, Baserga R (1999) Biological activities and signaling pathways of the granulin/epithelin precursor. *Cancer Res* (UNITED STATES) 59:5331-5340.

Zerial M, McBride H (2001) Rab proteins as membrane organizers. *Nat Rev Mol Cell Biol* (England) 2:107-117.

Zhang D, Iyer LM, He F, Aravind L (2012) Discovery of novel DENN proteins: Implications for the evolution of eukaryotic intracellular membrane structures and human disease. *Front Genet (Switzerland)* 3:283.

Zhang K et al (2015) The C9orf72 repeat expansion disrupts nucleocytoplasmic transport. *Nature (England)* 525:56-61.

Zhang YJ, Xu YF, Dickey CA, Buratti E, Baralle F, Bailey R, Pickering-Brown S, Dickson D, Petrucelli L (2007) Progranulin mediates caspase-dependent cleavage of TAR DNA binding protein-43. *J Neurosci (United States)* 27:10530-10534.

Zhang YQ, Gamarra S, Garcia-Effron G, Park S, Perlin DS, Rao R (2010) Requirement for ergosterol in V-ATPase function underlies antifungal activity of azole drugs. *PLoS Pathog (United States)* 6:e1000939.

Zhou J, Tan SH, Nicolas V, Bauvy C, Yang ND, Zhang J, Xue Y, Codogno P, Shen HM (2013) Activation of lysosomal function in the course of autophagy via mTORC1 suppression and autophagosome-lysosome fusion. *Cell Res (England)* 23:508-523.

Zhou X, Sun L, Bastos de Oliveira F, Qi X, Brown WJ, Smolka MB, Sun Y, Hu F (2015) Prosaposin facilitates sortilin-independent lysosomal trafficking of progranulin. *J Cell Biol (United States)* 210:991-1002.

Zhu J, Nathan C, Jin W, Sim D, Ashcroft GS, Wahl SM, Lacomis L, Erdjument-Bromage H, Tempst P, Wright CD, Ding A (2002) Conversion of proepithelin to epithelins: Roles of SLPI and elastase in host defense and wound repair. *Cell (United States)* 111:867-878.

Zimprich A et al (2011) A mutation in VPS35, encoding a subunit of the retromer complex, causes late-onset parkinson disease. *Am J Hum Genet (United States)* 89:168-175.

Zoncu R, Bar-Peled L, Efeyan A, Wang S, Sancak Y, Sabatini DM (2011) mTORC1 senses lysosomal amino acids through an inside-out mechanism that requires the vacuolar H(+)-ATPase. *Science (United States)* 334:678-683.

Zu T, Liu Y, Banez-Coronel M, Reid T, Pletnikova O, Lewis J, Miller TM, Harms MB, Falchook AE, Subramony SH, Ostrow LW, Rothstein JD, Troncoso JC, Ranum LP (2013) RAN proteins and RNA foci from antisense transcripts in C9ORF72 ALS and frontotemporal dementia. *Proc Natl Acad Sci U S A (United States)* 110:E4968-77.